NASA Contractor Report 175059

Enhanced Mixing of an Axisymmetric Jet by Aerodynamic Excitation

Ganesh Raman
Cleveland State University
Cleveland, Ohio

March 1986

Prepared for
Lewis Research Center
Under Grant NCC 3-49

National Aeronautics and
Space Administration

ABSTRACT

The main objective of acoustic excitation studies is to gain a high level of control over processes governing free shear flow characteristics. The basic premise is that inherent instability waves in free shear flows are excitable by external perturbations with frequencies close to the natural instability frequency of the flow.

In the present work an 8.89 cm diameter axisymmetric jet was acoustically excited by four loudspeakers placed upstream of the nozzle exit. Measurements were made at Mach numbers of 0.435 and 0.2 (quiet and noisy valve conditions). A single hot-wire probe was used to obtain turbulence levels at the nozzle exit and along the centerline, and a microphone at the nozzle exit was used to study the resonance characteristics of the rig.

A Pitot probe was stationed at X/D = 9 downstream along the nozzle axis to study the Strouhal number dependence and to look at threshold levels for excitation.

The test results were obtained after a preliminary evaluation and facility improvement.

Excitation at the correct Strouhal number enhanced mixing significantly. The effects were most prominent in the Strouhal number range between 0.4 and 1.0. The effects of acoustic excitation also depended considerably on the sound pressure level at the nozzle exit and were more pronounced at higher sound levels. Other factors which influenced the excitability were valve noise, exit turbulence levels, extraneous noise and a flanged nozzle. Analysis of the hot-wire signal, in conditions of optimum jet mixing, showed vortex pairing to occur between 2 and 3 diameters downstream.

TABLE OF CONTENTS

LIST OF SYMBOLS

b	Constant (Eq. (B-2))
D	Diameter, in.
F,f	Frequency, Hz
M	Mach number
St	Strouhal number
T	Temperature, °R
U	Mean velocity, ft/sec
u'	Fluctuating velocity, ft/sec
x	Axial coordinate
y	Radial coordinate

Greek Symbols

θ	Momentum thickness
δ	Constant (Eq. (b-1))

Subscripts

c	Centerline
e	Exit
d	Based on diameter

CHAPTER I

INTRODUCTION

The objective of jet shear layer excitation studies stated very broadly is to gain a high level of control over the processes governing the flow. What makes this possible is the ability of the applied perturbation to interact with the inherent instability in the shear layer. The benefits of this study, in addition to gaining a better understanding of subsonic shear layer dynamics, include technological applications in mixing processes and jet exhaust noise.

As cited by Crow and Champagne (1971) the first documented evidence of acoustic excitation dates back to the mid-nineteenth century. Like most other beginnings it was accidental, but a result of a keen observation. This occurred during an evening of chamber music when a medical doctor among the audience observed a gas flame dance in response to the violoncello. Leconte (1858) in his paper states, "A deaf man might have seen the harmony." Later Lord Rayleigh (1896) studied the behavior of sensitive jets. Subsequent to this many investigations have focused on the phenomenon of acoustic

excitation but to date the phenomenon is still not completely understood.

In excitation studies the turbulent jet is often the focus of attention. Figure 1 is a schematic diagram of an axisymmetric jet. When a jet of air issues from a nozzle into a stationary medium, the kinetic energy of such a jet dissipates through reaction with the surrounding fluid. As a result the kinetic energy of the oncoming stream steadily converts to the kinetic energy of turbulence which in turn decays through viscous dissipation. This results in a shrinkage of the potential core and in a widening of the flow section. Details on the theory of turbulent jets have been stated by Abramovich (1963).

There are growing instability waves that are inherent in the shear layer of an unexcited jet. The growing instability waves eventually roll up into vortices. These vortices then pair up, entraining ambient air and coalesce. The developmental features are easily observable in a flow visualization study using a schlieren system. Moore (1977) described the vortex pairing process as the growth of a larger-scale instability wave at the expense of the smaller scale wave that was present on the thinner upstream shear layer.

When a sinusoidal perturbation is applied upstream of a nozzle in the form of an acoustic wave the instability wave is created at the nozzle exit with a corresponding frequency. Under favorable conditions the instability wave could be amplified and pairing may occur between the resulting large scale vortical structures. The final result is an increase in the jet spreading rate and turbulence

intensity. The 'favorable conditions' for effective pure tone excitation are influenced by the forcing frequency, amplitude, flow Mach number and initial conditions such as the nature of the exit boundary layer, its thickness and the intensity of turbulence at the nozzle exit.

In engineering applications the excitation amplitude level from acoustic sources may be insufficient particularly if turbulence is high under unexcited conditions. The excitation, however does not have to be acoustic. It could, for example, be in the form of a piezo electric perturbation or a velocity perturbation from an oscillating plate. The conditions of excitation therefore do not include a specific source of perturbation.

PRESENT WORK:

This study was focussed on the effect of upstream excitation on free shear flows. An axisymmetric jet was selected since it was a common form of free shear flow. The objectives were to study the dependence of excitation on the frequency, the Mach number, the Strouhal number and to determine threshold levels for excitation. To accomplish these an existing jet facility at NASA Lewis Research Center was modified and improved.

Preliminary measurements of turbulence intensity and mean velocity were made using single hot wire probes in the plenum tank, at the nozzle exit and along the centerline at several axial stations. The above evaluation coupled with a study of resonance characteristics of the rig and measurement of exit velocity profiles using a Pitot probe was used to arrive at a tentative test plan.

Following the facility improvement the preliminary measurements were repeated and a final test plan was formulated. This plan included measurements using a Pitot probe at X/D = 9 over a range of acoustic excitation frequencies and sound levels at two Mach numbers for both noisy and quiet valve conditions. In addition hot-wire measurements were made with a single wire probe at various locations along the centerline.

CHAPTER II

LITERATURE REVIEW

A brief summary of the previous work pertaining to acoustic excitation is presented in this section. Background information on jet theories and large scale structures of turbulence is also included.

JET THEORIES:

Taylor (1921) assumed that the turbulent shearing stress in a stream must be determined by the lateral transfer of vorticity. He obtained velocity and temperature fields which agreed with experiments.

Prandtl (1932) assumed that the mixing length at any cross section of a jet was constant. The similarity of boundary layers in different cross sections provides sufficient basis for Prandtl's assumption. Therefore, it is sufficient to establish a law for the growth of a jet as a function of distance along the x-axis, in order to define the way in which the mixing length increases. In the fully developed region of a jet due to similarity of velocity profiles in different cross sections the rate of growth of the jet can be obtained by the product of the axial velocity and the rate of increase in the radius of the jet with axial distance. In addition it is usually assumed that the

pressure in a jet is virtually constant and equal to the pressure in the surrounding space. Due to this the total momentum is conserved (see Abramovich (1963)).

Comparing Prandtl's theory with Taylor's, one finds that Prandtl's theory neglected local instantaneous pressure gradients that substantially affect momentum exchange but not vorticity transfer. Taylor eliminated this inconsistency by using the vorticity concept and one experimental constant. A point worth noting is that Prandtl's theory gave velocity profiles which agreed closely with Taylor's predictions.

Prandtl later published a new theory of free turbulence in which Newton's laws of viscous friction were used to determine the turbulent shearing stress in a jet as Boussinesq (1877) had suggested. Prandtl assumed the coefficent of turbulent viscosity to be proportional to the product of density, velocity difference and jet thickness. Using Prandtl's new theory Gortler (1942) obtained asymptotic velocity profiles at the lateral cross sections of the jet which can be determined by simple analytical formulas.

Reichardt (1951) neglected the pressure gradients in the equation of motion constructed for instantaneous values of the variables. Reichardt further assumed that the lateral transport of momentum was proportional to the transverse gradient of the streamwise component of momentum. The parameter with the dimensions of length, introduced by Reichardt characterizes the mixing in analogy with Prandtl's mixing length. Reichardt assumed that this parameter was constant on each cross-section of the jet but variable along the jet.

ACOUSTIC EXCITATION:

Crow and Champagne (1971) highlighted "order in disorder," or the remarkable degree of order in turbulent flows. Since the development of the jet itself is dictated by the evolution of these large scale coherent structures, interest was therefore diverted to coherent structures. They showed that by exciting an axisymmetric jet at a Strouhal number of 0.3 based on the jet diameter the entrained volume increased by 32 percent over the unexcited case. Future works established that the coherent structures do play an important role in mixing and heat, mass and momentum transfer (Hussain (1983)).

Several authors have emphasized the importance of the dimensionless Strouhal number ($St_d = fD/U_e$). Moore (1977) showed that the acoustic level required for effective enhancement of turbulent mixing and a consequential increase in broadband noise was only 0.08% of the jet dynamic head provided it was done at the correct Strouhal number. In addition, when a low level acoustic source was used the instability wave locked on to it and responded in accordance with linear shear layer instability theory. However, at higher excitation levels the wave extracted energy from the mean flow and the response became nonlinear as some of this energy was converted to turbulent energy.

Crighton (1981) in a review paper explained that, "forcing", such as acoustic excitation, which amounts to control of the upstream boundary condition on the jet or shear layer, restores a degree of control to an otherwise chaotic flow, fixing the frequency, phase and azimuthal coherence of vortical wavetrains. Due to their nature as

instabilities these vortical wavetrains are raised above the level of the fine-scale background turbulence. Much of the turbulent energy in frequency bands around the forcing frequency and its harmonics and subharmonics is locked to the forcing frequency.

It has been shown by Vlasov and Ginevskii (1980), Zaman and Hussain (1981), and Ahuja et al. (1982) that excitation at a jet Strouhal number between 2 and 4 decreased turbulence intensities along the centerline from corresponding unexcited values. More explicitly, the result was an attenuation in turbulent mixing: roll up and breakdown of shear layer instabilities occurred earlier, the shear layer became thinner and the length of the potential core increased.

In contrast at a jet Strouhal number between 0.2 and 0.8 the effect of excitation was quite the reverse. Turbulent mixing was enhanced: Shear layer vortices grew to larger sizes, there was successive pairing between these large-scale structures, the shear layer broadened, the length of the potential core decreased and the turbulence intensity level increased.

Zaman and Hussain (1980) showed that jet mixing enhancement or supression depended not merely on the jet Strouhal number but also very strongly on the type of the nozzle exit boundary layer (laminar or turbulent) and on the nozzle exit boundary layer thickness. They found that for a laminar exit boundary layer, the vortex pairing in the jet shear layer occurred regularly in space and time, but became intermittent with increasing Reynolds number.

Ahuja et al. (1982) explained excitation and jet noise production to be a three step process. In the first step, the large scale

instability wave inherent even in an unexcited jet was modified by the upstream excitation leading to an amplification of this instability wave.

The second part of the process involved the coupling between the large scale structure and the fine scale turbulence.

The final link was the relationship between the jet-flow characteristics and the noise radiated to the far-field. The excited jet has a modified mean flow and turbulence intensity and will therefore generate noise slightly different from the unexcited case.

Heavens (1980) examined the response of a subsonic round jet to excitation using flow visualization and noise measurements. These measurements indicate that the effects of pure tone excitation depend considerably on the forcing amplitude and frequency. Heavens also points out that the interaction of the sound field with the nozzle flow is a nonlinear process resulting in an amplification of the broadband noise field of the jet.

Tam (1978) studied the effect of forced excitation of unstable waves in a two-dimensional shear layer. A mathematical analysis was made by formulating the problem as an inhomogeneous boundary-value problem. The advantage of this approach is that the arbitrary spatial distribution of the incident sound wave amplitude was automatically taken care of. Tam used an inviscid model because it has been shown for a plane shear layer at moderate Reynolds numbers that viscosity is not important as far as instability characteristics are concerned (Michalke (1965) and Freymuth (1966)). In the mathematical analysis the coupling constants between the incident sound wave and the excited

instability wave are calculated and for a given mean flow profile are seen to depend on the frequency and flow Mach numbers.

VORTEX PAIRING AND LARGE-SCALE STRUCTURES:

Winant and Browand (1974) believe that vortex pairing is the mechanism which controls the growth of the mixing layer in the initial region. These large scale vortical structures have their axes perpendicular to the direction of the mean flow. Two adjoining vortices interact to form a single larger vortex and a repetition of this process controls the mixing layer growth in the initial region of the jet.

Ho and Huang (1982) emphasized that the subharmonic amplification was the cause, rather than the outcome of vortex pairing. They forced a plane mixing layer over a range of frequencies. Measurements of the amplification of the fundamental and subharmonic made it clear that the amplification of the fundamental and its saturation under nonlinear effects do not determine where vortex pairing occurs. They believe that vortex pairing occurs at the locations where the subharmonic wave achieves its maximum amplitude.

Chan (1977) observed that large scale eddies in a turbulent jet behave much like a wavetrain propagating in a shear flow. Chan showed that an axisymmetric turbulent jet can support in addition to the plane wave mode, a helical wavetrain with the azimuthal mode index equal or greater than unity.

Acton (1980) studied large eddies in an axisymmetric jet and found that changes in frequency and amplitude of harmonic excitation caused distinct changes in the wavelengths of jet eddies. The resulting

large eddy behavior was consistent with many features of nonlinear behavior observed in experimentally forced jets.

Armstrong (1981) experimentally obtained cross-spectral densities of turbulent pressure and its azimuthal constituents using condensor microphones in a round jet. The coherent structures which were thus determined appear not to be strongly influenced by Mach number. The author also noticed a difference in eddy-wave behavior between acoustically forced and unforced jets.

CHAPTER III

EXPERIMENTAL APPARATUS

THE JET FACILITY:

The jet facility consisted of a plenum chamber, an excitation ring and a convergent nozzle. The plenum chamber was supplied by 40 psig pressurized air through an 8-in. line. An 8-in. butterfly valve bypassed by a 1.5-in. valve allowed the regulation and control of the total pressure in the plenum. Details of the air supply system and plenum are shown in Figures 2 and 3. Figure 4 shows the valve system.

An adaptor ring installed between the plenum tank and the nozzle inlet housed the excitation system. This system consisted of four acoustic drivers and microphones that were equally spaced about the circumference. Each driver was enclosed in a sealed can and vented to the nozzle inlet to equalize pressure across the speaker diaphragm. The acoustic drivers had a rated power of 40 W over a frequency range between 50 and 20 000 Hz. Each driver was connected to a dual channel Altec Lansing 100 W power amplifier.

A flanged and an unflanged convergent nozzle with an exit diameter of 8.89 cm (3.5 in.) were available. All data described herein were taken using the flanged nozzle.

The convergent nozzle exhausted into the test cell and had an exit diameter of 8.89 cm (3.5 in.). A microphone array at the nozzle exit could be used to determine the nature of the output acoustic signals. Figure 5 shows the unflanged nozzle and the microphone array. The flanged nozzle is detailed in Figure 6.

PROBE POSITIONING:

Pitot probes, hot wires and microphones were mounted on a traversing mechanism and moved in the axial and radial directions. Figure 7 shows this capability. In addition it shows the flanged nozzle. The mechanism was capable of moving two probe holders (probe holders A and B). Probe holder A had an axial traverse of 36 in. and a radial traverse of 6 in. For any position of probe holder A, probe holder B could be positioned independently up to 18 in. axially and 12 in. radially. The position accuracy was within 0.035 in.

A motor driven single axis probe positioner actuator was used to measure radial profiles. The probe positioner was connected on the IEEE-488 bus to an HP computer. The computer could operate the actuator and move the probe positioner at a preset speed along a single axis, The positioner could support hot wires or Pitot probes.

DATA ACQUISITION:

A schematic diagram of the data acquisition set up is shown in Figure 8. At the heart of the data acquisition system was an HP 9835A computer. This high speed computational and controlling tool could be

programmed in the BASIC language. Internal Read/Write memory could be expanded to 256 Kbytes. A tape cartridge allowed data storage and retrieval. The HP 9835A could access digital voltmeters, relay switches, a scanner, a variphase tone generator and a Rockland Scientific 804 FFT signal analyzer through an IEEE-488 bus. Figure 9 shows the data acquisition set-up.

The HP computer read signals from the DISA constant temperature anemometer system using the Fluke digital voltmeters and scaled, plotted and stored this data as mean velocities and turbulence intensities. Figure 10 shows the anemometer system.

The Wavetek 152 programmable variphase tone generator was a precision source of selectable waveforms with variable phase relationships between its eight channels. The programmed frequency was applied to all channels. Amplitude, phase and waveform for each channel could be independently programmed. The generator could also be controlled locally with a front panel keyboard and could produce sine, cosine, triangle, square, variphase sine and variphase square waveforms of frequency between 1 Hz and 100 kHz and amplitudes from 10 mV peak to 9.99 V peak.

The Rockland Scientific 804 multichannel signal processor proved to be a very powerful and flexible analysis system. It could perform basic signal processing functions at the press of a few keys. The Rockland Scientific 804 could be programmed in SAMPL (Signal Analysis Macro Programming Language) and could calculate, plot and store power spectra, cross spectra and other correlation functions.

CHAPTER IV

EXPERIMENTAL PROCEDURE

MICROPHONE MEASUREMENTS:

Before each test run a microphone was calibrated using a B and K pistonphone so that the sound pressure levels in the power spectrum are relative to 20 μPa. The pistonphone generated a frequency of 250 Hz at 124 dB. The microphone was then mounted flush in the nozzle 0.25 in. from the nozzle exit.

For the resonance test the pressure in the plenum chamber was first adjusted to produce a predetermined Mach number at the nozzle exit. Following this a constant amplitude was set on the variphase tone generator and the computer stepped through frequencies from 500 to 1600 Hz at intervals of 50 Hz. The microphone at the nozzle exit then measured sound pressure levels and a power spectrum was recorded on the signal analyzer.

PITOT PROBE MEASUREMENTS:

To study the mean velocity at X/D = 9, with and without excitation, a Pitot probe was stationed there and the plenum pressure was adjusted to produce the desired Mach number at the nozzle exit.

The tone generator was then set at a predetermined frequency and the amplitude was varied to produce different sound levels at the nozzle exit. For each sound pressure level the computer recorded velocities based on the Pitot probe pressure. The test was repeated at several frequencies.

Exit velocity profiles were measured using a similar procedure. The difference being that the single axis probe positioner moved the Pitot probe radially across the jet for each set of test conditions.

SINGLE HOT-WIRE MEASUREMENTS:

The single hot-wire calibration procedure using a DISA constant temperature anemometer is provided in Appendix A along with a test check-list and a run summary.

In a typical test run involving single wire measurements of turbulence intensities and mean velocities the following procedure was followed. The pressure in the plenum chamber was adjusted to produce a desired Mach number at the nozzle exit (up to Mach 0.5). At the beginning of each run the Altec Lansing power amplifiers were adjusted manually to provide the desired voltage input to the acoustic drivers, and the frequency and amplitude were set on the variphase tone generator by the HP 9835A computer. Finally the hot wire was positioned. The HP computer read a Fluke voltmeter to determine the ac and dc anemometer voltages. It then time averaged dc and ac signals separately and converted them to mean and fluctuating velocities respectively. Simultaneously the Rockland Scientific 804 signal analyzer averaged and stored spectra. The frequency was then changed on the variphase tone genarator. During changes in frequency

the amplitude was automatically reduced to zero and gradually stepped up after a frequency change to prevent damage to the drivers due to transients.

SUMMARY OF TESTS:

PRELIMINARY TESTS

(1) Measurement of turbulence intensities using a single hot-wire at nozzle exit, in plenum tank and along the centerline axis, Mach number = 0.1, 0.173, 0.199, 0.223, and 0.28, locations: X/D = 0.463, 1.9, 3.3, 4.75, 6.2, 7.6, 9, and 10.46.

(2) Single hot-wire measurements along centerline axis with excitation at Mach number = 0.1, 0.3, locations X/D = 1.90, 4.75, 6.2, and 9.0.

(3) Measurements of resonance characteristics of rig with and without flow.

(4) Single hot-wire measurements at the radial position for half velocity with excitation at constant sound levels, Mach number = 0.4 and 140 dB, X/D= 1.9, 4.75, 6.2, and 9, (at X/D = 9, two hot wires, one behind another by an inch were used) frequencies = 910, 1040, 1510, 1580, and 2510 (Strouhal number = 0.49, 0.56, 0.82, 0.856, and 1.36).

(5) Pitot probe measurements of radial velocity profiles at X/D = 1 and 2, Mach number = 0.07, 0.2, and 0.435.

(6) Pitot probe measurements at X/D = 9 with and without excitation, Mach number = 0.435, frequency = 1590 Hz, fluctuating pressure level = 135 dB.

(7) Pressure drop test with different thicknesses of felt (1/8, 1/4, and 3/8 in. thickness).

TESTS WITH IMPROVED FACILITY

(1) Measurement of turbulence intensity at exit and in plenum tank.

(2) Measurement of resonance characteristics of modified rig.

(3) Single hot-wire measurements of axial velocity decay and turbulence intensities, Mach number = 0.2 (quiet and noisy valve settings), Strouhal number = 0.5, fluctuating pressure level = 140.7 dB, X/D = 1.9, 3.3, 6.2, 7.6, and 9.

(4) Pitot probe measurements of radial velocity profiles, Mach numbers = 0.435,0.2 (quiet and noisy valve settings), X/D = 0, 1, and 2, Strouhal number = 0.5, fluctuating pressure level = 140 dB.

(5) Pitot probe measurements at X/D = 9, frequencies: 400 to 2500 Hz, Mach number = 0.435.

(6) Pitot probe measurements at X/D = 9, frequencies: 400 to 1300, Mach number = 0.2.

(7) Radial traverse with Pitot probe at X/D= 9, Mach number = 0.2 (quiet and noisy valve settings), 0.435, Strouhal number = 0.5, fluctuating pressure level = 140 dB.

CHAPTER V

DISCUSSION OF RESULTS

A. Preliminary Evaluation of Jet Facility:

TURBULENCE MEASUREMENTS

At the start of the test program turbulence measurements were made with single hot wires at the jet exit and in the plenum tank. The turbulence intensity was obtained by dividing the RMS value of the fluctuating longitudinal component by the mean velocity. The turbulence intensities were measured to be about 40 percent in the plenum tank and less than 1.5 percent at the nozzle exit. The axisymmetric contraction with an area ratio of 64 was responsible for this reduction. This is consistent with observations in the literature (Tan-Atichat (1980)) which predicted that for such a contraction the turbulence intensity would be reduced to less than 5 percent of the original value by the contraction. Effects of flow contraction on the evolution of turbulence have been studied in detail by Shinichi Tsuge' (1984).

Measurements of mean velocities and turbulence intensities were also made axially along the centerline up to X/D = 9 for Mach number

equal to 0.1, 0.144, 0.173, 0.199, 0.223, and 0.28. These are shown in Figures 11 to 16. For this low Mach number test the jet was naturally excited by valve system noise. The length of the potential core was seen to gradually increase from X/D = 3 for a Mach number of 0.1 to X/D = 4 for a Mach number of 0.22. The turbulence intensity curves display a prominent hump in the region of the potential core followed by a linear increase and an apparent leveling off in the self-preserving region ($X/D \geq 10$). The 'hump' as pointed out by Ahuja et al. (1982) is due to a massive large scale activity in the vicinity of X/D = 2. This is a region where the growth of an instability wave controls the total turbulence. The turbulence intensity values were as high as 25 percent because local mean velocities were used to normalize the rms value of the fluctuating component obtained from the single hot-wire probe.

RESONANCE CHARACTERISTICS OF RIG

The resonance characteristics of the plenum tank, excitation adaptor and nozzle (which behaved like an organ pipe in resonance) were studied. Although the voltage input to the acoustic drivers was constant at all frequencies, the exit fluctuating pressure levels varied in a range of 23 dB. Figure 17 shows these characteristics. This test was repeated at a Mach number of 0.3 and showed some changes in the resonance characteristics (Figure 18). (In the figures the caption pressure levels refers to fluctuating pressure levels.)

EXCITABILITY TESTS:

Single hot-wire measurements were made along the centerline of the jet at four axial stations. At a Mach number of 0.1 the

frequencies were varied from 700 to 1600 Hz at intervals of 50 Hz. There was no control over the sound levels which were essentially governed by the resonance characteristics of the rig. The results are shown in Figures 19 and 20.

At a Mach number of 0.3 the measurements were repeated at the same axial stations but at frequencies between 500 and 2450 Hz at intervals of 50 Hz. The results are shown in Figures 21 and 22. Corresponding to an increase or decrease in the mean centerline velocity was an opposite effect in the rms value of the fluctuating velocity. For example a decrease in the mean centerline velocity at 1000 Hz and a Mach number of 0.3 was accompanied by an increase in the RMS value of the fluctuating velocity. The small effect of excitation on the flow is attributed to the high turbulence intensities at the nozzle exit and the low sound pressure levels used to excite the flow.

EXCITATION AT CONSTANT SOUND LEVELS

In an attempt to identify a frequency dependence a test was performed along the velocity half-width line (the velocity half-width line joins points in the shear layer at which the velocity is half the centerline velocity of the jet). Five frequencies (910, 1040, 1510, 1580, and 2510 Hz) which corresponded to peaks in the resonance test were selected. The sound level was maintained constant at 140 dB at the nozzle exit. At a Mach number of 0.4, mean velocity suppression and turbulence enhancement was seen around 1510 Hz. The corresponding Strouhal number was 0.8 based on the jet exit diameter. The results for different axial locations are presented in Table (1-A) to (1-E). For the measurement at X/D = 9 two hot wires were used, both along

the centerline and one trailing the other by an inch. These are presented in Tables (1-A) and (1-B).

RADIAL VELOCITY PROFILES

Radial velocity measurements were made using a Pitot probe at X/D = 1 and 2 at Mach number of 0.07, 0.2 and 0.435. The data is presented in Tables C-6(a-f) of Appendix C. The momentum thickness (a measure of the loss of momentum due to viscosity) was calculated in the following manner:

$$\theta = \int_0^y \frac{U}{U_e}\left(1 - \frac{U}{U_e}\right)dy$$

A sample calculation is provided in Appendix B and some values thus obtained are in Table II.

A radial traverse was also made at X/D = 9. The excitation frequency was 1590 Hz with a sound pressure level of 135 dB at Mach number 0.435. Figure 23 shows the results of this test. With the application of the tone the centerline mean velocity was suppressed to 0.93 of the unexcited value. This decrease in the centerline velocity was accompanied by a widening of the flow section as seen by the crossover of curves. Very plainly this crossover is a result of axial momentum being conserved.

B. JET FACILITY IMPROVEMENT:

In an attempt to reduce turbulence levels at the nozzle exit it was decided to explore the effect of inserting a sheet of felt directly into the direction of flow in the plenum tank. Preliminary measurements of pressure drop were made with felt pieces of different

thicknesses mounted in the nozzle between two flanges (see Figure 24). Since the pressure drop across the jet was negligible at low plenum velocities the 3/8-in. felt was selected.

TURBULENCE MEASUREMENTS ON MODIFIED RIG

Measurements of turbulence intensities were repeated at the jet exit and in the plenum tank with the 3/8-in. felt in place. The exit turbulence was down to about 0.5 percent and the turbulence intensity in the plenum tank was reduced drastically to 0.6 percent. The axisymmetric contraction was therefore ineffective in reducing turbulence intensities significantly in this case. The probable cause was a sudden contraction between the plenum tank and the excitation adaptor (area ratio 1.5). The disturbance caused by this region was introducing additional turbulence into the flow. The measurements are compared with 'no felt' measurements in Table III.

RESONANCE CHARACTERISTICS OF MODIFIED RIG

The resonance characteristics of the modified rig were much like those of the original rig. They were expected to be different due to a change in the effective plenum length caused by the felt. The unchanged characteristics suggest that radial resonances could be predominating over axial resonances. These characteristics and a comparison are shown in Figure 25.

The pressure levels for the modified rig at the nozzle exit were about 5 dB higher. A probable explanation could be sound waves bouncing off the felt and back into the flow.

In addition to reducing turbulence levels at the exit and increasing sound levels the felt also muffled valve noise. This

increased the excitability of the jet, which was severely hindered by the valve system.

VALVE NOISE

The pressure in the plenum was regulated by an 8-in. butterfly valve bypassed by a 1.5-in. annin plug valve.

There were therefore many possible combinations of the butterfly and bypass valves to achieve a desired plenum pressure. It was observed that the background noise varied considerably depending on the combination selected. When this seemingly unimportant observation was followed up at a Mach number of 0.2 it was seen that the background sound pressure level varied by about 15 dB, 113 and 128 dB being extreme values . The structure and excitability of the jet was therefore quite different depending on the valve combination. Valve noise was at its minimum when the bypass was fully closed and only the main valve was open, and reached a maximum when the main valve was closed and the flow was regulated using the bypass.

Of course the bypass made more noise, because valve noise depends on the multiplicity of openings which were used to regulate the flow (more the number of ports, less is the valve noise), the total differential pressure across the valve, and the ratio of differential pressure to inlet pressure. All of these were unfavorable for the bypass valve. Understandably the velocity through the bypass opening was much higher than that through the butterfly valve. The power emitted by the flow is proportional to the 8th power of the velocity (Lighthill (1952)). The observations are therefore qualitatively consistent.

An indepth analysis was not attempted since valves were really not the focus of attention. An involved calculation could use Lighthill's theory for jets applied to confined flows and account for corrections required due to nonsymmetric throttling. Several empirical correlations are available in the literature (Hutchison (1976)). Standard handbooks on valves (Driskell (1983), Hutchison (1976)) suggest either source control or path control to reduce valve noise. For example the felt used to reduce turbulence intensities actually muffled some of the valve noise, and this constitutes path control.

Power spectra from the microphone which was mounted flush in the nozzle 0.25 in. from the exit show that the valve noise peak (590 Hz) was very close to the tone peak (550 Hz). At a Mach number of 0.2 this gave a Strouhal number of 0.5. Figures 26 to 31) show these spectra.

MEAN FLOW MEASUREMENTS

Measurements were made axially along the centerline at regular intervals up to X/D = 9, using hot wires. These measurements were made with and without excitation at a Mach number of 0.2, for both quiet and noisy valve positions. The velocity decayed faster for the noisy case (Figure 32) when no tone was applied. This difference was negligible when the tone was applied (Figure 33). For the quiet valve position (Figure 34) the difference between the excited and unexcited decay profiles was significant, the excited jet decaying faster than the unexcited one. For the noisy case the difference was not so significant since the unexcited case was already excited to some

degree by the valve system (Figure 35). Comparison of axial decay profiles with those obtained without the felt in the plenum tank showed that the decay was much slower with the felt in the plenum tank (Figure 36). The turbulence intensities for quiet and noisy valve positions with and without excitation are plotted in Figure 37).

Wygnanski and Fiedler (1969) reported mean velocities and turbulence intensities measured along the axis of the jet, using both X-wires and a single normal wire, in two separate tests. The RMS values of longitudinal fluctuations obtained with single wires were identical with those from the X-wires. The single wires used are thus assumed to provide valid RMS values of longitudinal fluctuations.

RADIAL VELOCITY PROFILES

Radial velocity profiles were measured using a Pitot probe at X/D = 0, 1, and 2 at Mach number of 0.2 (quiet and noisy valve positions) and 0.435. Excitation was at a Strouhal number of 0.5 and a level of 140 dB. The data is presented in Tables C-12(a-r) of Appendix C.

The jet was traversed radially at X/D = 9 with and without excitation at Mach number of 0.435 and 0.2 (quiet and noisy valve positions). The Strouhal number was kept at 0.5 and the sound level at 140 dB. The results are illustrated in Figures 38 to 40. Values of momentum thickness derived from the profiles are compared in Table II.

C. TEST RESULTS

THE STROUHAL NUMBER DEPENDENCE

A Pitot probe was positioned at X/D = 9 and frequencies were varied to yield Strouhal numbers from 0 to 1.6 at two different Mach numbers (0.435 and 0.2). The test was first conducted without maintaining constant sound levels and later at constant sound levels. There was a strong Strouhal number dependence which is illustrated in Figures 41 to 42.

Figure 43 is a plot of relative velocity versus Strouhal number. This shows a maximum supression in the mean velocity at a Strouhal number of 0.54 for a case when the Mach number was 0.2 at a constant sound level of 131 dB.

At a Mach number of 0.435 the supression was only half as much although the constant sound levels were raised to 133 dB. This however, did not come as a surprise as the jet dynamic head was now much higher (Figure 44). Figures 45 and 46 show the effect of the felt.

SOUND LEVEL EFFECTS

In order to observe a sound pressure level dependence, tests were performed with the Pitot probe at X/D = 9, keeping the frequency constant and varying the sound levels from the no tone level to about 140 dB. These tests were performed for three different valve positions and therefore three different turbulence levels at the nozzle exit. Threshold levels for excitation are therefore identifiable by looking at the plots of relative velocity versus sound pressure level for the three cases Figures 47 to 61.

Figures 47 and 48 are plots of relative velocity versus sound pressure levels at the nozzle exit for the case when the exit Mach number was 0.435. With increase in sound levels the effects of excitation became more pronounced, for example at a frequency of 1050 Hz the relative velocity was 1.0 at 110 dB, 0.985 at 120 dB, 0.96 at 130 dB and 0.86 at 140 dB. The region of maximum slope being between 130 and 140 dB. A strong frequency dependence is also noticed in Figures 47 and 48. As the frequency is stepped up from 550 Hz the slope of the sound pressure level curve increased, reaching a maximum at around 1050 Hz and then backtracing the earlier path with further increase in frequency. A reproducibility test was performed at 1300 Hz to check the reliability of the measurements (Figure 49).

Figure 50 shows plots for the case when the Mach number was 0.2 (quiet valve). At the starting frequency (450 Hz) the slope of the sound pressure level curve is already high as this frequency was in the sensitive Strouhal number range. At a sound pressure level of 137 dB the relative velocity was supressed to 0.86 at 550 Hz. After 700 Hz the prominence of the slopes is diminished. At frequencies higher than 1150 Hz mixing is supressed , or the slopes increase in the opposite direction.

Figures 51 to 61 are results of the noisy valve test at a Mach number of 0.2. The trends are not as clear as those of the other two cases, though very distinctly, excitation at almost all frequencies supresses turbulent mixing (quite reverse as compared to the quiet valve case). Also as background sound levels are higher, very little effect is observed at sound levels less than 130 dB. Threshold levels

are thus much higher, however the maximum effect is observed at 550 Hz (same as quiet valve case). The noisy valve data is provided merely for the sake of completeness. Since this test was disturbed by extraneous noise a detailed analysis could only result in erroneous conclusions.

Itemized tabulated data is provided in Appendix B to aid in a detailed analysis of plotted data. For example the tabulated data indicate fluctuations in the plenum tank pressure, changes in valve positions and other information which could not be incorporated in the plots.

SPECTRAL ANALYSIS

Results of hot-wire measurements along the centerline are shown in Figures 62 to 107. These include microphone power spectra, hot-wire power spectra, coherence and transfer functions for both the noisy and quiet valve positions at Mach number 0.2. The excitation frequency was 550 Hz at a sound pressure level of 140 dB. The Strouhal number based on the jet exit diameter was 0.5. Figures 62 to 67 are provided for qualitative comparison. Details are in Figures 68 to 87 for the quiet case and in Figures 88 to 107 for the noisy case.

For the quiet case the hot-wire spectrum showed a subharmonic growth at $X/D = 1.9$ which peaked around $X/D = 3.3$. Several authors have shown that the location at which the subharmonic peaks is the location at which vortex pairing culminates (Zaman and Hussain (1981)). A probable explanation would be that the forcing raises the large scale structures above the background random turbulence levels in the vicinity of the forcing frequency. The hot-wire spectrum

therefore shows a peak at the forcing frequency because one measures a vortical frequency which is close to the forcing frequency. When pairing commences, the subharmonic grows and the fundamental peak decays indicating that the vortical frequency has halved or that two vortices merge into one at some point along the vortical wavetrain.

At $X/D = 6$ and 7.6 the background turbulence grows and the peaks are not visible anymore. This is the second step in the acoustic excitation phenomenon as explained by Ahuja et al. (1982): the link between the large scale structures and the fine scale turbulence. At $X/D = 9$ the subharmonic is noticed to grow again.

Coherence between the microphone at the nozzle exit and the hot wire is noted to be very high, almost equal to 1, near the fundamental at $X/D = 1.9$ and is slightly less at $X/D = 3.3$. For $X/D \geq 6.2$ the coherence is extremely low indicating a very weak link between the excitation and the hot-wire signal. At $X/D = 9$ the coherence grows again.

The transfer function was noticed to be growing at $X/D = 1.9$ and peaked around $X/D = 3.3$. Subsequently it was extremely low and a slight growth was detected at $X/D = 9$.

For the noisy case the trends were similar and yet different from the quiet case. The hot-wire spectrum showed a broader subharmonic at $X/D = 1.9$. Pairing was complete even before $X/D = 3.3$ where the peak was barely visible at the fundamental frequency. The broader subharmonic could indicate that a 'collective interaction' of vortices could be occurring (Ho and Huang (1982)) or that the jet may be excited at other modes. The exit boundary layer could be different

for the noisy case and Hussain and Zaman (1981) have shown that in such a case vortex pairing is intermittent in space and time. Background turbulence levels are always higher in the noisy case as compared to the quiet case, although there is little difference at $X/D \geq 6.2$.

The coherence shows little change at $X/D = 1.9$ whereas at $X/D = 3.3$ it drops to 0.5 versus 0.8 for the quiet case.

The transfer function for the noisy case peaks at 900 Hz at $X/D = 1.9$. The peak visible at 550 Hz at this location grows to a maximum at $X/D = 3.3$ and decays to near zero values for $X/D \geq 6.2$.

CHAPTER VI

APPLICABILITY

JET EJECTORS:

The jet ejector is used in the chemical industry to produce low pressures. Its principle of operation involves fluid being entrained in a high velocity stream of a second fluid.

Enhanced mixing by acoustic excitation can improve ejector performance considerably. This application is a direct outcome of the analogy between the velocity fields in the ejector and in a free jet. Abramovich (1963) explains this as an obvious similarity due to the universality of the effective laws of turbulent mixing.

Figure 108 shows this similarity. The velocity field at each of the cross-sections of the ejector chamber appears like the velocity field at corresponding cross sections of the central part of a free jet bounded by the walls of the chamber. The extension of acoustically controlled jets to jet ejectors is therefore straightforward.

THE COMBUSTION CHAMBER:

Another example of enhanced mixing dependency is the combustion chamber. The entrainment of hot furnace gases by a jet in a combustion chamber heated by secondary air is responsible for a fuel-air jet increasing in temperature and thereby igniting. This ignition process is essentially complete within a few diameters from the nozzle and hence control of jet characteristics in the initial region is useful.

Subsequent to ignition the flame structure and the overall rate of combustion in a jet flame are determined by the mixing of the reactants and the hot combustion products. This is because the rate of chemical reaction is very high at flame temperatures compared to the rate of mixing, and is therefore negligible.

In the third step a better mixing of the hot combustion products and the diluting air ensures lower pollutant concentrations.

The advantages of acoustic excitation in combustion are therefore manifold. Fine control over a turbulent jet is useful for earlier ignition, combustion instability supression and pollution minimization.

HEAT EXCHANGER:

The characteristics of flow past a tube bundle in a heat exchanger determines the heat transfer effectiveness. Slots formed by the first column of tubes cause the airflow through them to resemble turbulent jets. These jets spread as they are propagated between columns. Air from the regions located behind the tubes is entrained by the main core of the jet. The heat exchanger is therefore an orderly arrangement of jets and closed recirculation zones.

Low frequency acoustic excitation would cause the jet cross sections to be wider, reducing the closed circulation zones to a minimum. In this fashion the effective area for heat transfer is increased considerably. Figure 109 shows this schematically.

FLOW OVER AN AIRFOIL:

Acoustic excitation can influence flow over an airfoil considerably. Ahuja et al. (1982) showed that separated flow over an airfoil reattaches with excitation at a Strouhal number equal to 4 (based on the wing chord).

Flow separation is a cause for concern as it could cause a loss of lift or stall in aircraft. The acoustic excitation energizes the boundary layer and helps in overcoming the adverse pressure gradients which cause separation.

POTENTIAL AEROSPACE APPLICATIONS:

Several potential applications have been explained by Stone and Mckinzie (1984). These include supersonic jet noise reduction, reducing V/STOL (Vertical and Short Take off and Landing) and STOVL (Short Take Off and Vertical Landing) ground effects, internal mixers, separation control, stall prevention/recovery, enhanced maneuverability for fighter aircraft, skin friction reduction and impingement control.

CHAPTER VII

SUMMARY AND CONCLUSIONS

(1) The present work examined some effects of upstream excitation on an axisymmetric jet.

(2) Preliminary evaluation of the jet facility included turbulence measurements at the nozzle exit, plenum tank and along the axis using a single hot-wire probe. Radial velocity profiles were measured using a Pitot probe and the resonance characteristics of the rig were studied using a microphone at the nozzle exit.

(3) Following this preliminary study the facility was modified by inserting a 3/8-in. thick felt in the plenum tank. The felt reduced turbulence intensities in the tank and at the nozzle exit, muffled valve noise, increased sound pressure levels when a tone was applied and also increased the length of the potential core. Though the excitability of the jet was enhanced significantly the resonance characteristics of the rig were essentially unchanged.

(4) The test plan consisted of measurements at $X/D = 9$ using a Pitot probe at Mach number of 0.435 and 0.2 (quiet and noisy valve conditions), at various sound pressure levels and frequencies. Single

hot-wire measurements were made at regular axial stations along the centerline.

(5) Tests performed at a constant frequency helped identify threshold sound pressure levels for excitation and its dependence on exit turbulence intensities. The effects of excitation became more apparent with increasing sound levels, though the slopes depended considerably on the frequency and exit turbulence levels.

(6) The dimensionless Strouhal number was seen to play a key role in the the excitation process. Constant sound level tests clearly indicated a range between 0.4 and 1.0 where acoustic excitation enhanced mixing. Other factors which influenced the excitability were background noise, exit boundary layer conditions, Mach number and exit turbulence levels.

(7) Valve noise was a reason for concern as the effects of tone excitation varied considerably with valve positions. In addition to valve noise, extraneous noise from a nearby facility acted as a source of external excitation and disturbed some of the measurements. Also the flanged nozzle affected jet development in the initial region.

(8) Signal analysis of single hot-wire measurements showed vortex pairing (the mechanism for mixing layer growth in the initial region) to occur between $X/D = 2$ and 3 and this occurred earlier for the noisy valve condition.

(9) The phenomenon of acoustic excitation has its applications in mixing devices, a host of aerospace applications and in jet noise studies. In addition the excitation mechanism provides an insight into the intricacies of subsonic shear layer dynamics.

(10) The data and analysis presented here could be used as a starting point for structuring a more complete research plan. Some suggestions for future work are made in the next section.

CHAPTER VIII

SUGGESTIONS FOR FUTURE WORK

Deficiencies in the present work are outlined and some suggestions to overcome these are made in this section.

In the present work, mean jet characteristics, spreading rate, potential core length, valve noise, excitability, Strouhal number dependence and sound pressure level effects are addressed, though with a limited knowledge of the nozzle exit boundary layer.

Turbulence measurements with a single hot-wire probe proved simple both in operation and analysis but limited the measurements to a single velocity component.

Inherent deficiencies in the system included high turbulence at the nozzle exit, insufficient sound levels at certain frequencies, valve noise interference, extraneous noise, pressure transducer limitations, a flanged nozzle and a sudden contraction between the plenum tank and the excitation adaptor.

As a first step towards resolving these problems a piece of felt was inserted in the plenum tank during the course of this work.

Introducing more felt in the tank and at the sudden contraction near the excitation adaptor could reduce turbulence intensities further.

Replacing the flanged nozzle by a regular nozzle would take the improvement program a step further. Due to the presence of standing waves in the nozzle the location at which sound pressure levels are measured is critical. An indepth study of standing waves in the nozzle followed by calibration of an external microphone with respect to a microphone at the nozzle exit may provide enhanced universality and reproducibility of measurements.

If the above are accomplished, a knowledge of exit velocity and shear layer profiles would then be invaluable as they would lend new meaning to the subsequent measurements. To accomplish these a two transducer capability is being developed. When the Pitot probe nears the edge of the jet the computer would actuate a valve which would switch to a more sensitive transducer.

Finally extensive mapping using cross wires would provide comprehensive data and a phenomenological insight into the excitation process. Currently an effort is underway to develop the cross-wire capability along with the possibility of using hot films where breakage of hot wires prevents their use.

The new computer controlled three axis probe positioner would take automation to a new dimension when properly utilized in conjunction with the present data acquisition system and the new HP 9836 computer.

In the long run a quiet valve system, a smooth contraction between the plenum tank and the excitation adaptor, data transmittal to the main frame computer for desktop data acquisition systems and a

schlieren system for flow visualization studies would aid in the quest for improvement.

REFERENCES

Abramovich, G.N., "The Theory of Turbulent Jets," MIT press, (1963).

Acton,E., "A Modeling of Large Eddies in an Axisymmetric Jet," J.Fluid Mech., 98, pp. 1-31, (1980).

Ahuja, K.K., J. Lepicovsky, C.K.W. Tam, P.J. Morris, and R.H.Burrin, "Tone-Excited Jet, Theory and Experiments," NASA contractor report 3538, (1982).

Armstrong, R.R., "Influence of Mach Number on Coherent Structure Relevant to Jet Noise," AIAA J., 19, pp. 677-683 (1981).

Boussinesq, J., Mem. Pres. par. div. Savants acad. Sci., Paris, 23, 46 (1877) (through Abramovich (1963)).

Gortler, H., "berechnung Von Aufgaben der freven turbulenz auf grund eines neuen Naherungsansatzes," ZAMM, 22, 5, (1942) (through Abramovich (1963).

Crighton, D.G., "Acoustics as a Branch of Fluid Mechanics," J. Fluid Mech., 106, pp. 261-298 (1980).

Crow, S.C. and F.H. Champagne, "Orderly Structure in Jet Turbulence," J. Fluid Mech., 48, pp. 547-591, (1971).

Driskell, L., "Control-Valve Selection and Sizing," Instrument Society of America (1983).

Freymuth P., "On Transition in a Separated Laminar Boundary Layer," J. Fluid Mech., 25, pp. 683-704 (1966).

Heavens, S.N., "Visualization of the Acoustic Excitation of a Subsonic Jet," J. Fluid Mech., 100, pp. 185-192 (1980).

Ho, C.M. and L.S. Huang, "Subharmonics and Vortex Merging in Mixing Layers," J. Fluid Mech., 119, pp. 443-473 (1982).

Hussain, A.K.M.F. and K.B.M.Q. Zaman, "The Preferred Mode of the Axisymmetric Jet," J. Fluid Mech., 110, pp. 39-71 (1981).

Hussain, A.K.M.F., "Coherent Structures - Reality and Myth," Phys. Fluids, 26, pp. 2816-2850 (1983).

Hutchison, J.W., "ISA Handbook of Control Valves," 2nd Ed., Instrument Society of America (1976).

Leconte, J., "On the Influence of Musical Sounds on the Flame of a Jet of Coal-Gas," Phil. Mag., 15, pp. 235-239 (1858).

Lighthill, M.J., "On Sound Generated Aerodynamically - I. General Theory," Proc. of Royal Soc., A211, pp. 564-587 (1951).

Michalke, A., "On Spatially Growing Disturbances in an Inviscid Shear Layer," J. Fluid Mech., 23, pp. 521-544 (1965).

Michalke, A., "Survey on Jet Instability Theory," Prog. Aerospace Sci., 21, pp. 159-199, (1984).

Moore, C.J., "The Role of Shear-Layer Instability Waves in Jet Exhaust Noise," J.Fluid Mech., 80, pp. 321-367 (1977).

Prandtl, L., "Zur turbulenten Stomung in Rohren und langs platten," Ergeb AVA Gottingen IV, Lfg. 18-29 (1932) (through Abramovich (1963)).

Rayleigh, J.W.S., "Theory of Sound, 2 Vols., Macmillan (1896).

Reichardt (1951) (through Abramovich).

Shinichi Isuge', "Effects of flow Contraction on Evolution of Turbulence," Phys. Fluids, 27, pp. 1948-1956 (1984).

Stone, J.R. and Mckinzie, J.M., "Acoustic Excitation - A Promising New Means of Controlling Shear Layers," NASA TM-83772 (1984).

Tam, C.K.W., "Excitation of Instability Waves in a Two-Dimensional Shear Layer by Sound," J.Fluid Mech., 89, pp. 357-371 (1978).

Tan-Atichat, J., "Effects of Axisymmetric Contraction on Turbulence of Various Scales," Masters Thesis, Mech. and Aerospace Dept., III Chicago (1980).

Taylor, G.I., "Diffusion by Continuous Movements," Proc. London Math. Soc., 20, Ser., 2, 196 (1921) (through Abramovich (1963)).

Vlasov, E.V. and A.S. Ginevskii, "The Aeroacoustic Interaction Problem (review)," Sov. Phys. Acoust, 26, pp. 1-7 (1980).

Winant, C.D. and F.K. Browand, "Vortex Pairing: The Mechanism of Turbulent Mixing Layer Growth at Moderate Reynolds Number," J. Fluid Mech., 63, pp. 237-255 (1974).

Wygnanski, I., and H. Fiedler, "Some Measurements in a Self-Preserving Jet," J. Fluid Mech., 38, pp. 577-612 (1969).

Zaman, K.B.M.Q., and A.K.M.F. Hussain, "Vortex Pairing in a Circular Jet under Controlled Excitation, General Jet Response," J. Fluid Mech., Vol. 101, pp. 449-491 (1980).

Zaman, K.B.M.Q. and A.K.M.F. Hussain, "Turbulence Supression in Free Shear flows by controlled Excitation," J. Fluid Mech., 103, pp. 133-159 (1981).

TABLE (I-A). - CONSTANT SOUND LEVEL TEST

[Fluctuating pressure level = 140 dB re 20 μPa; X/D = 9; jet exit Mach number = 0.4; plenum pressure = 1.688 psi; leading hot wire.]

Frequency, Hz	Strouhal number	Mean velocity, ft/sec	Fluctuating velocity, ft/sec	Turbulence intensity,
910	0.493	199.79	132.20	0.6617
1040	.564	199.79	129.73	.6493
1510	.819	190.22	128.38	.6749
1580	.856	209.57	140.39	.6699
2510	1.361	199.79	129.35	.6474

TABLE (1-B). - CONSTANT SOUND LEVEL TEST

[Fluctuating pressure level = 140 dB; X/D = 9; jet exit Mach number = 0.4; plenum pressure = 1.688 psi; trailing hot wire.]

Frequency, Hz	Strouhal number	Mean velocity, ft/sec	Fluctuating velocity, ft/sec	Turbulence intensity
910	0.493	185.53	75.33	0.4060
1040	.564	185.53	78.85	.4250
1510	.819	177.10	78.85	.4452
1580	.856	179.47	78.81	.4467
2510	1.361	185.53	78.77	.4246

TABLE (I-C). - CONSTANT SOUND LEVEL TEST

[Fluctuating pressure level = 140 dB; X/D = 4.75; jet exit Mach number = 0.4; plenum pressure = 1.688 psi.]

Frequency, Hz	Strouhal number	Mean velocity, ft/sec	Fluctuating velocity, ft/sec	Turbulence intensity
910	0.493	260.75	145.49	0.5580
1040	.564	260.75	152.55	.5850
1510	.819	259.77	150.58	.5796
1580	.856	265.85	155.36	.5844
2510	1.361	260.75	146.59	.5622

TABLE (1-E). - CONSTANT SOUND LEVEL TEST

[Fluctuating pressure level = 140 dB; X/D = 1.90; jet exit Mach number = 0.4; plenum pressure = 1.690 psi.]

Frequency, Hz	Strouhal number	Mean velocity, ft/sec	Fluctuating velocity, ft/sec	Turbulence intensity
910	0.493	270.48	147.81	0.5465
1040	.564	270.48	154.00	.5693
1510	.819	257.85	153.05	.5936
1580	.856	276.59	154.35	.5580
2510	1.361	270.48	142.72	.5276

TABLE (I-D). - CONSTANT SOUND LEVEL TEST

[Fluctuating pressure level = 140 dB; X/D = 6.20; jet exit Mach number = 0.4; plenum pressure = 1.688 psi.]

Frequency, Hz	Strouhal number	Mean velocity, ft/sec	Fluctuating velocity, ft/sec	Turbulence intensity
910	0.493	252.26	149.59	0.5930
1040	.564	252.26	150.52	.5967
1510	.819	246.43	151.21	.6136
1580	.856	232.13	140.32	.6045
2510	1.361	252.26	144.48	.5727

TABLE II. - MOMENTUM THICKNESS

Axial location, X/D	With felt (unexcited)			With felt (excited)			Without felt (unexcited)		
	b	δ	θ, cm (in.)	b	δ	θ, cm (in.)	b	δ	θ, cm (in.)
Mach number = 0.435									
0	8	1.08	0.149 (0.059)	8	1.08	0.149 (0.059)	-----	----	-------
1	3.125	1.13	0.396 (0.156)	3.125	1.13	0.396 (0.156)	4.16	1.40	0.371 (0.146)
2	1.78	1.15	0.701 (0.276)	1.78	1.15	0.701 (0.276)	2.083	1.42	0.711 (0.280)
Mach number = 0.2 (quiet valve setting)									
0	8.33	1.07	0.139 (0.055)	8.33	1.07	0.139 (0.055)	-----	----	-------
1	3.57	1.07	0.333 (0.131)	2.5	1.07	0.472 (0.186)	-----	----	-------
2	1.56	1.2	0.815 (0.321)	1.56	1.15	0.789 (0.311)	-----	----	-------
Mach number = 0.2 (noisy valve setting)									
0	8.33	1.10	0.149 (0.059)	8.33	1.10	0.149 (0.059)	-----	----	-------
1	2	1.0	0.531 (0.209)	2.5	1.15	0.508 (0.200)	3.57	1.25	0.388 (0.153)
2	1.56	1.3	0.853 (0.336)	1.56	1.3	0.853 (0.336)	1.785	1.45	0.805 (0.317)

TABLE III. - TURBULENCE INTENSITIES AT NOZZLE EXIT

[September 1985; thickness of felt = 3/8 in.; nozzle diameter = 3.5 in.]

Tank ΔP	Exit Mach number	Turbulence intensity	
		Without felt	With felt
0.1	0.1	1.07	0.6548
.2	.14	1.4847	.951
.3	.175	1.3716	.7494
.4	.2	0.8045	.39939
.5	.223	0.7839	.4394

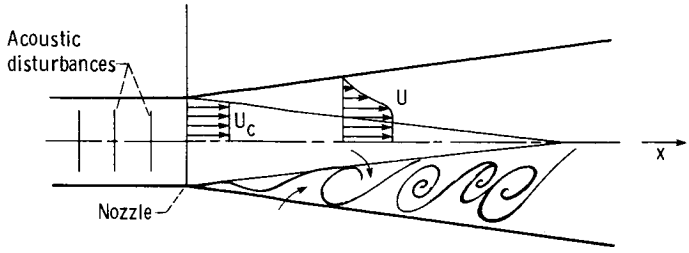

Figure 1. - Schematic diagram of an excited jet shear layer.

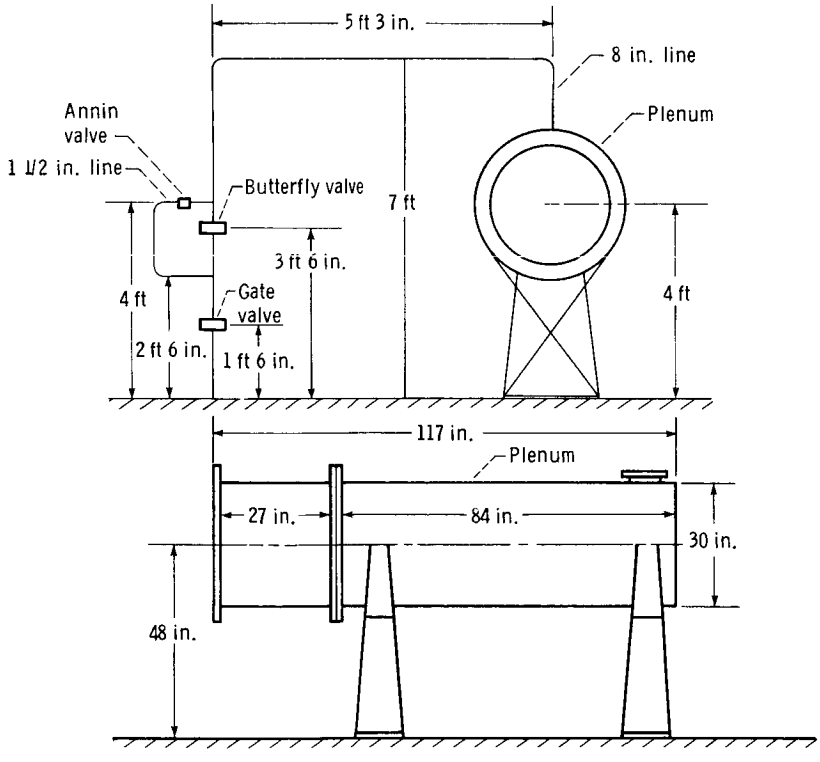

Figure 2. - Schematic drawing of plenum and valve system.

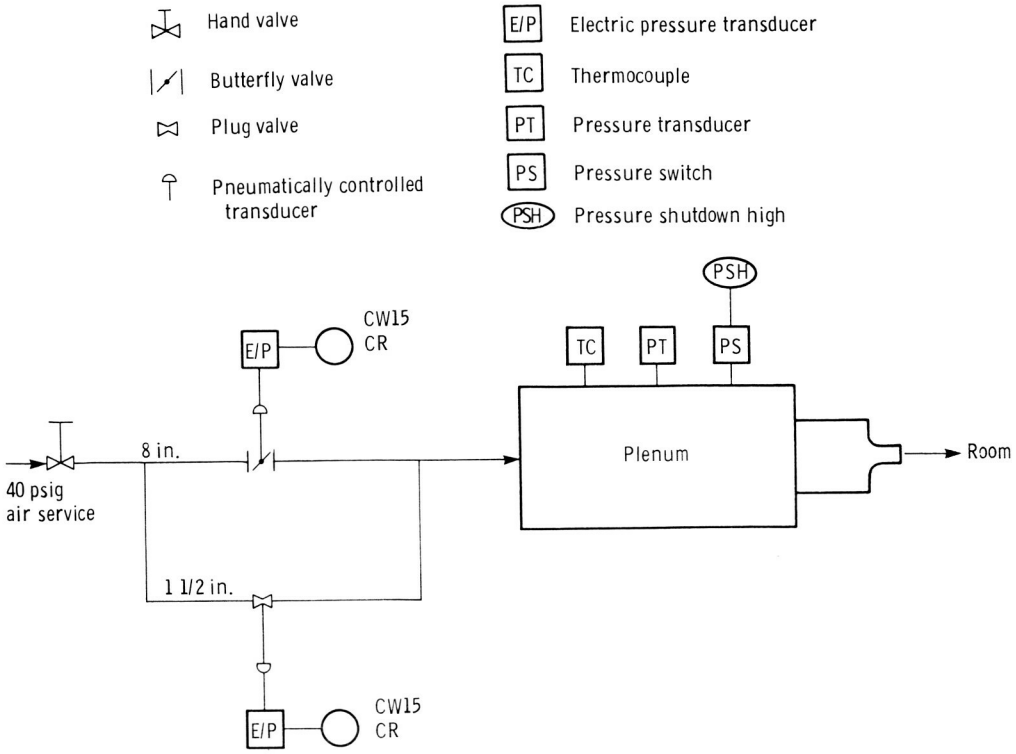

Figure 3. - Schematic representation of air system.

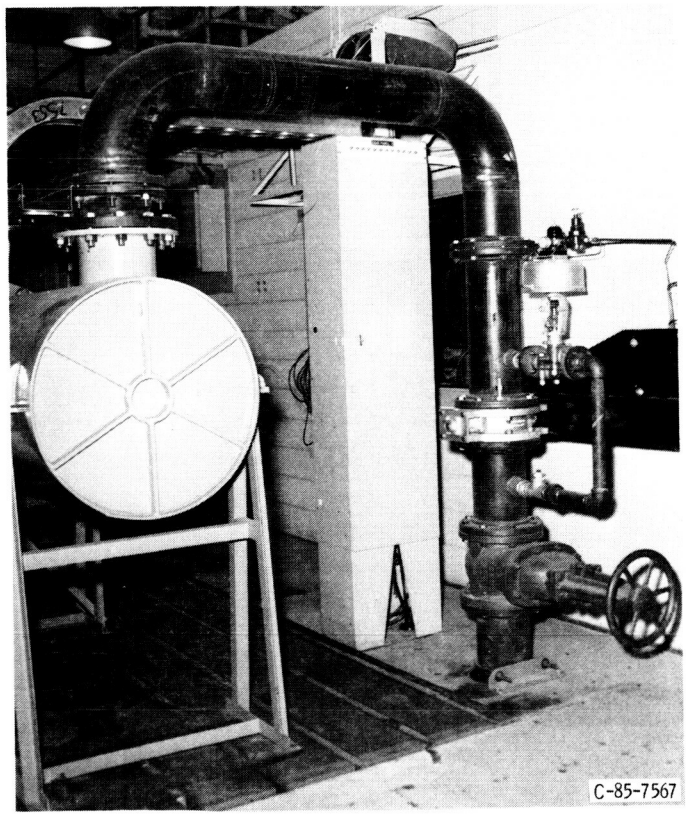

Figure 4. - Plenum and valve system.

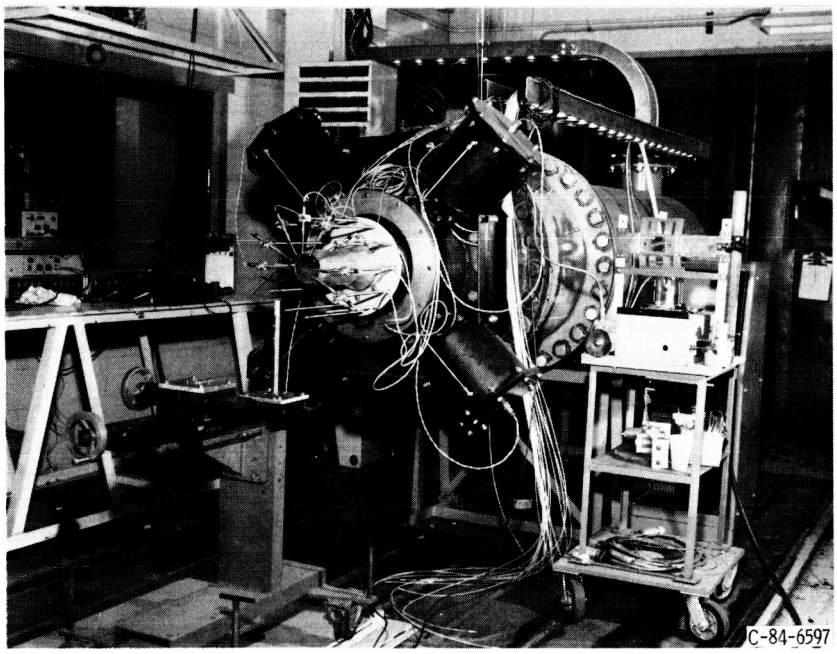

Figure 5. - The axisymmetric jet facility.

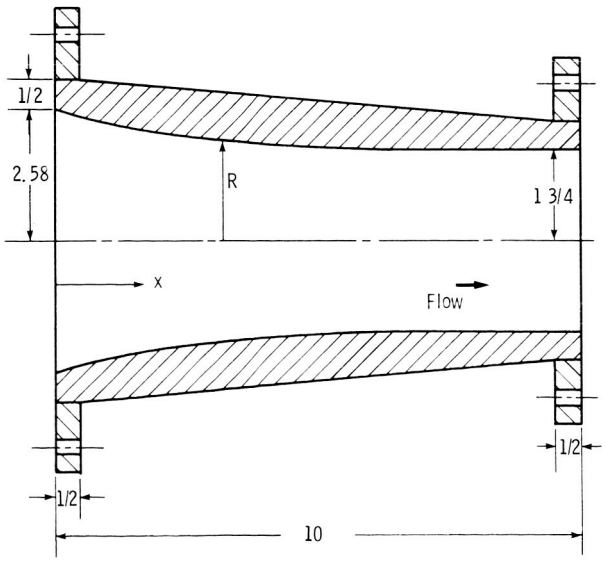

Figure 6. - Details of flanged nozzle. (All dimensions in inches.)

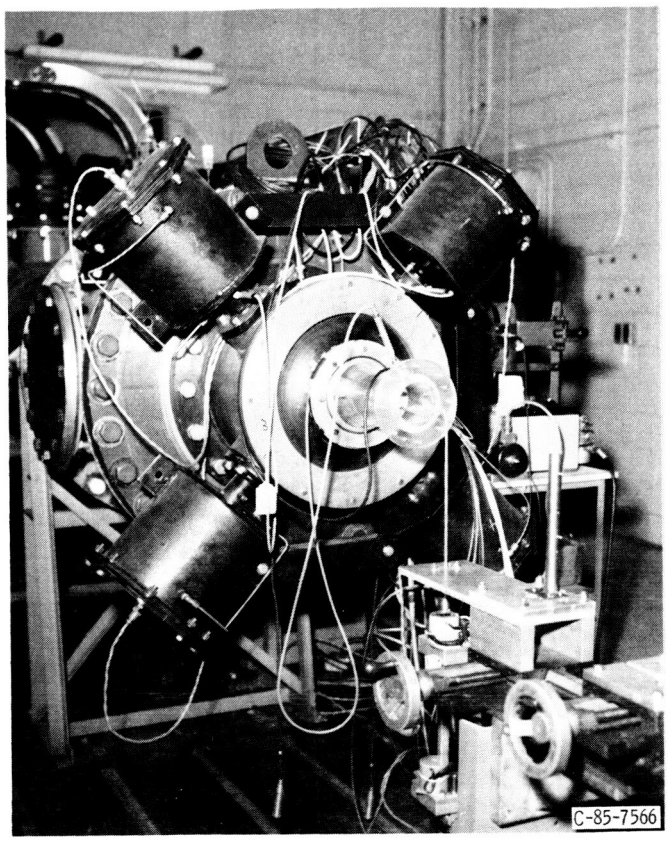

Figure 7. - The jet facility and traversing mechanism.

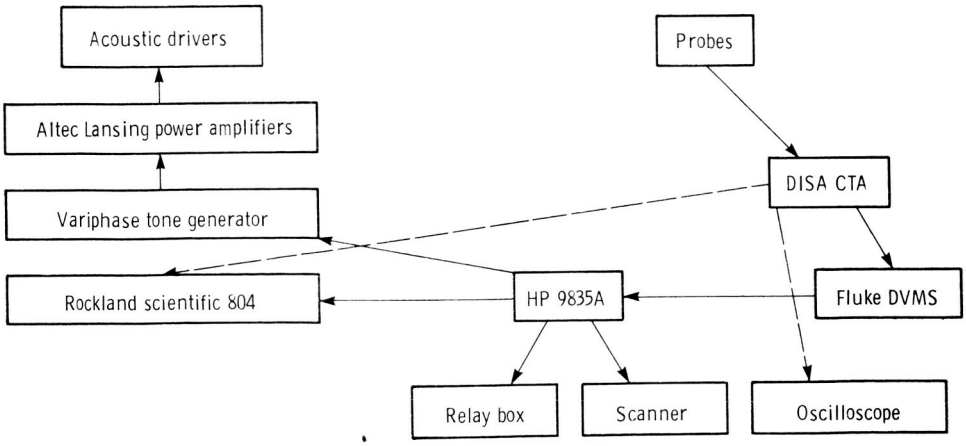

Figure 8. - Schematic representation of the data acquisition system.

Figure 9. - Data acquisition system.

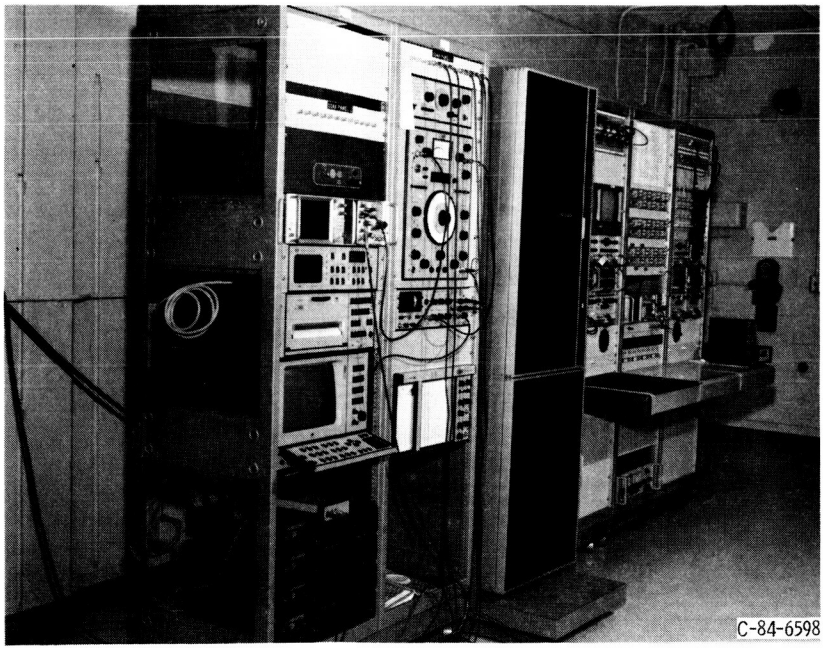

Figure 10. - The constant temperature anenometer set-up.

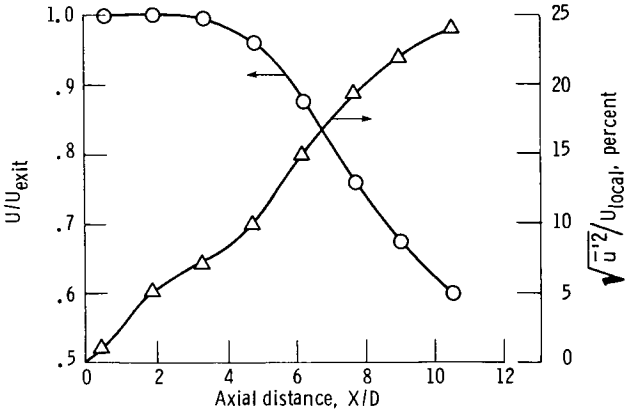

Figure 11. - Variation of mean velocity and turbulence intensity along jet axis measured with single hot wire (M = 0.1).

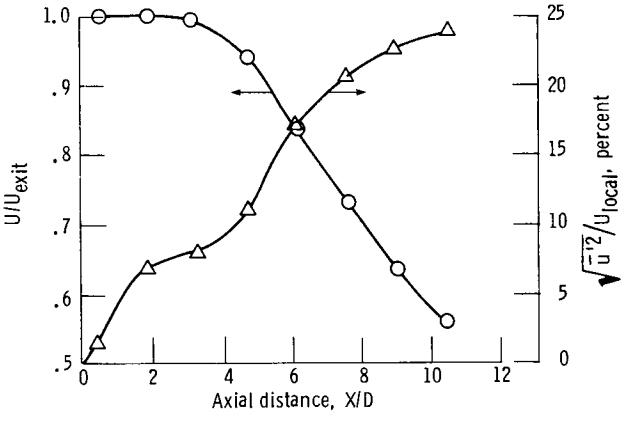

Figure 12. - Variation of mean velocity and turbulence intensity along jet axis measured with single hot wire (M = 0.141).

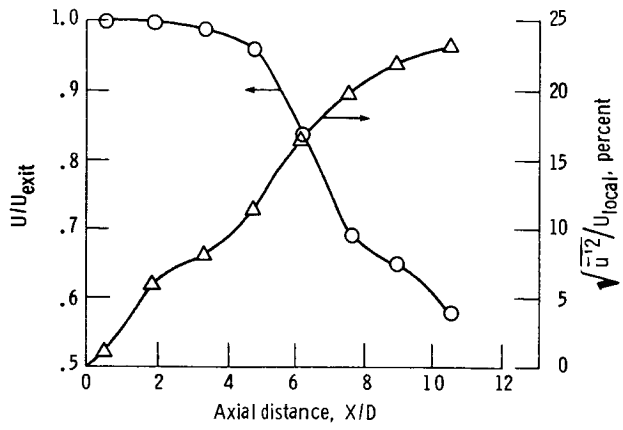

Figure 13. - Variation of axial velocity and turbulence intensity along jet axis measured with single hot wire (M = 0.173).

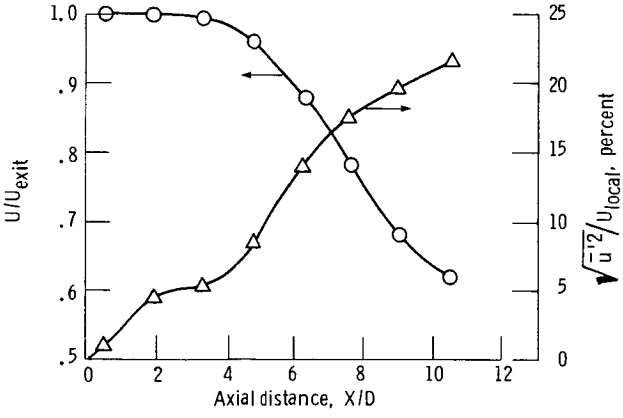

Figure 14. - Variation of axial velocity and turbulence intensity along jet axis measured with single hot wire (M = 0.199).

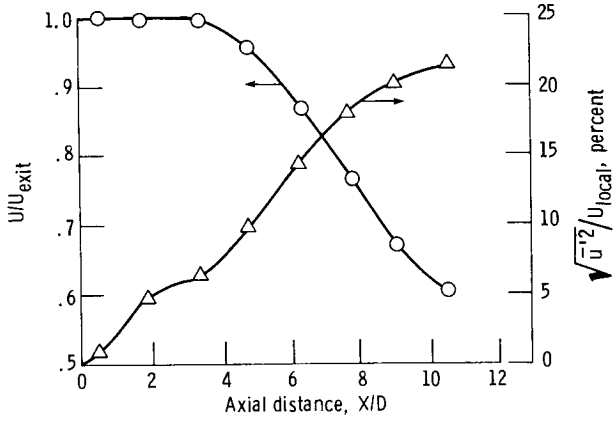

Figure 15. - Variation of axial velocity and turbulence intensity along jet axis measured with single hot wire (M = 0.22).

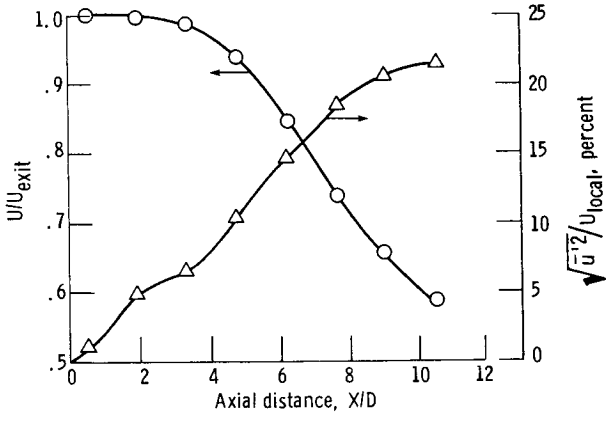

Figure 16. - Variation of axial velocity and turbulence intensity along jet axis measured with single hot wire (M = 0.28).

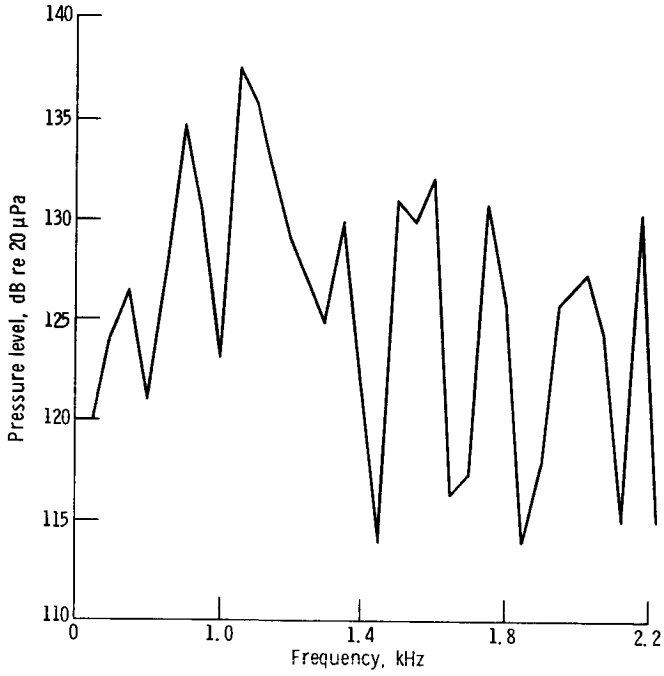

Figure 17. - Resonance characteristics of original rig without airflow.

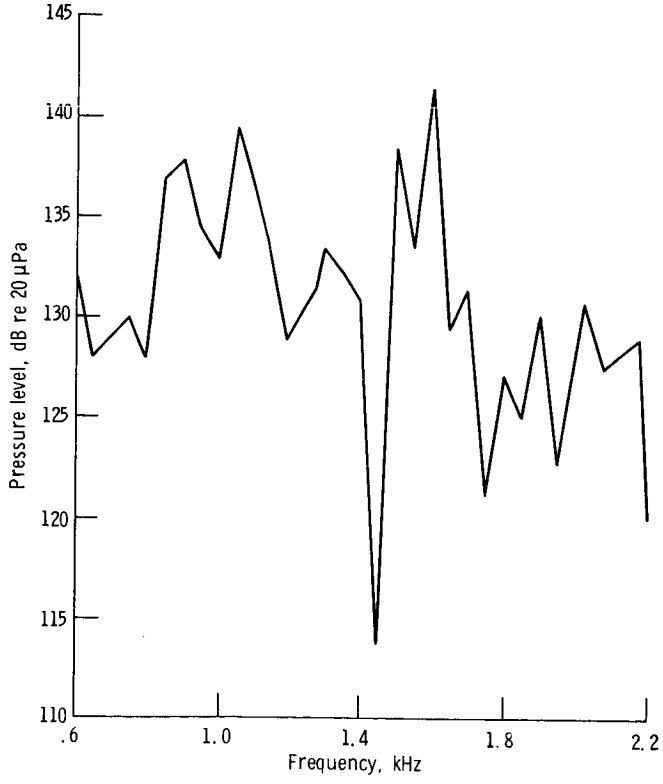

Figure 18. - Resonance characteristics of original rig with airflow (M_1 = 0.3).

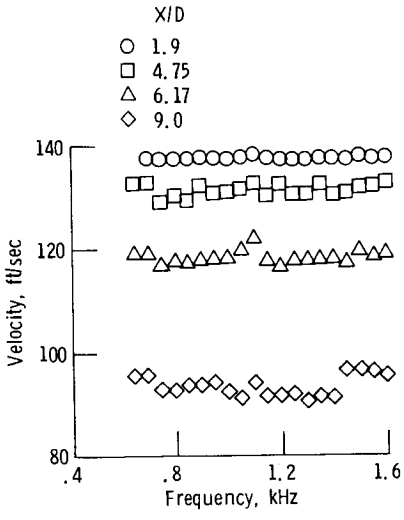

Figure 19. - Variation of mean velocity with frequency at X/D = 1.9, 4.75, 6.17, and 9.0 along jet axis (M = 0.1).

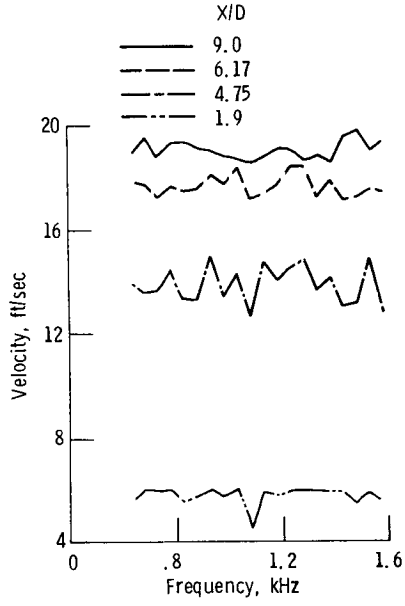

Figure 20. - Variation of rms velocity with frequency at X/D = 1.9, 4.75, 6.17, and 9.0 along jet axis (M = 0.1).

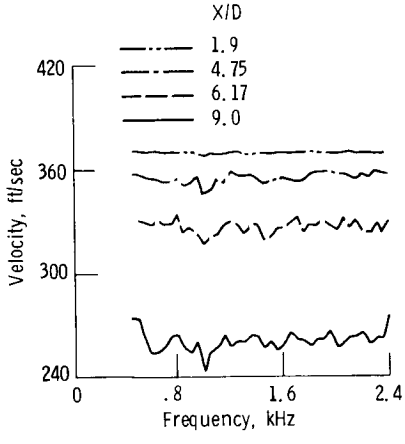

Figure 21. - Variation of mean velocity with frequency at X/D = 1.9, 4.75, 6.17, and 9.0 along jet axis (M = 0.3).

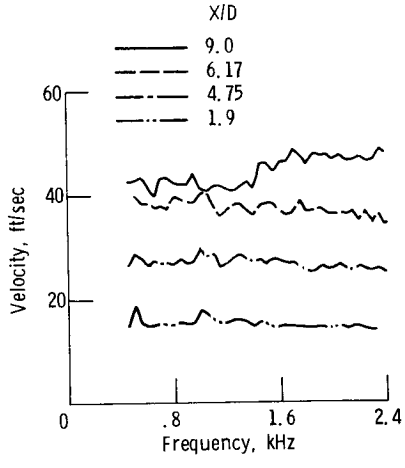

Figure 22. - Variation of rms velocity with frequency at X/D = 1.9, 4.75, 6.17, and 9.0 along jet axis (M = 0.3).

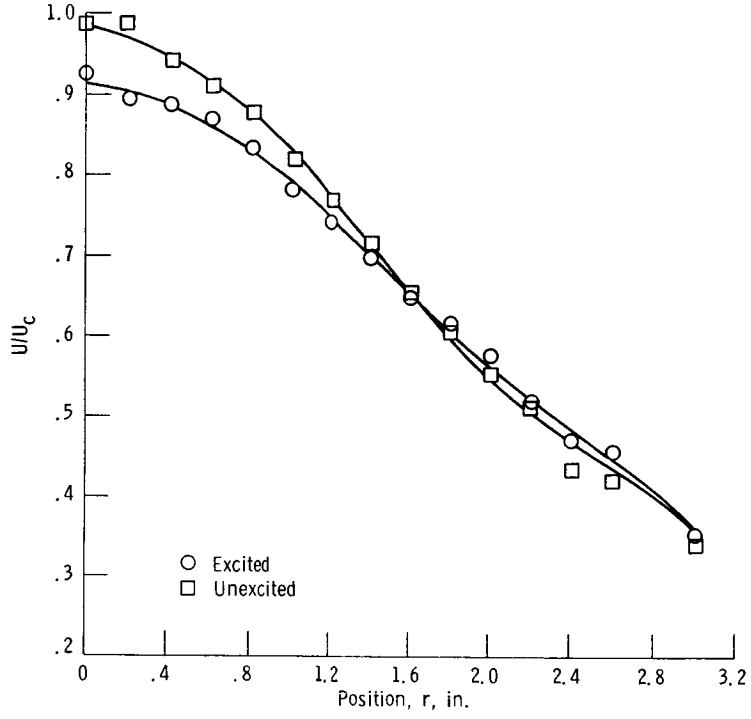

Figure 23. - Effect of excitation on radial variation of mean velocity at X/D = 9 (M = 0.45). Excitation level, 135 dB re 20 μPa; excitation frequency, 1590 Hz.

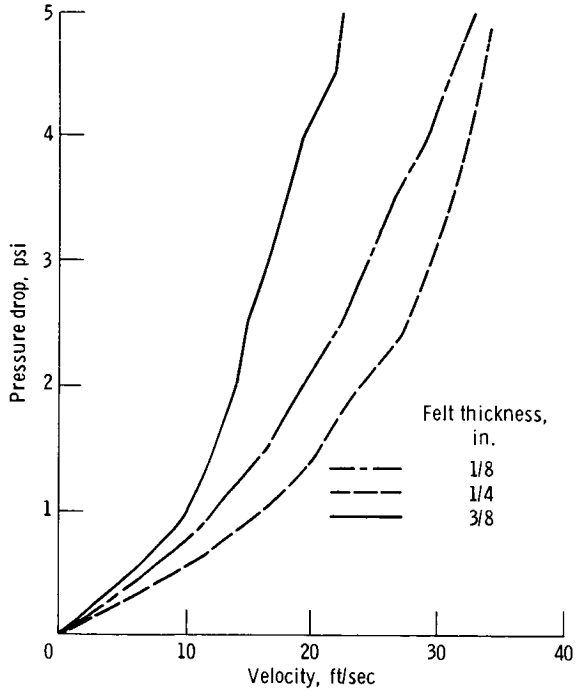

Figure 24. - Pressure drop variation with velocity.

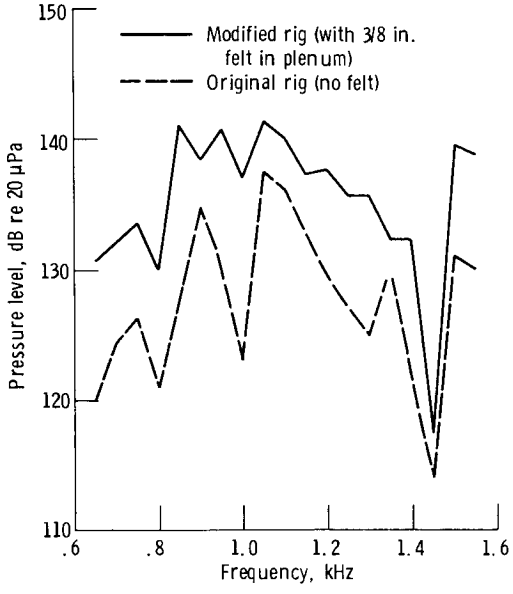

Figure 25. - Comparison of resonance characteristics of jet facility without airflow.

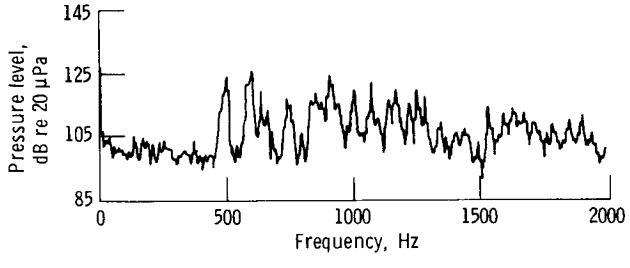

Figure 26. - Pressure spectrum at nozzle exit with no tone applied (M = 0.2, noisy valve).

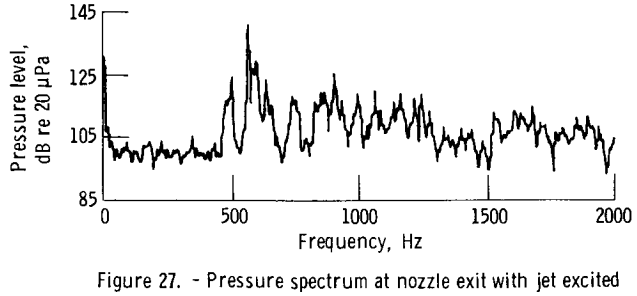

Figure 27. - Pressure spectrum at nozzle exit with jet excited at 550 Hz (M = 0.2, noisy valve).

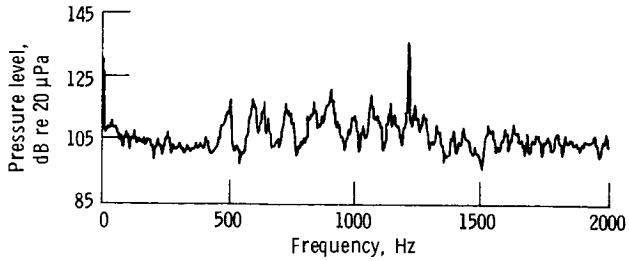

Figure 28. - Pressure spectrum at nozzle exit with no tone applied (M = 0.435).

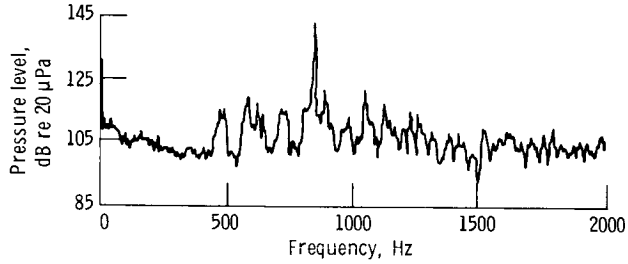

Figure 29. - Pressure spectrum at nozzle exit with jet excited at 850 Hz (M = 0.435).

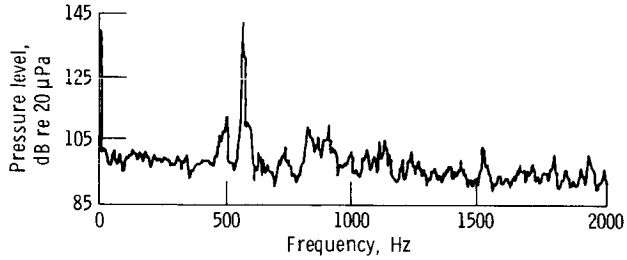

Figure 30. - Pressure spectrum at nozzle exit with jet excited at 550 Hz (M = 0.2, quiet valve).

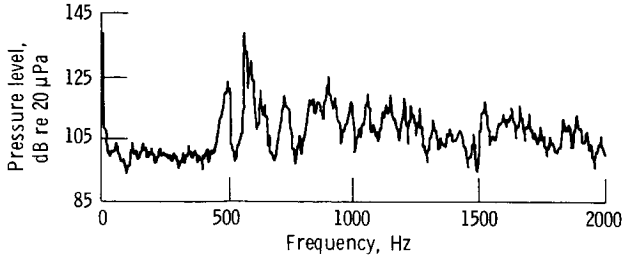

Figure 31. - Pressure spectrum at nozzle exit with jet excited at 550 Hz (M = 0.2, noisy valve).

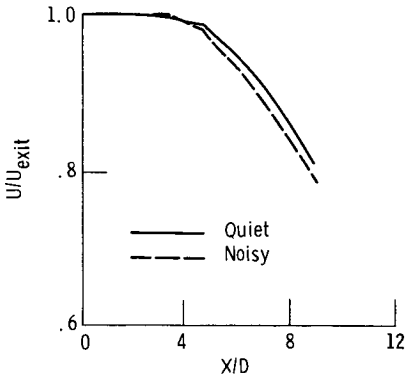

Figure 32. - Effect of valve settings on centerline mean velocity distribution (M = 0.2).

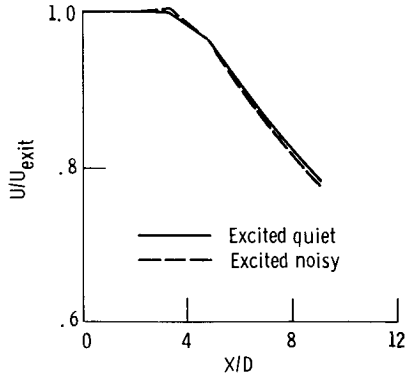

Figure 33. - Effect of valve settings on centerline mean velocity distribution with jet excited at 550 Hz tone (M = 0.2, excitation level = 140 dB re 20 μPa).

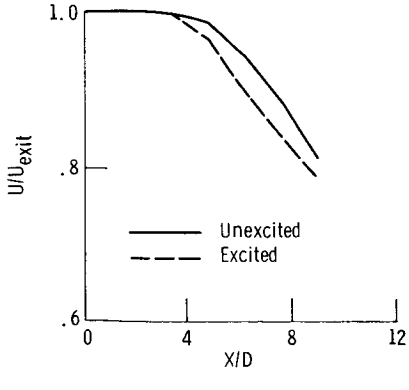

Figure 34. - Effect of excitation on centerline mean velocity distribution (M = 0.2, quiet valve) with jet excited at 550 Hz and a level of 140 dB re 20 μPa.

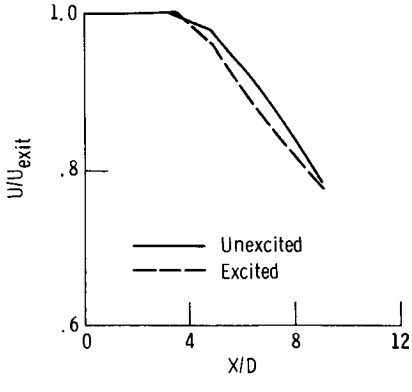

Figure 35. - Effect of excitation on centerline mean velocity distribution (M = 0.2, noisy valve) with jet excited at 550 Hz and a level of 140 dB re 20 μPa.

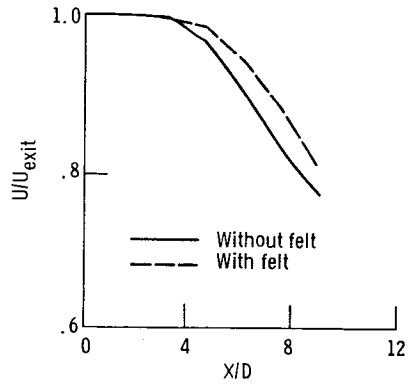

Figure 36. - Effect of felt on centerline mean velocity distribution (M = 0.2).

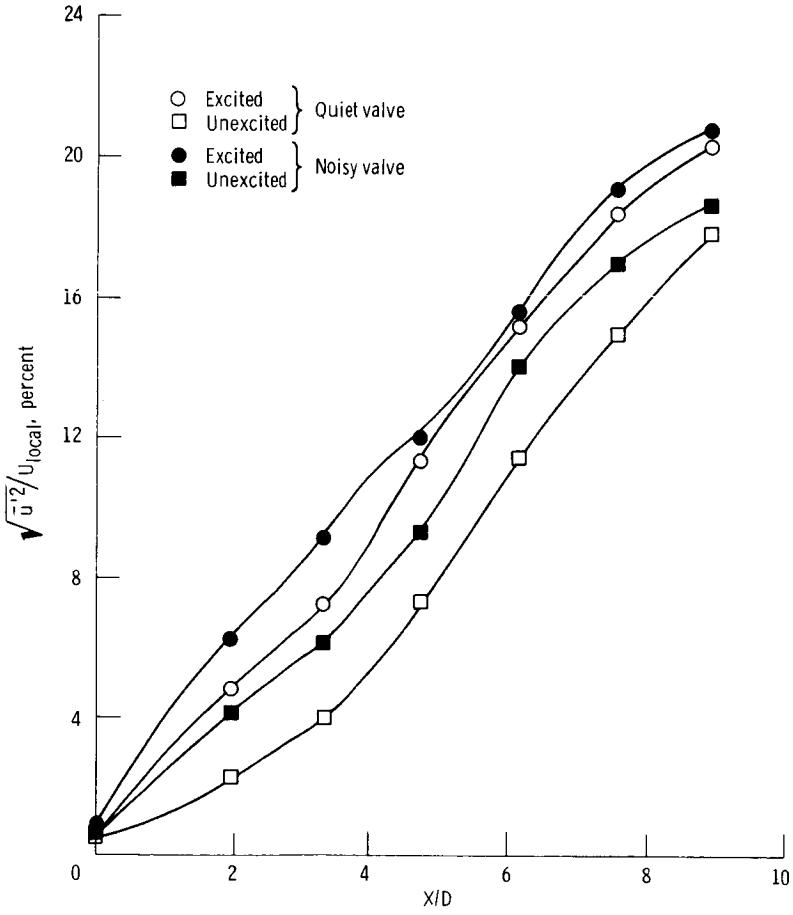

Figure 37. - Effect of excitation and valve settings on centerline turbulence intensities with jet excited by 550 Hz tone at 140 dB re 20 μPa (M = 0.2).

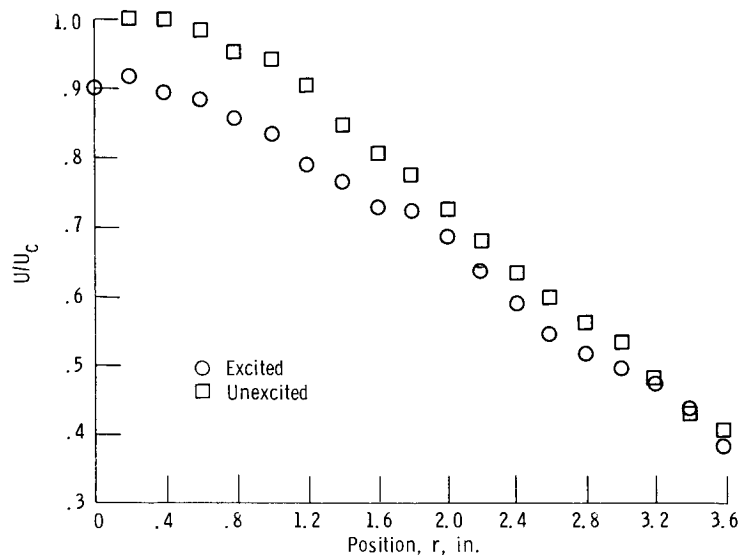

Figure 38. - Effect of excitation on radial variation of mean velocity at X/D = 0 (M = 0.435). Excitation level, 140 dB re 20 μPa; excitation frequency, 850 Hz; modified jet facility (with 3/8-in.-thick felt in plenum).

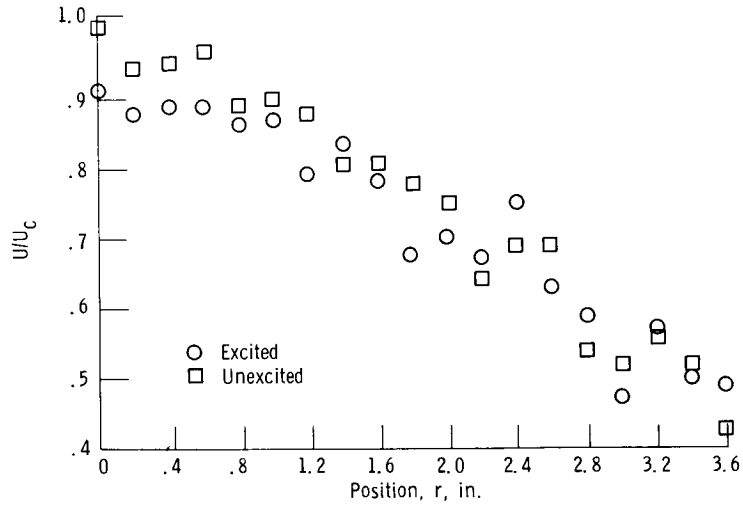

Figure 39. - Effect of excitation on radial variation of mean velocity at X/D = 9 (M = 0.2, quiet valve). Excitation level, 140 dB re 20 μPa; excitation frequency, 550 Hz; modified jet facility (with 3/8-in.-thick felt in plenum).

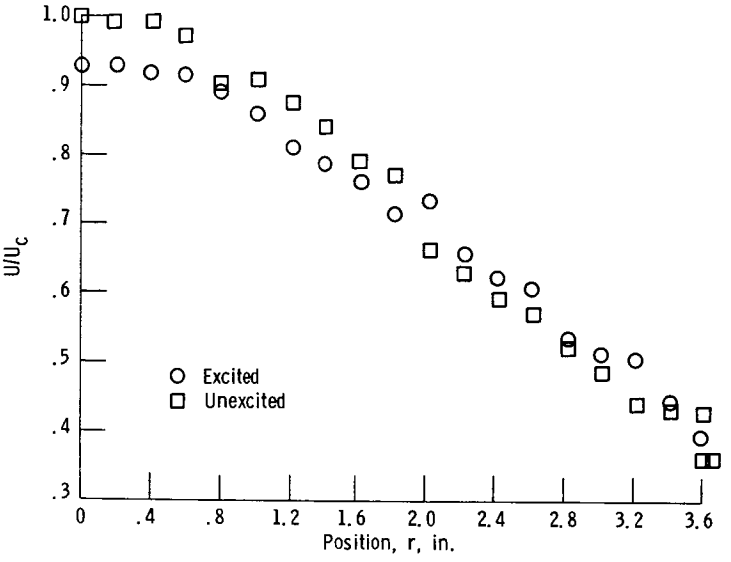

Figure 40. - Effect of excitation on radial variation of mean velocity at X/D = 9 (M = 0.2, noisy valve). Excitation level, 140 dB re 20 μPa; excitation frequency, 550 Hz; modified jet facility (with 3/8-in.-thick felt in plenum tank).

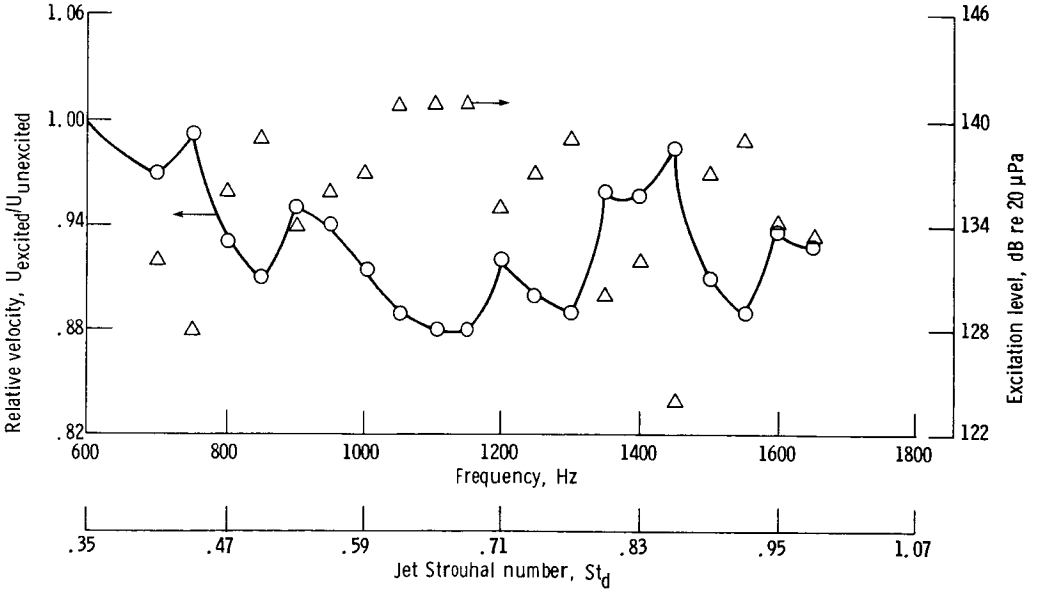

Figure 41. - Excitation Strouhal number effects on relative velocity on jet axis at X/D = 9 (M = 0.435).

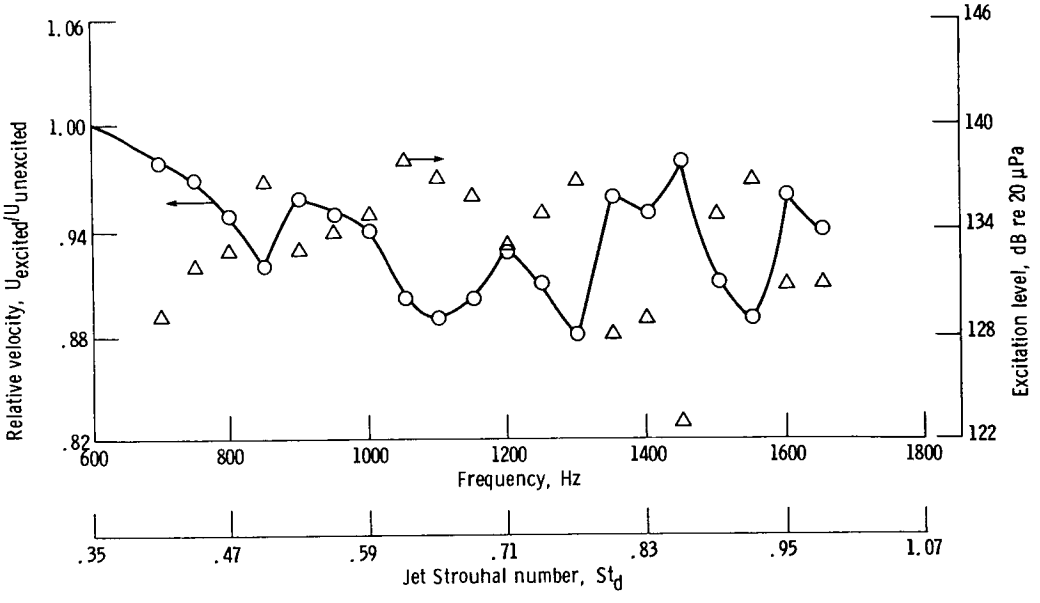

Figure 42. - Excitation Strouhal number effects on relative velocity on jet axis at X/D = 9 (M = 0.435).

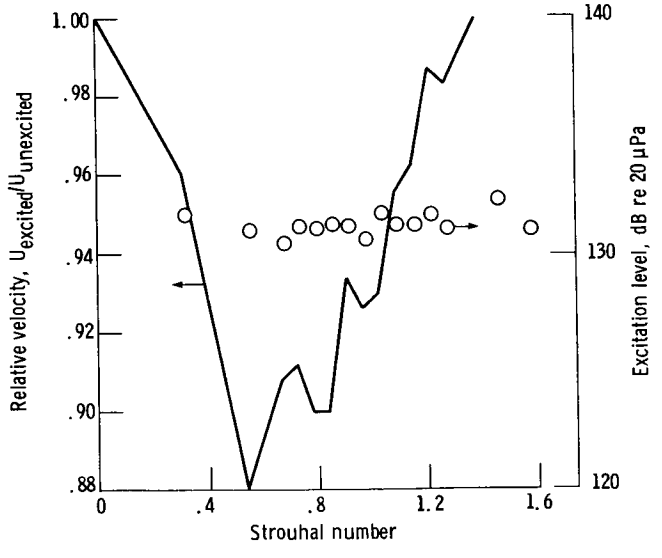

Figure 43. - Excitation Strouhal number effects on relative velocity on jet axis at X/D = 9 (M = 0.2, T = 541 ^{0}R).

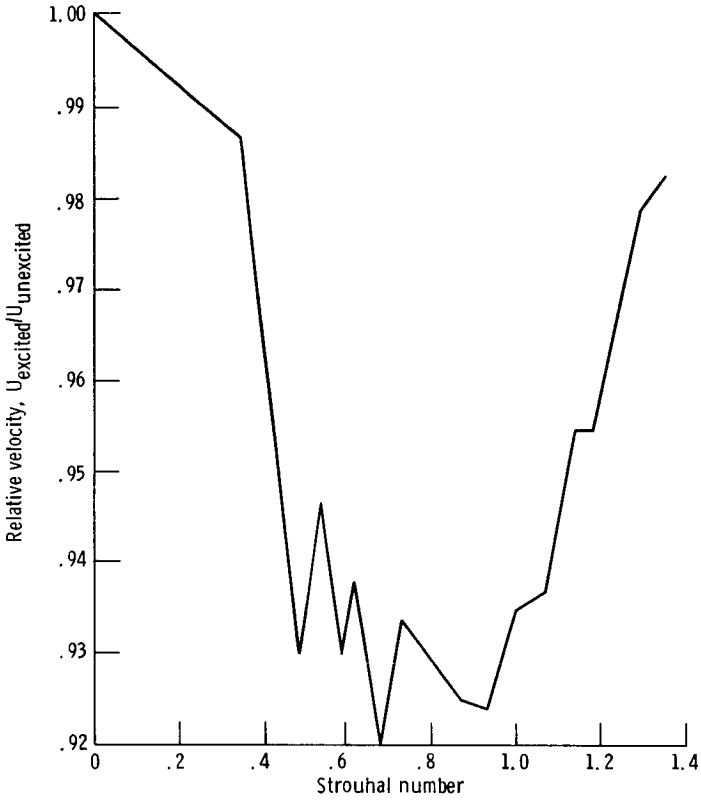

Figure 44. - Excitation Strouhal number effects on relative velocity on jet axis at X/D = 9 (M = 0.435, T = 541 ^{0}R, excitation level ≈ 135 dB re 20 μPa).

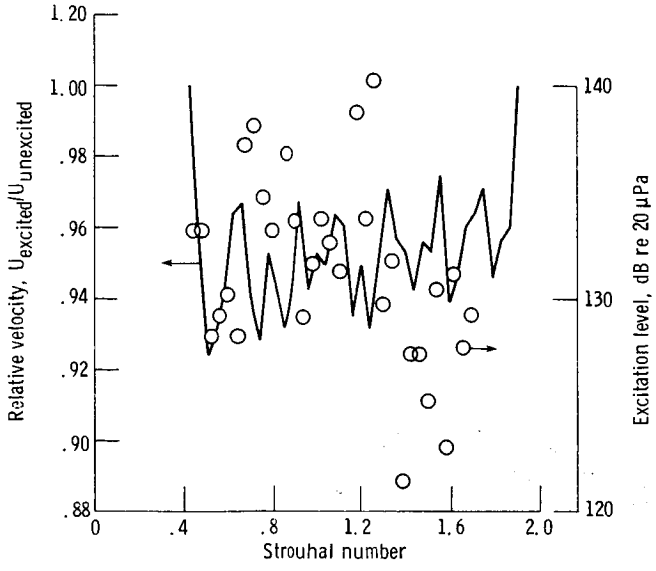

Figure 45. - Excitation Strouhal number effects on relative velocity on jet axis at X/D = 9 in original rig (M = 0.3).

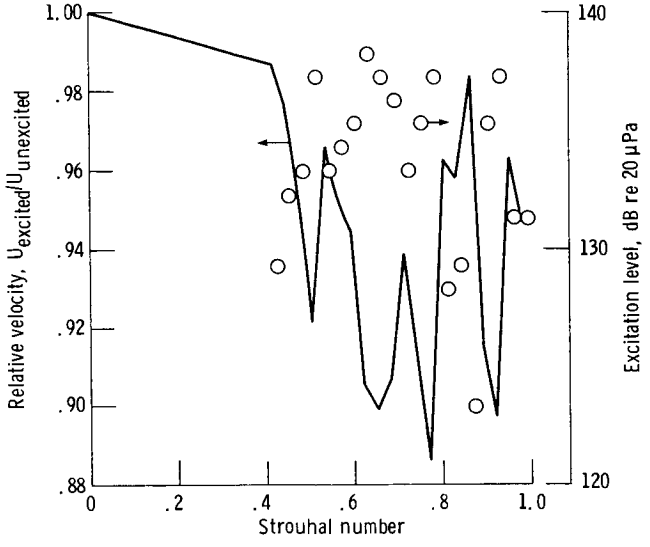

Figure 46. - Excitation Strouhal number effects on relative velocity on jet axis at X/D = 9 in modified rig (with 3/8-in. felt; M = 0.435).

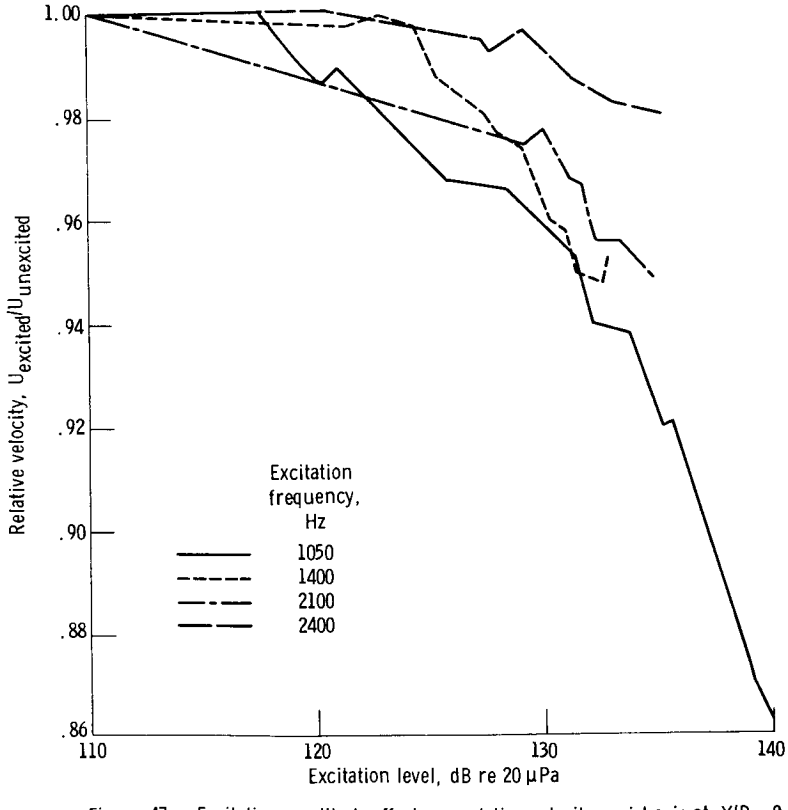

Figure 47. - Excitation amplitude effects on relative velocity on jet axis at X/D = 9 (M = 0.435, T = 540 ^{o}R).

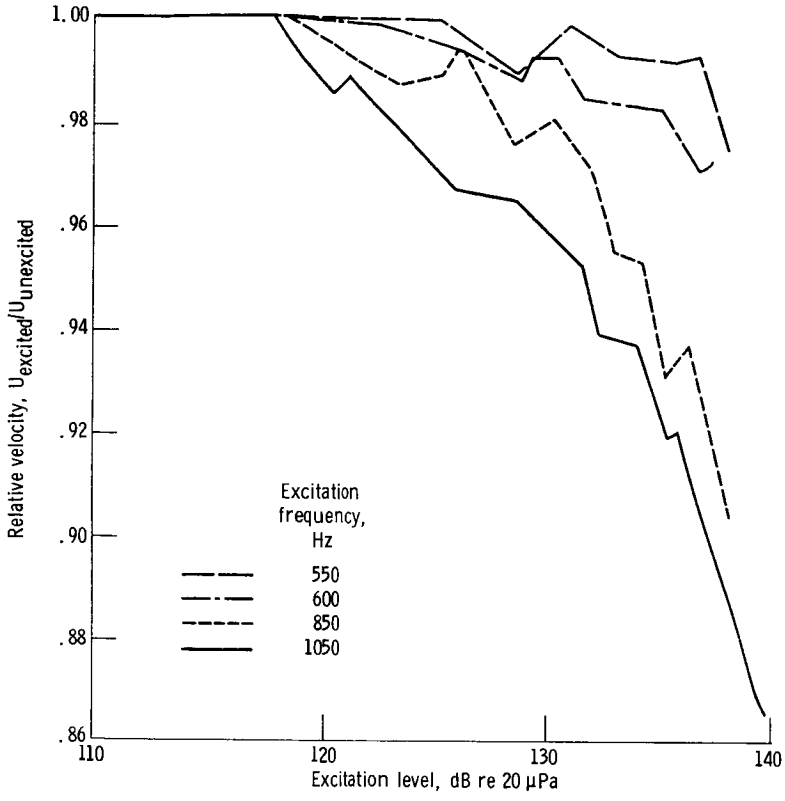

Figure 48. - Excitation amplitude effects on relative velocity on jet axis at X/D = 9 (M = 0.435, T = 540 ^{0}R).

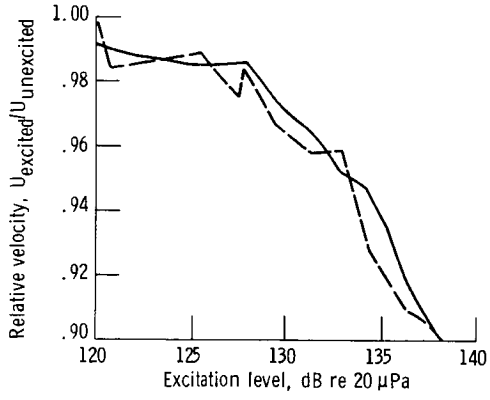

Figure 49. - Reproducibility test for excitation amplitude dependence of relative velocity on jet axis at X/D = 9 (M = 0.435, T = 540 ^{0}R)

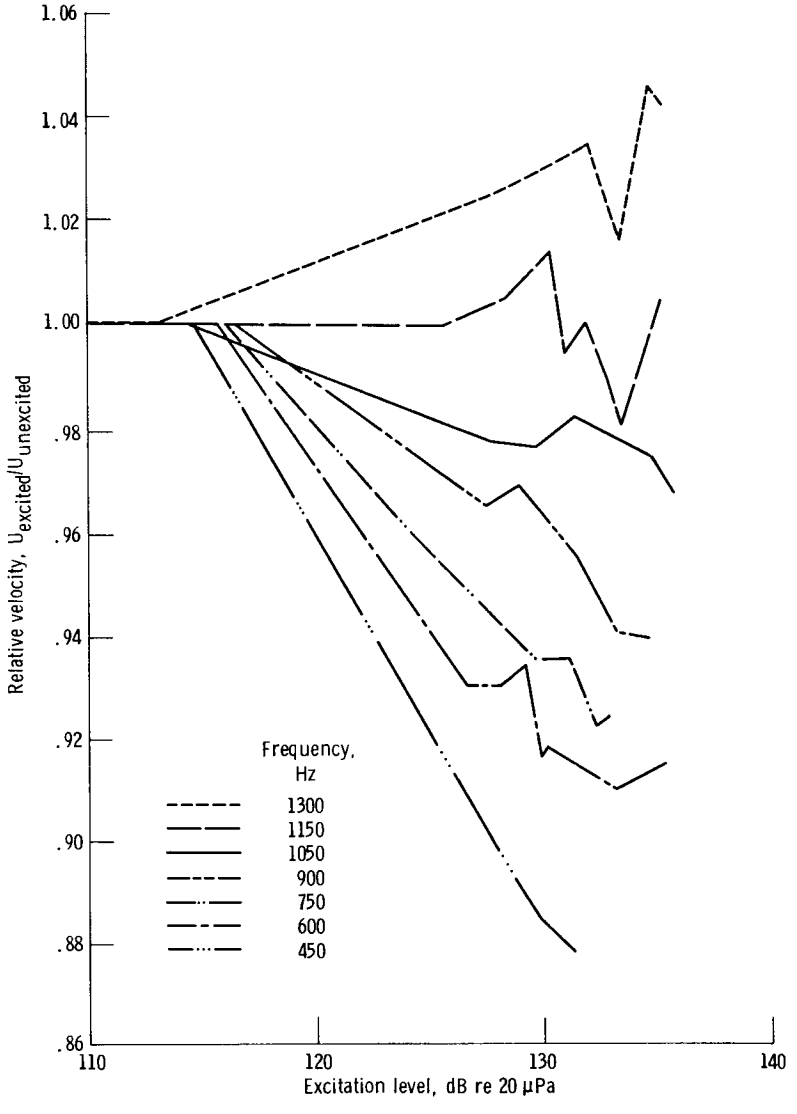

Figure 50. - Excitation amplitude effects on relative velocity on jet axis at X/D = 9 (M = 0.2, quiet valve, T = 541 ^{0}R).

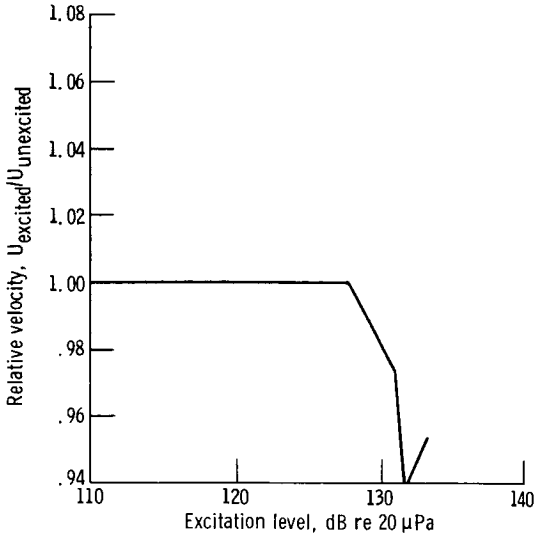

Figure 51. - Excitation amplitude effects on relative velocity on jet axis at X/D = 9 (M = 0.2, T = 540 ^{0}R, F = 450 Hz, noisy valve).

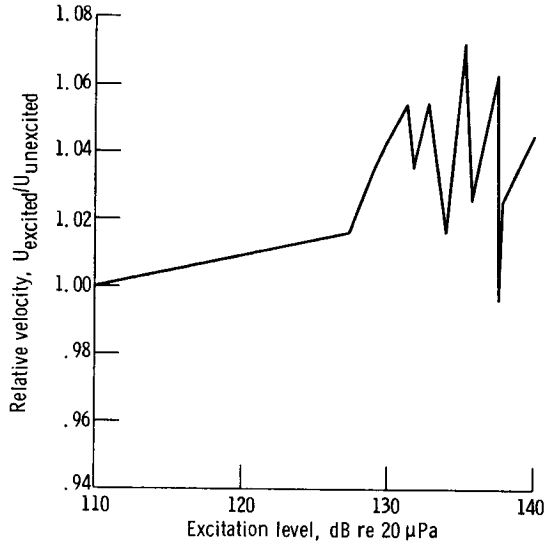

Figure 52. - Excitation amplitude effects on relative velocity on jet axis at X/D = 9 (M = 0.2, T = 540 ^{0}R, F = 550 Hz, noisy valve).

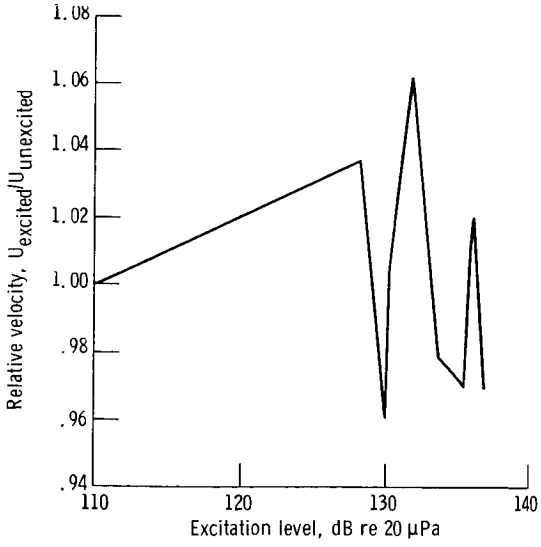

Figure 53. - Excitation amplitude effects on relative velocity on jet axis at X/D = 9 (M = 0.2, T = 540 ^{0}R, F = 575 Hz, noisy valve).

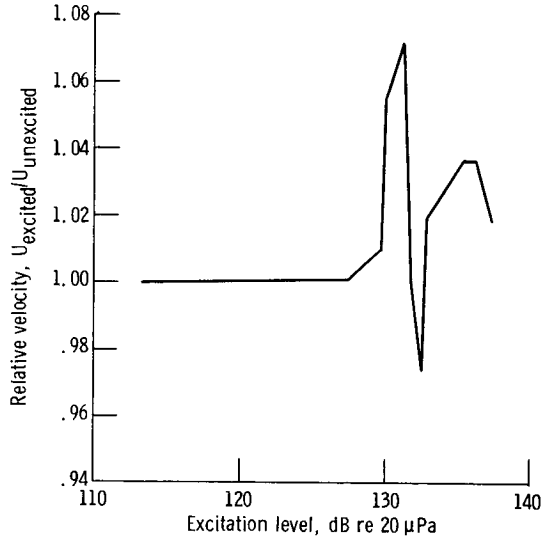

Figure 54. - Excitation amplitude effects on relative velocity on jet axis at X/D = 9 (M = 0.2, T = 540 ^{0}R, F = 600 Hz, noisy valve).

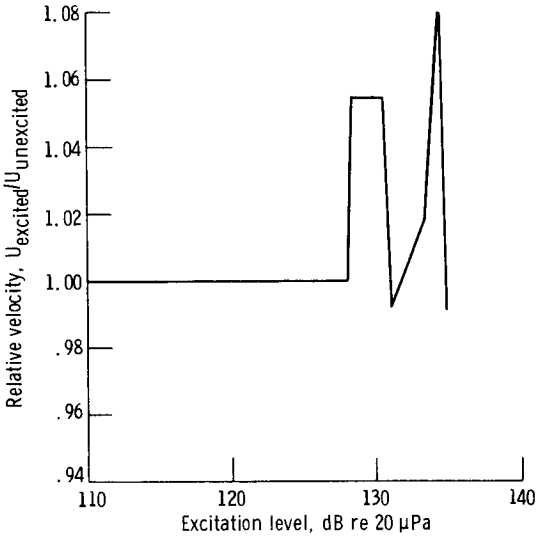

Figure 55. - Excitation amplitude effects on relative velocity on jet axis at X/D = 9 (M = 0.2, T = 540 ^{0}R, F = 700 Hz, noisy valve).

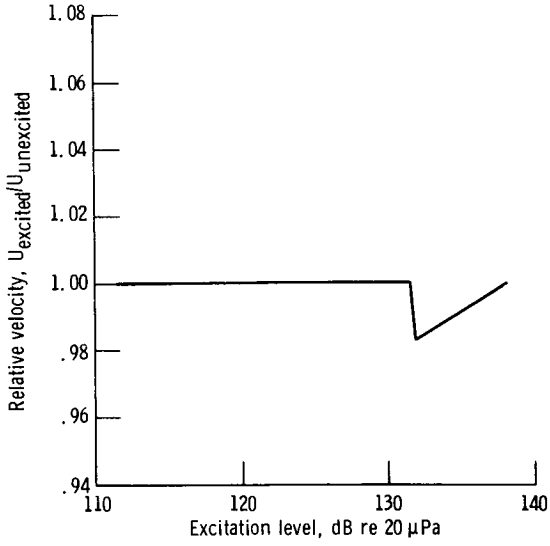

Figure 56. - Excitation amplitude effects on relative velocity on jet axis at X/D = 9 (M = 0.2, T = 540 ^{0}R, F = 850 Hz, noisy valve).

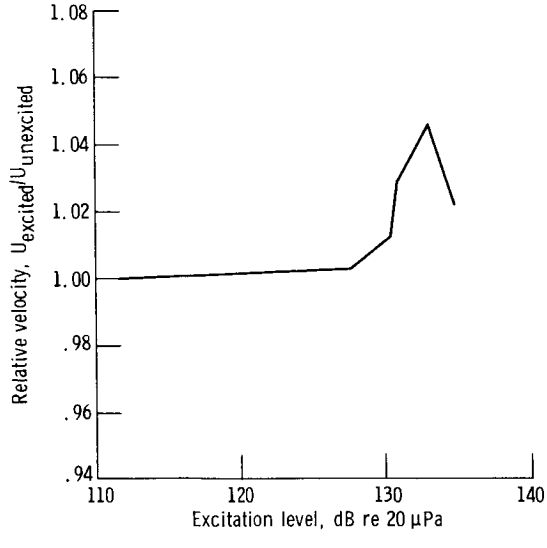

Figure 57. - Excitation amplitude effects on relative velocity on jet axis at X/D = 9 (M = 0.2, T = 540 ^{0}R, F = 950 Hz, noisy valve).

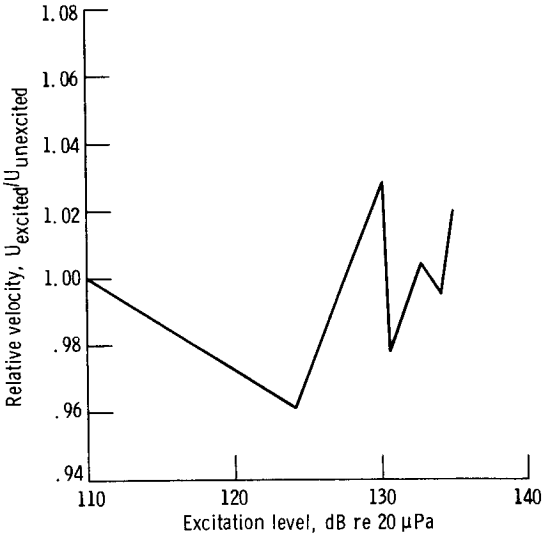

Figure 58. - Excitation amplitude effects on relative velocity on jet axis at X/D = 9 (M = 0.2, T = 540 ^{0}R, F = 1050 Hz, noisy valve).

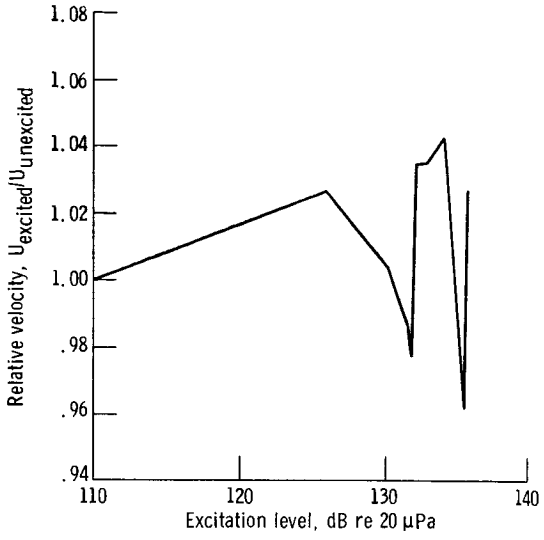

Figure 59. - Excitation amplitude effects on relative velocity on jet axis at X/D = 9 (M = 0.2, T = 540 ^{0}R, F = 1150 Hz, noisy valve).

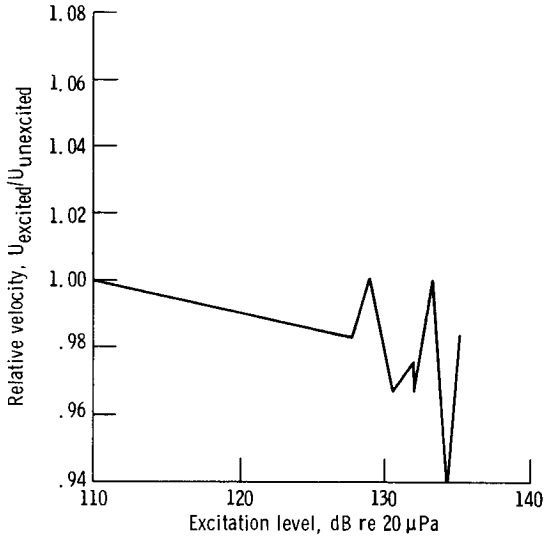

Figure 60. - Excitation amplitude effects on relative velocity on jet axis at X/D = 9 (M = 0.2, T = 540 ^{0}R, F = 1200 Hz, noisy valve).

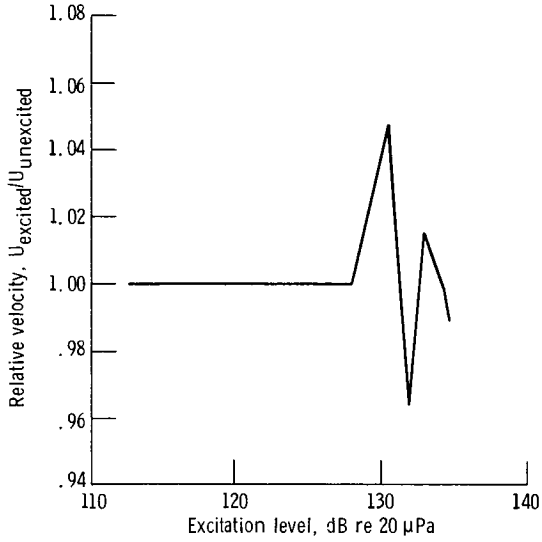

Figure 61. - Excitation amplitude effects on relative velocity on jet axis at X/D = 9 (M = 0.2, T = 540 ^{0}R, F = 1300 Hz, noisy valve).

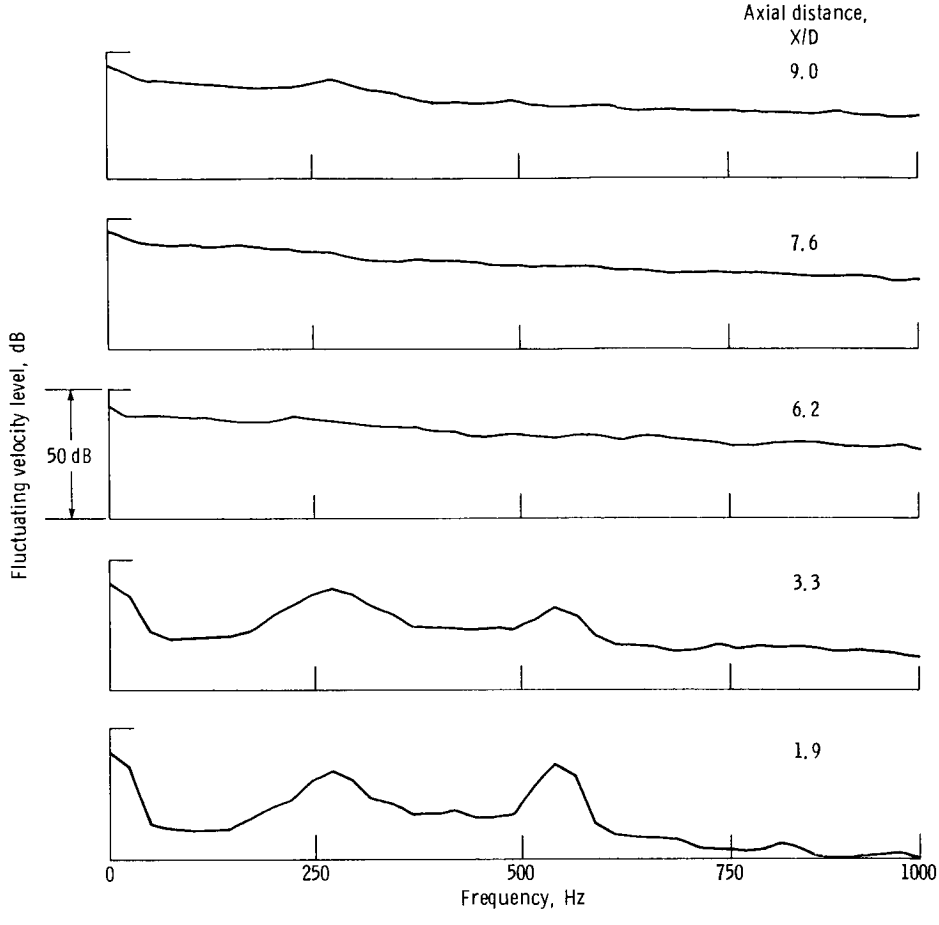

Figure 62. - Velocity spectrum at X/D = 1.9, 3.3, 6.2, 7.6, and 9.0 with jet excited by 550 Hz tone (M = 0.2, quiet valve).

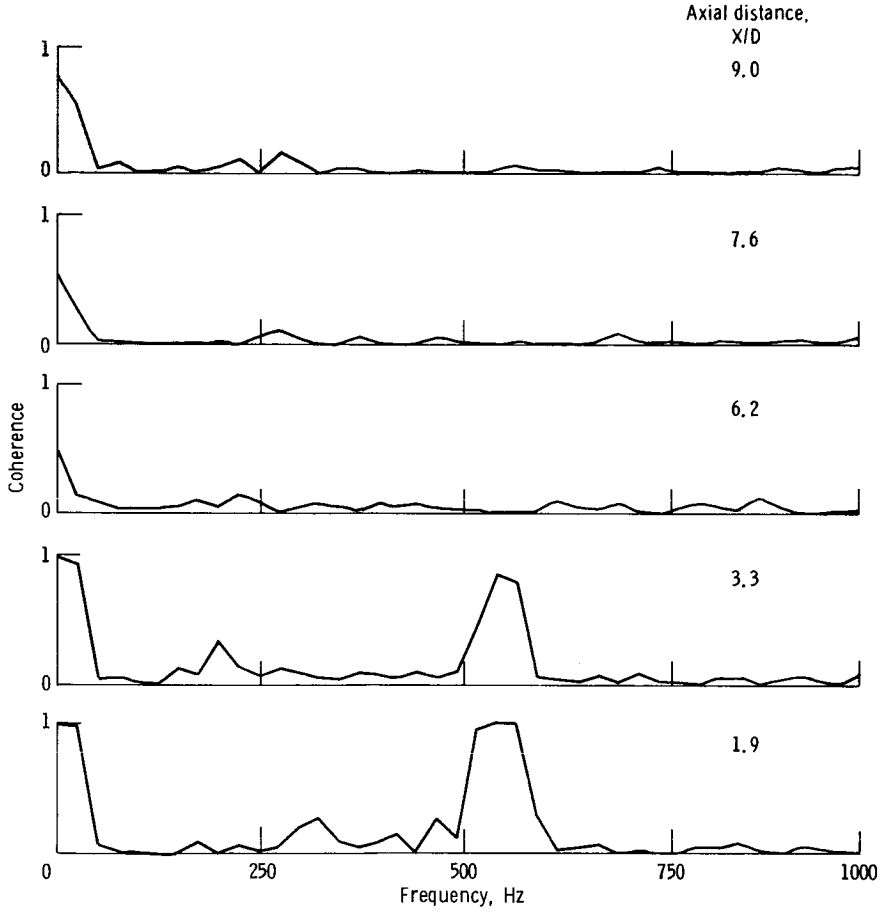

Figure 63. - Coherence between microphone at nozzle exit and hot wire at X/D = 1.9, 3.3, 6.2, 7.6, and 9.0 with jet excited by 550 Hz tone (M = 0.2, quiet valve).

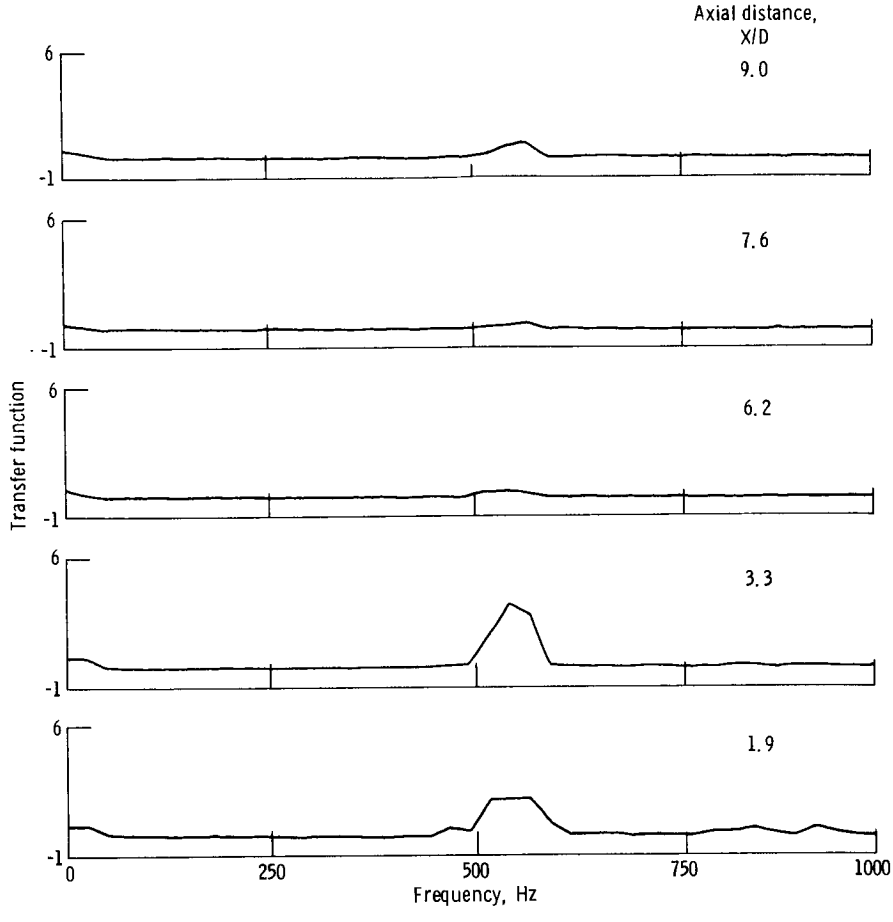

Figure 64. - Transfer function between microphone at nozzle exit and hot wire at X/D = 1.9, 3.3, 6.2, 7.6, and 9.0 with jet excited by 550 Hz tone (M = 0.2, quiet valve).

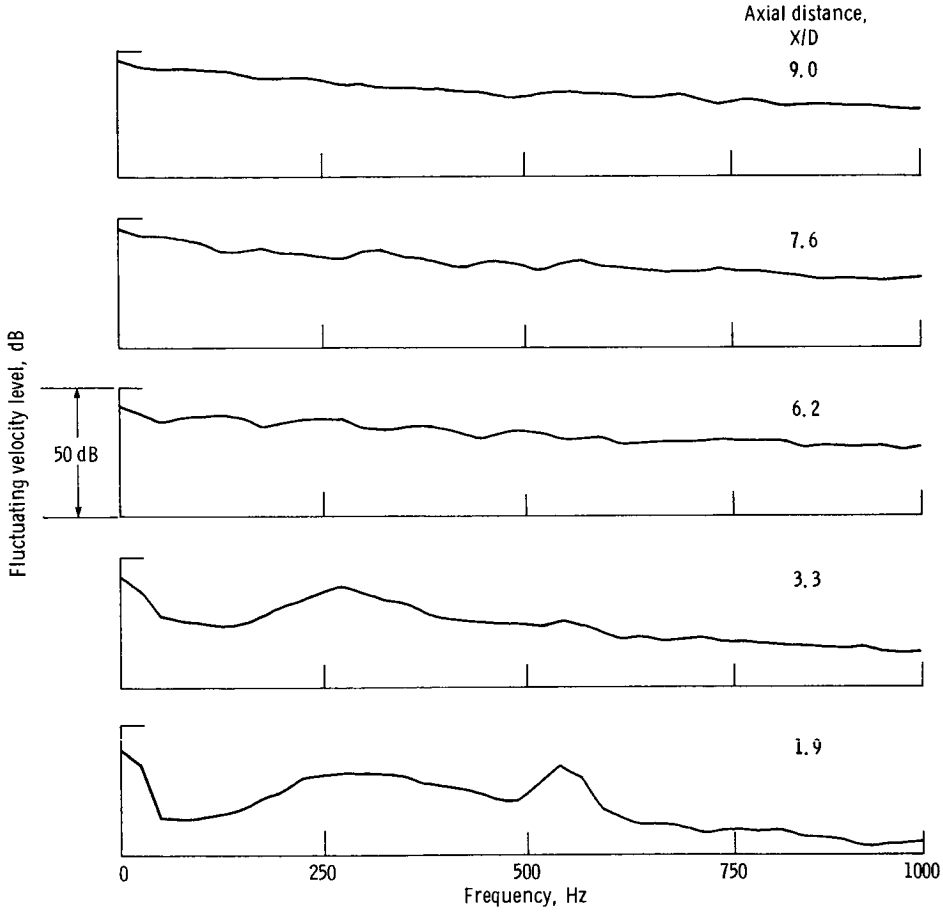

Figure 65. - Velocity spectrum at X/D = 1.9, 3.3, 6.2, 7.6, and 9.0 with jet excited by 550 Hz tone (M = 0.2, noisy valve).

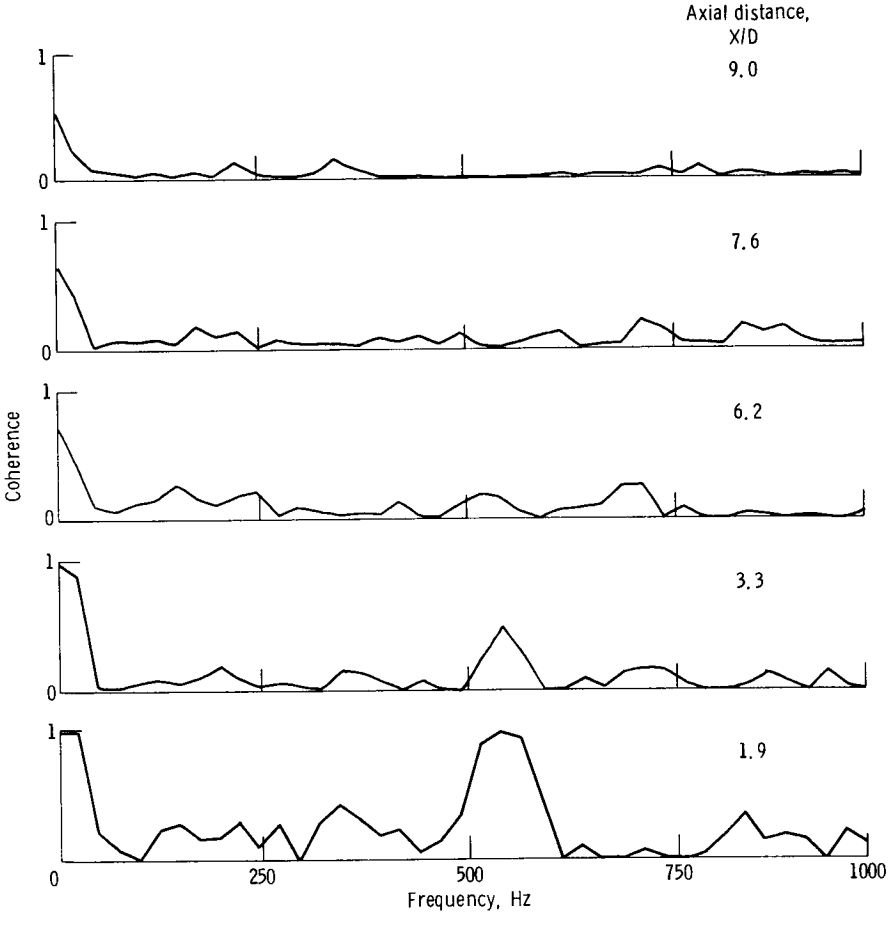

Figure 66. - Coherence between microphone at nozzle exit and hot wire at X/D = 1.9, 3.3, 6.2, 7.6, and 9.0 with jet excited by 550 Hz tone (M = 0.2, noisy valve).

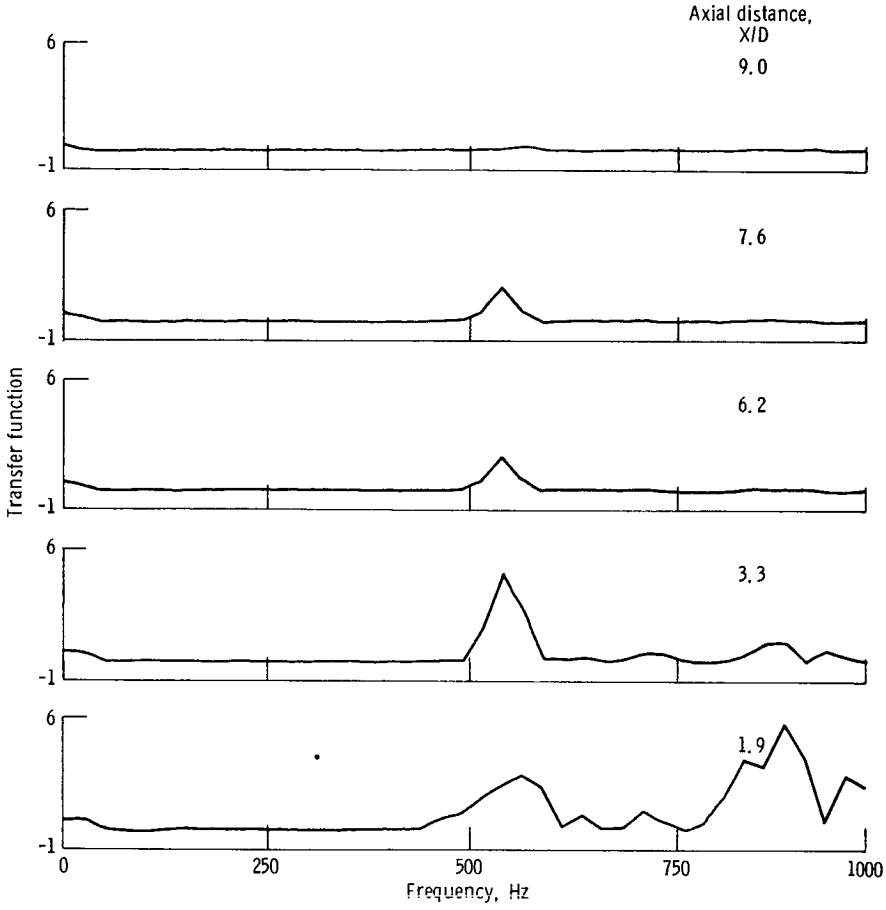

Figure 67. - Transfer function between microphone at nozzle exit and hot wire at X/D = 1.9, 3.3, 6.2, 7.6, and 9.0 with jet excited by 550 Hz tone (M = 0.2, noisy valve).

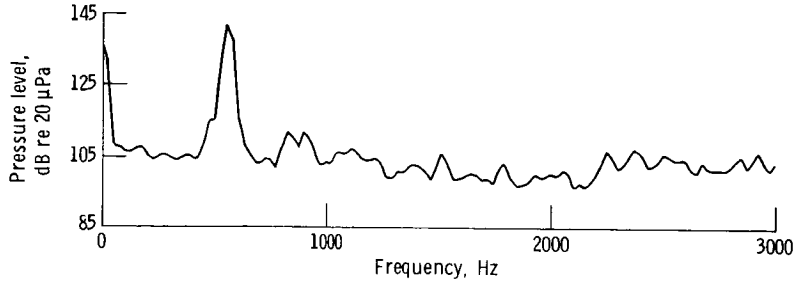

Figure 68. - Pressure spectrum at nozzle exit with jet excited by 550 Hz tone (M = 0.2, quiet valve).

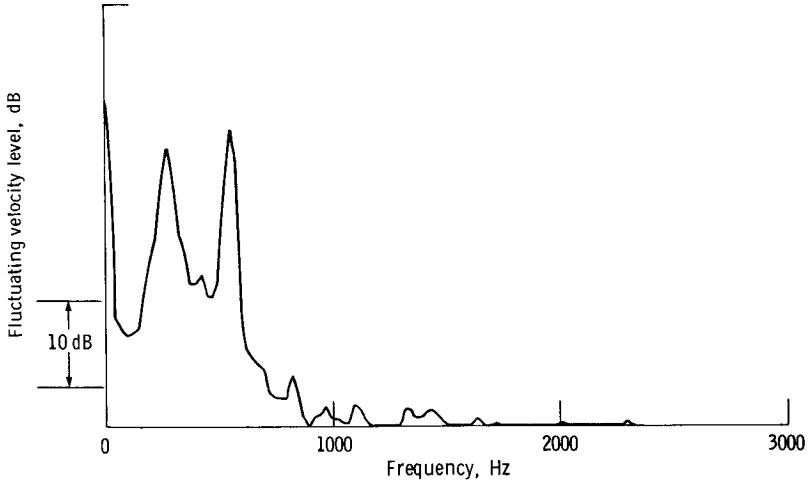

Figure 69. - Velocity spectrum at X/D = 1.9 with jet excited by 550 Hz tone (M = 0.2, quiet valve.

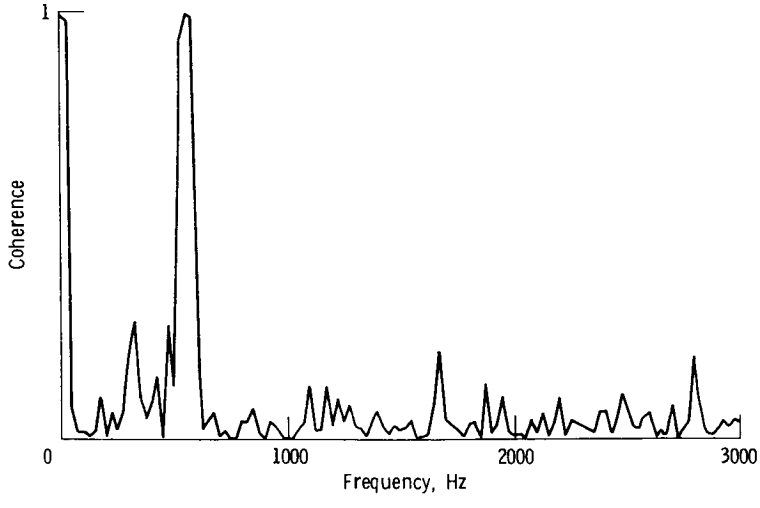

Figure 70. - Coherence between microphone at nozzle exit and hot wire at X/D = 1.9 with jet excited by 550 Hz tone (M = 0.2, quiet valve).

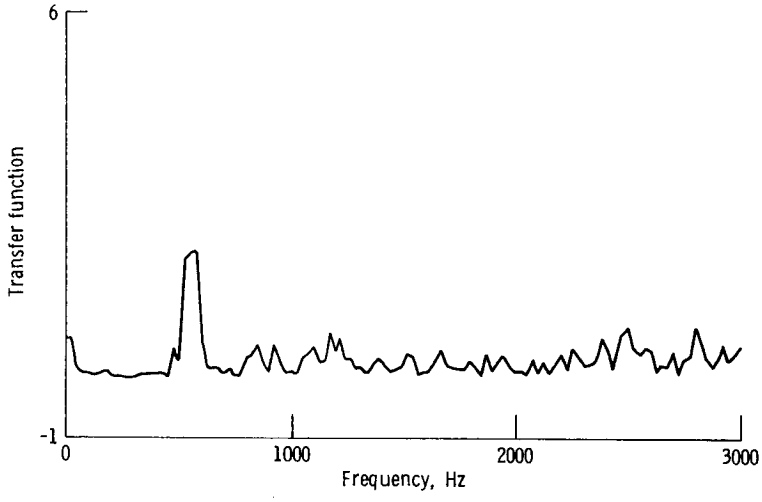

Figure 71. - Transfer function between microphone at nozzle exit and hot wire at X/D = 1.9 with jet excited by 550 Hz tone (M = 0.2, quiet valve).

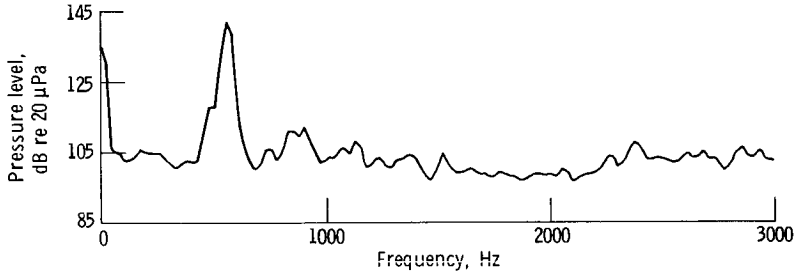

Figure 72. - Pressure spectrum at nozzle exit with jet excited by 550 Hz tone (M = 0.2, quiet valve).

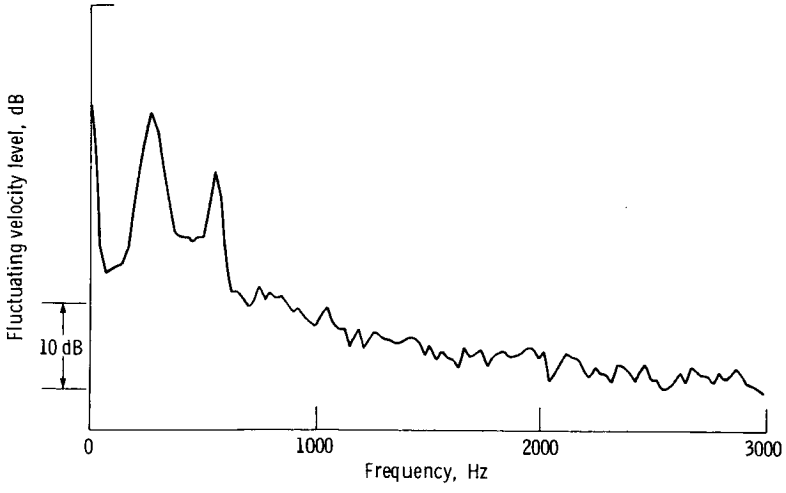

Figure 73. - Velocity spectrum at X/D = 3.3 with jet excited by 550 Hz tone (M = 0.2, quiet valve).

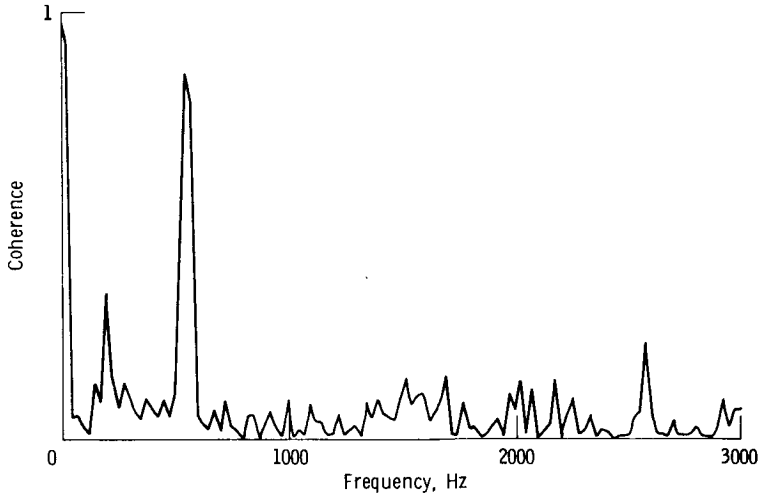

Figure 74. - Coherence between microphone at nozzle exit and hot wire at X/D = 3.3 with jet excited by 550 Hz tone (M = 0.2, quiet valve).

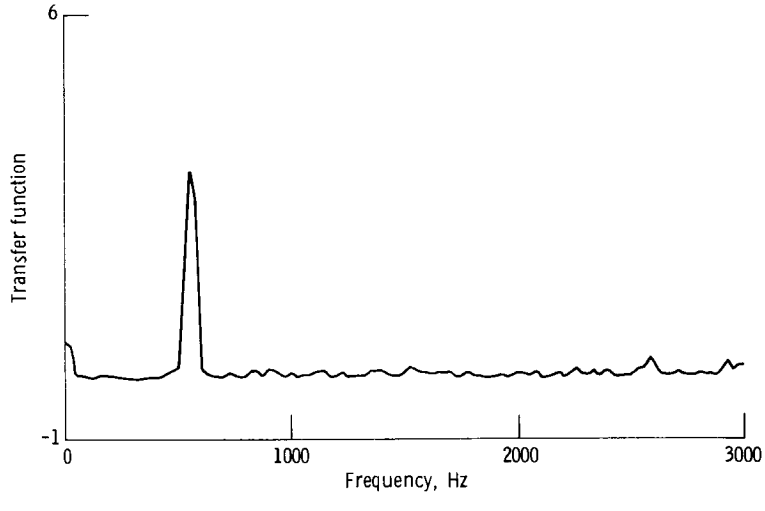

Figure 75. - Transfer function between microphone at nozzle exit and hot wire at X/D = 3.3 with jet excited by 550 Hz tone (M = 0.2, quiet valve).

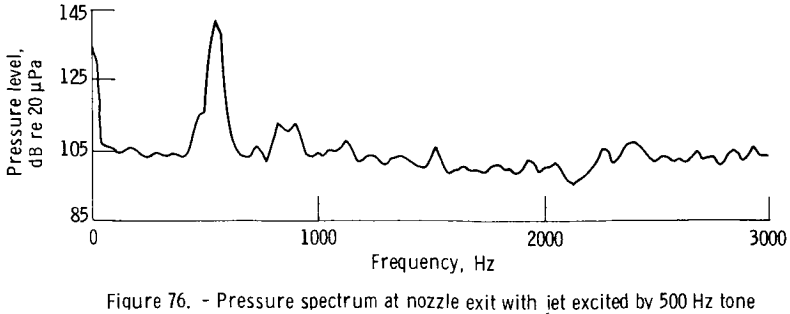

Figure 76. - Pressure spectrum at nozzle exit with jet excited by 500 Hz tone (M = 0.2, quiet valve).

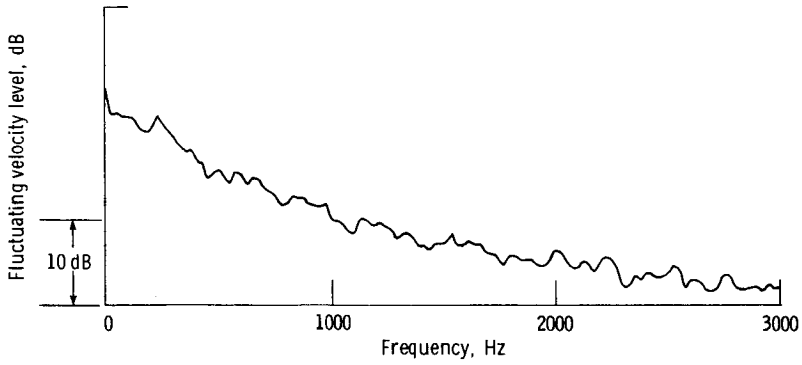

Figure 77. - Velocity spectrum at X/D = 6.2 with jet excited by 550 Hz tone (M = 0.2, quiet valve).

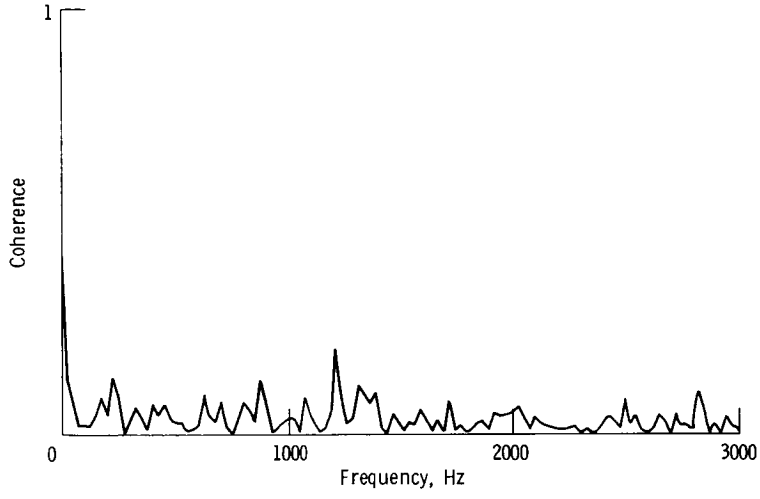

Figure 78. - Coherence between microphone at nozzle exit and hot wire at X/D = 6.2 with jet excited by 550 Hz tone (M = 0.2, quiet valve).

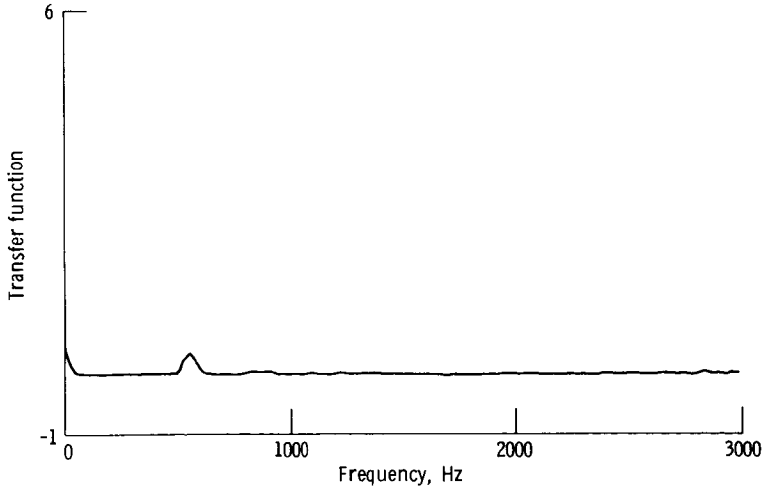

Figure 79. - Transfer function between microphone at nozzle exit and hot wire at X/D = 6.2 with jet excited by 550 Hz tone (M = 0.2, quiet valve).

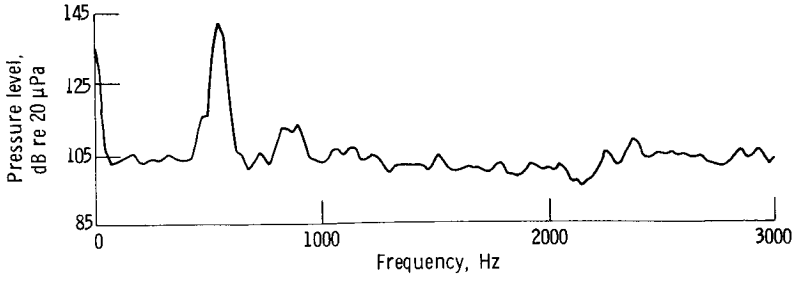

Figure 80. - Pressure spectrum at nozzle exit with jet excited by 550 Hz tone (M = 0.2, quiet valve).

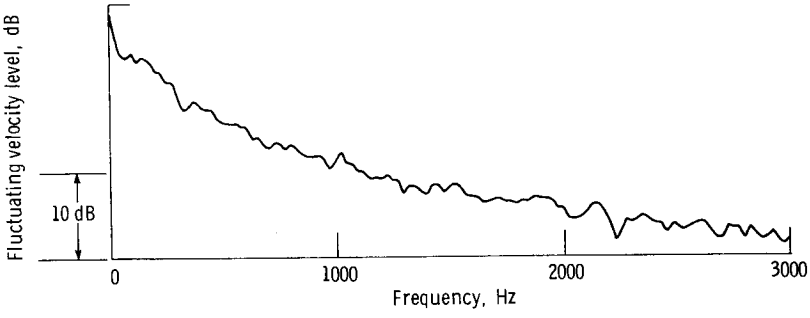

Figure 81. - Velocity spectrum at X/D = 7.6 with jet excited by 550 Hz tone (M = 0.2, quiet valve).

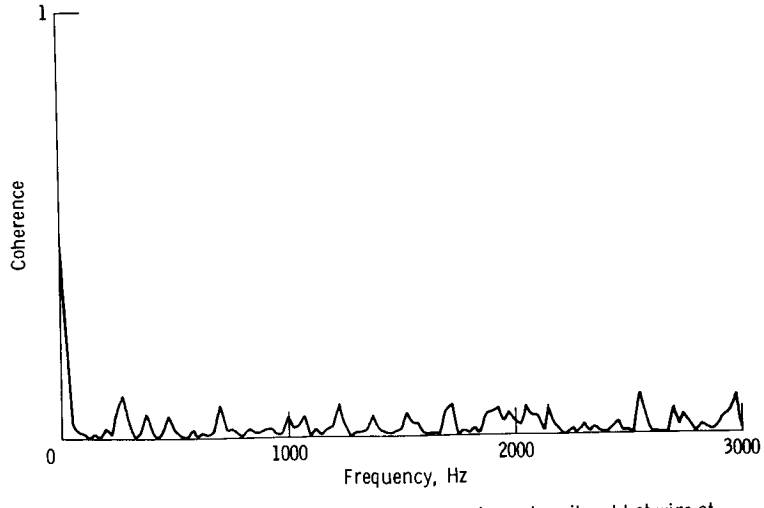

Figure 82. - Coherence between microphone at nozzle exit and hot wire at X/D = 7.6 with jet excited by 550 Hz tone (M = 0.2, quiet valve).

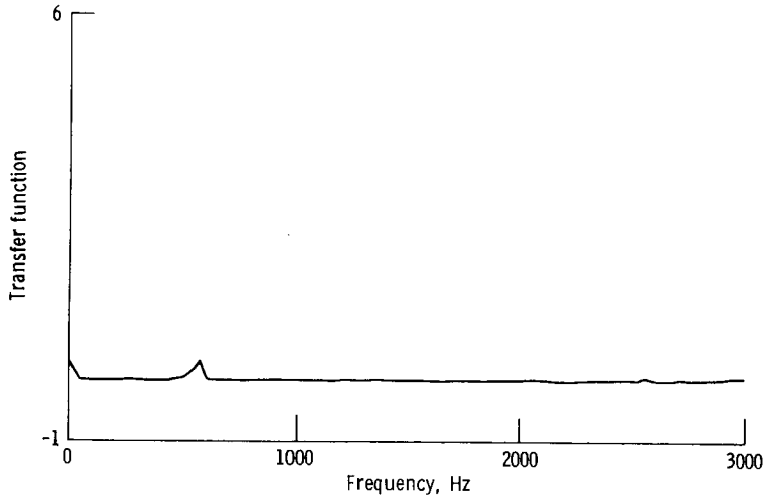

Figure 83. - Transfer function between microphone at nozzle exit and hot wire at X/D = 7.6 with jet excited by 550 Hz tone (M = 0.2, quiet valve).

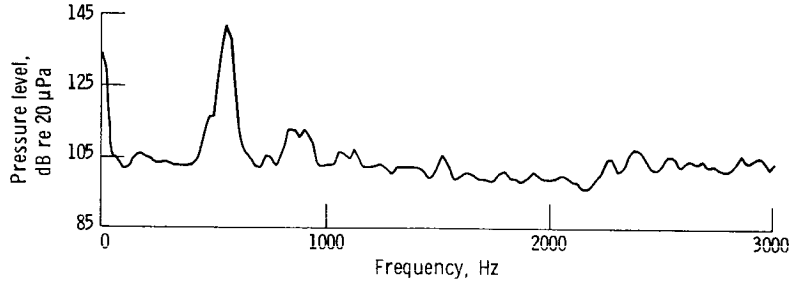

Figure 84. - Pressure spectrum at nozzle exit with jet excited by 550 Hz tone (M = 0.2, quiet valve).

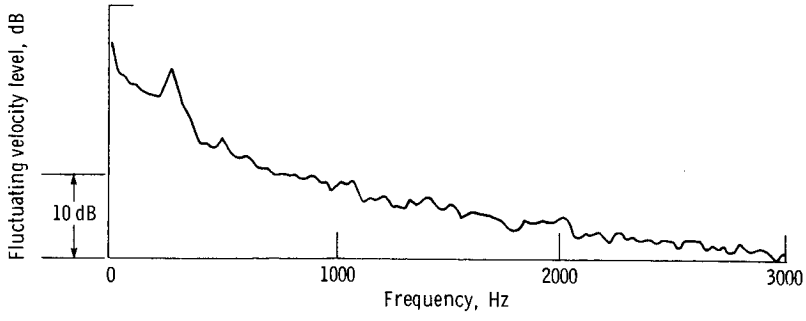

Figure 85. - Velocity spectrum at X/D = 9 with jet excited by 550 Hz tone (M = 0.2, quiet valve).

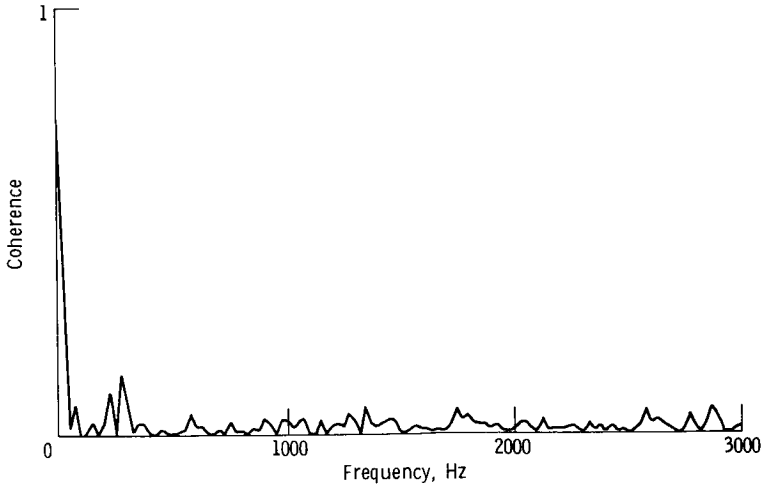

Figure 86. - Coherence between microphone at nozzle exit and hot wire at X/D = 9 with jet excited by 550 Hz (M = 0.2, quiet valve).

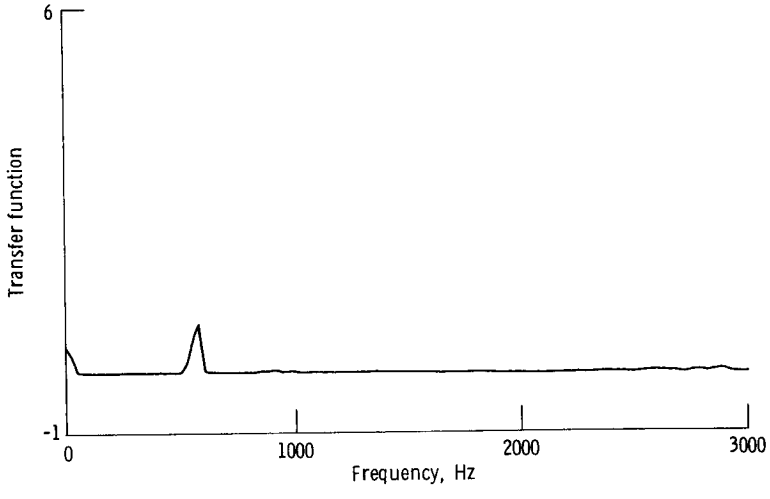

Figure 87. - Transfer function between microphone at nozzle exit and hot wire at X/D = 9 with jet excited by 550 Hz tone (M = 0.2, quiet valve).

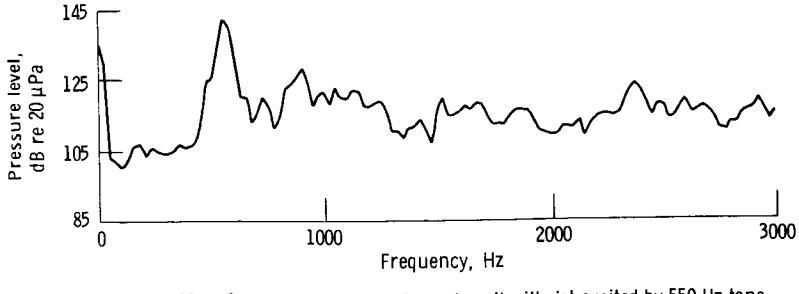

Figure 88. - Pressure spectrum at nozzle exit with jet excited by 550 Hz tone (M = 0.2, noisy valve).

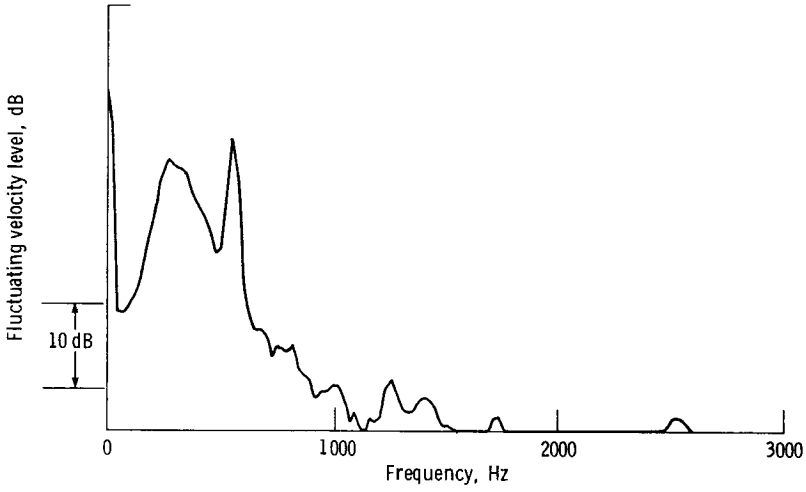

Figure 89. - Velocity spectrum at X/D = 1.9 with jet excited by 550 Hz tone (M = 0.2, noisy valve).

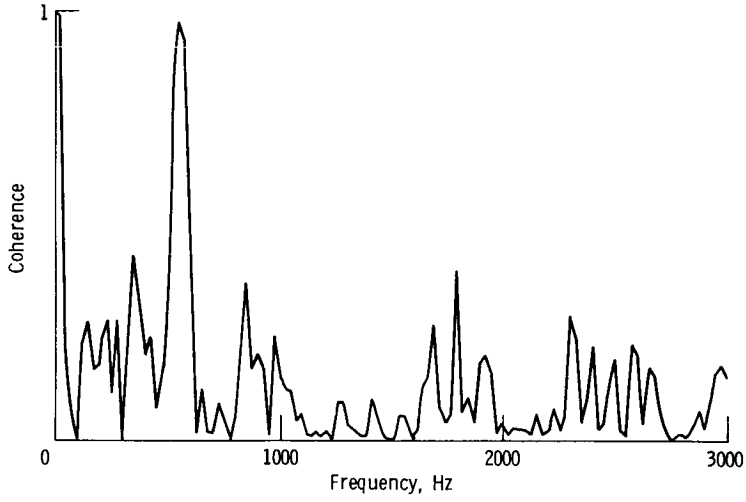

Figure 90. - Coherence between microphone at nozzle exit and hot wire at X/D = 1.9 with jet excited by 550 Hz tone (M = 0.2, noisy valve).

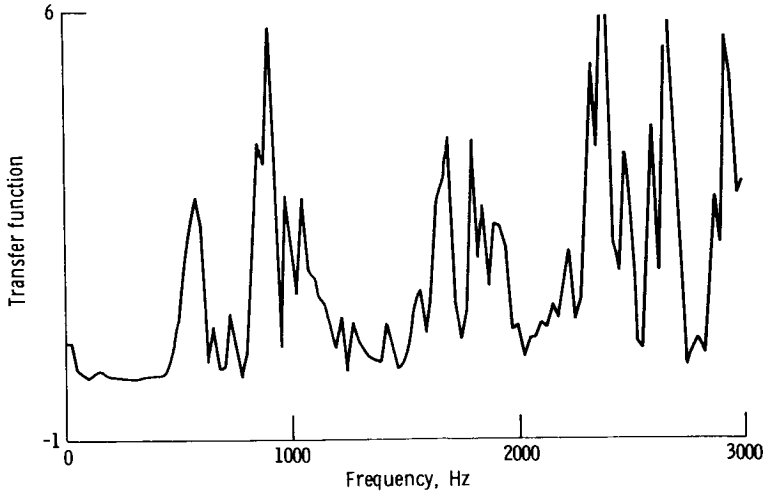

Figure 91. - Transfer function between microphone at nozzle exit and hot wire at X/D = 1.9 with jet excited by 550 Hz tone (M = 0.2, noisy valve).

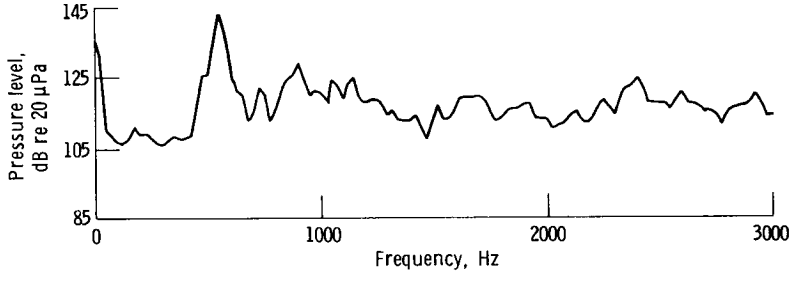

Figure 92. - Pressure spectrum at nozzle exit with jet excited by 550 Hz tone (M = 0.2, noisy valve).

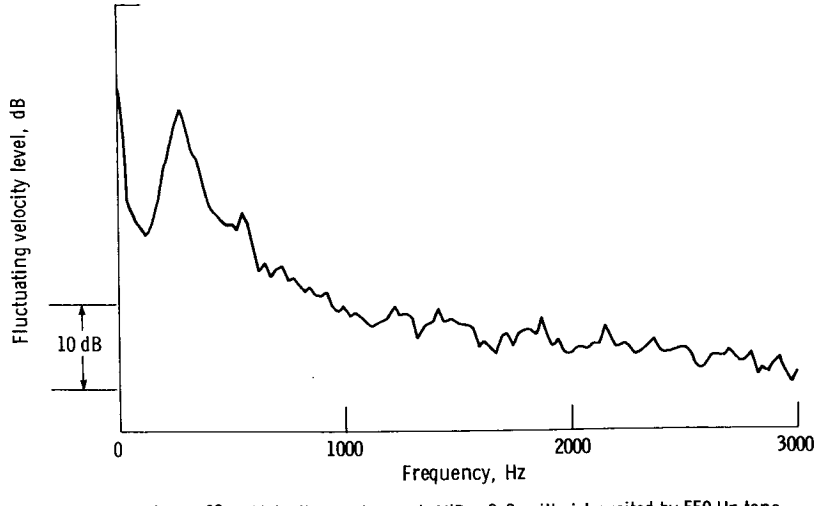

Figure 93. - Velocity spectrum at X/D = 3.3 with jet excited by 550 Hz tone (M = 0.2, noisy valve).

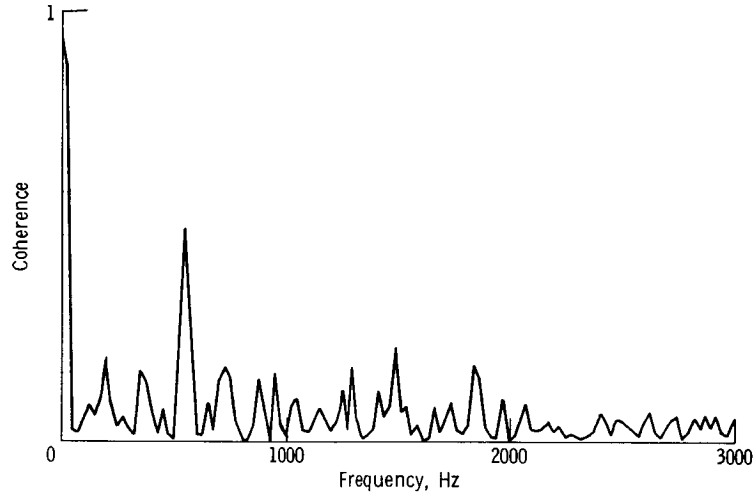

Figure 94. - Coherence between microphone at nozzle exit and hot wire at X/D = 3.3 with jet excited by 550 Hz tone (M = 0.2, noisy valve).

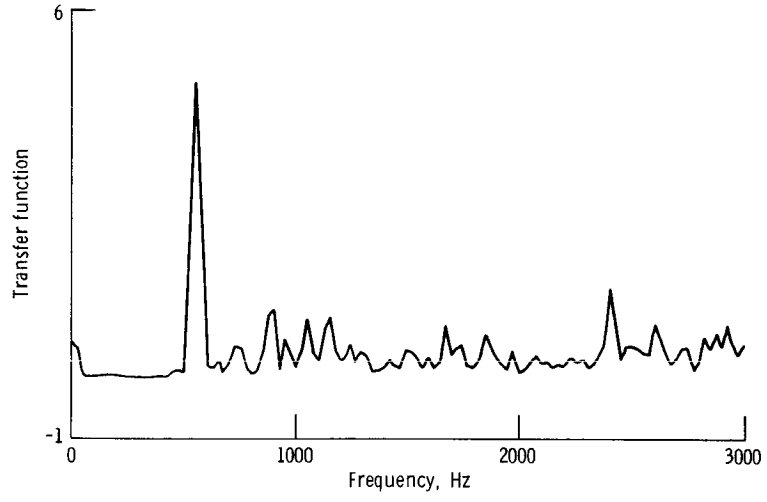

Figure 95. - Transfer function between microphone at nozzle exit and hot wire at X/D = 3.3 with jet excited by 550 Hz tone (M = 0.2, noisy valve).

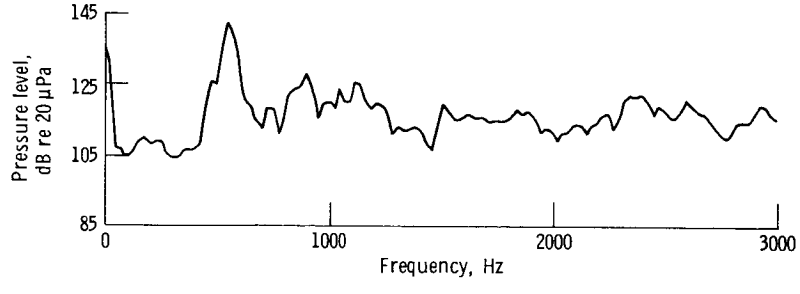

Figure 96. - Pressure spectrum at nozzle exit with jet excited by 550 Hz tone (M = 0.2, noisy valve).

C-2

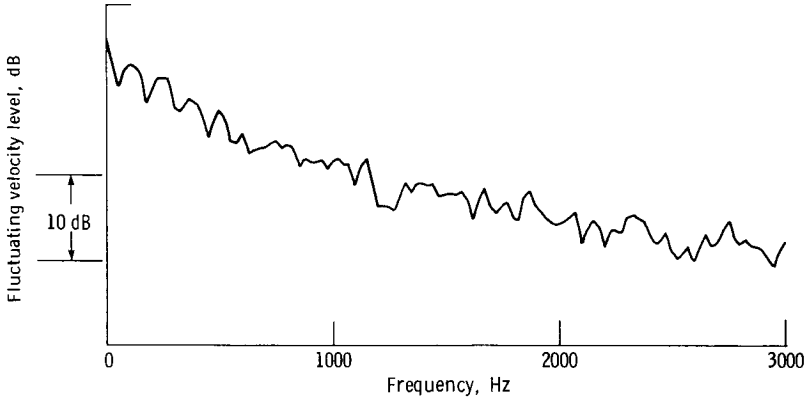

Figure 97. - Velocity spectrum at X/D = 6.2 with jet excited by 550 Hz tone (M = 0.2, noisy valve).

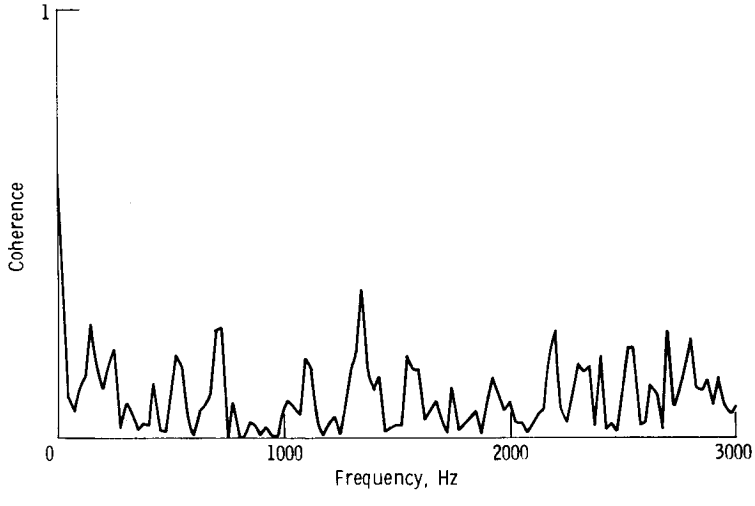

Figure 98. - Coherence between microphone at nozzle exit and hot wire at X/D = 6.2 with jet excited by 550 Hz tone (M = 0.2, noisy valve).

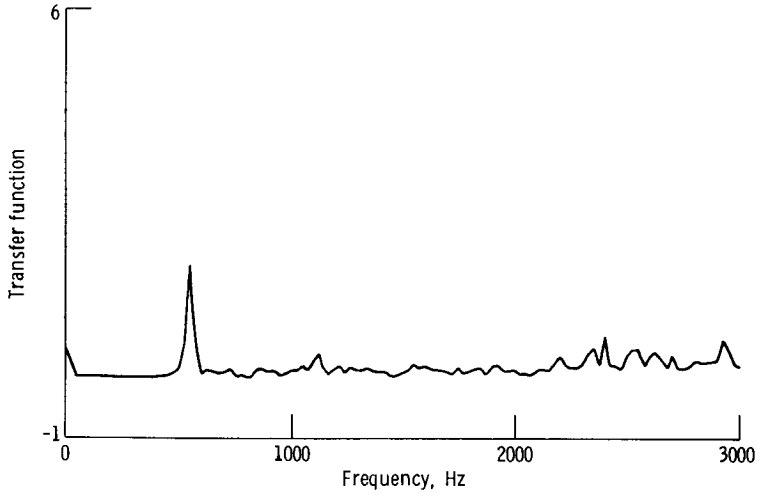

Figure 99. - Transfer function between microphone at nozzle exit and hot wire at X/D = 6.2 with jet excited by 550 Hz tone (M = 0.2, noisy valve).

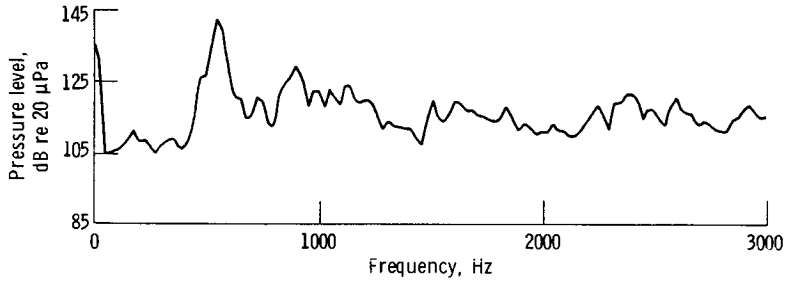

Figure 100. - Pressure spectrum at nozzle exit with jet excited by 550 Hz tone (M = 0.2, noisy valve).

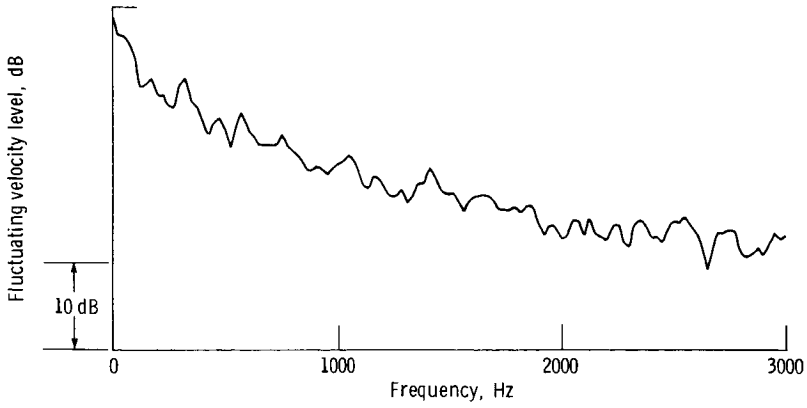

Figure 101. - Velocity spectrum at X/D = 7.6 with jet excited by 550 Hz tone (M = 0.2, noisy value).

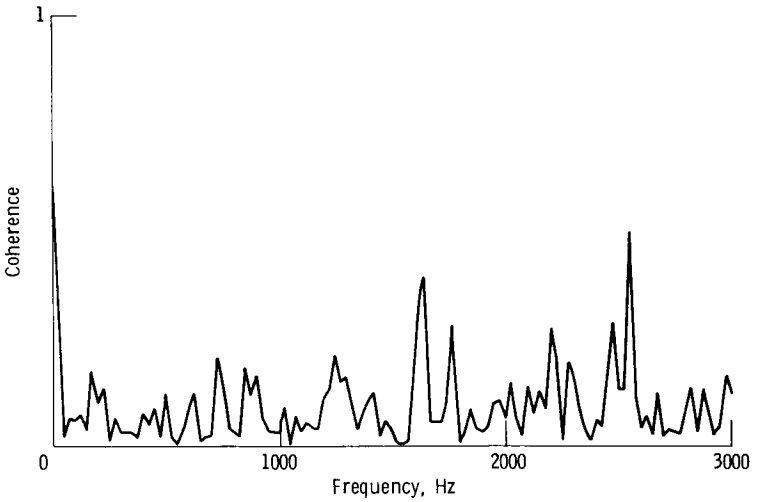

Figure 102. - Coherence between microphone at nozzle exit and hot wire at X/D = 7.6 with jet excited by 550 Hz tone (M = 0.2, noisy valve).

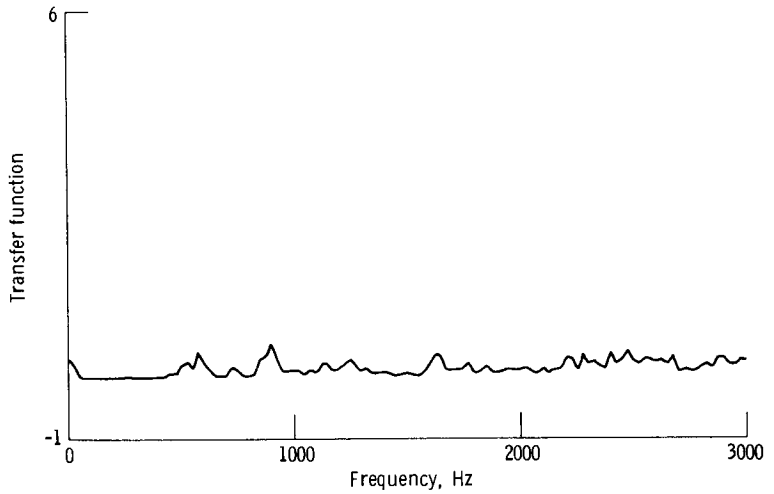

Figure 103. - Transfer function between microphone at nozzle exit and hot wire at X/D = 7.6 with jet excited by 550 Hz tone (M = 0.2, noisy valve).

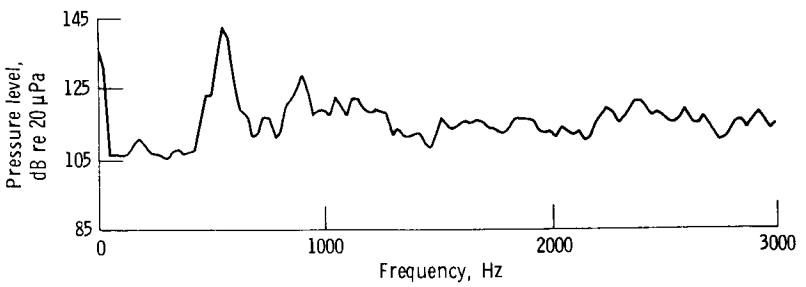

Figure 104. - Pressure spectrum at nozzle exit with jet excited by 550 Hz tone (M = 0.2, noisy valve).

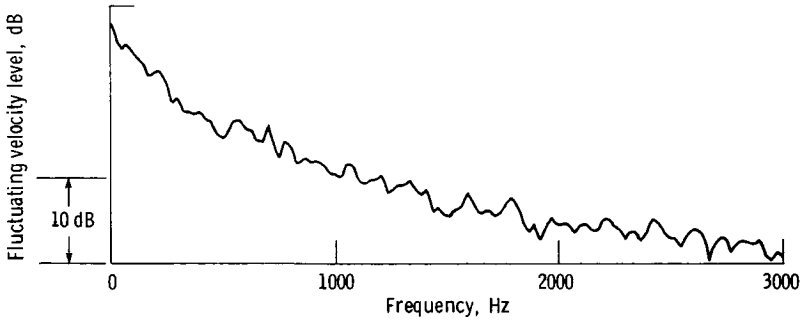

Figure 105. - Velocity spectrum at X/D = 9 with jet excited by 550 Hz tone (M = 0.2, noisy valve).

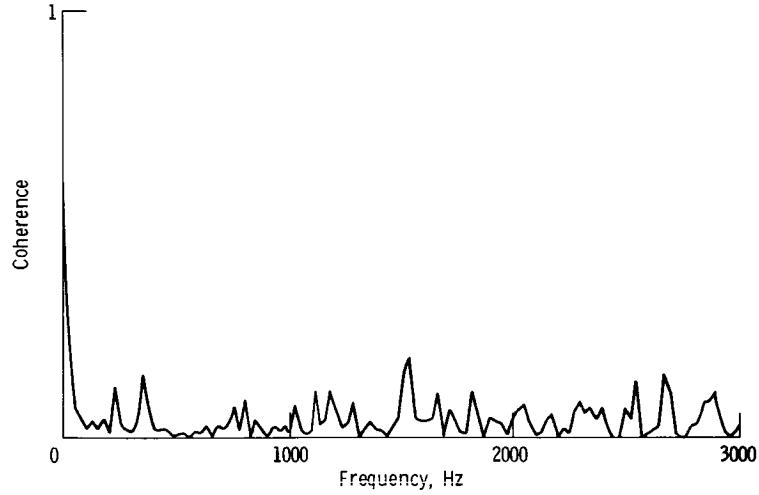

Figure 106. - Coherence between microphone at nozzle exit and hot wire at X/D = 9 with jet excited by 550 Hz tone (M = 0.2, noisy valve).

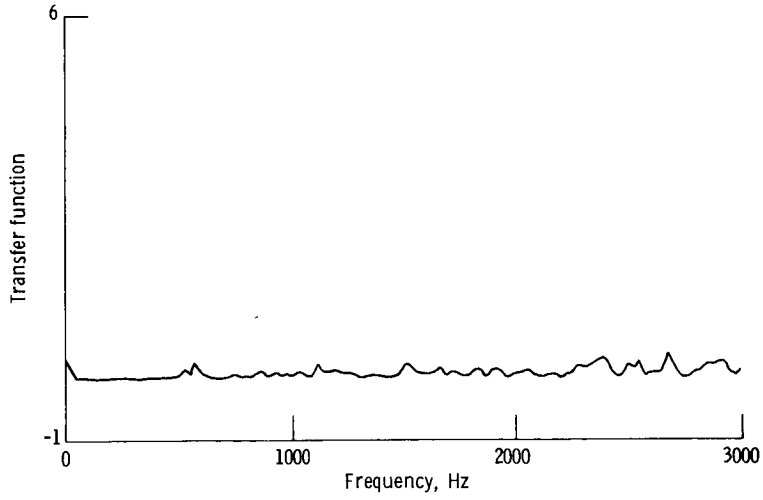

Figure 107. - Transfer function between microphone at nozzle exit and hot wire at X/D = 9 with jet excited by 550 Hz tone (M = 0.2, noisy valve).

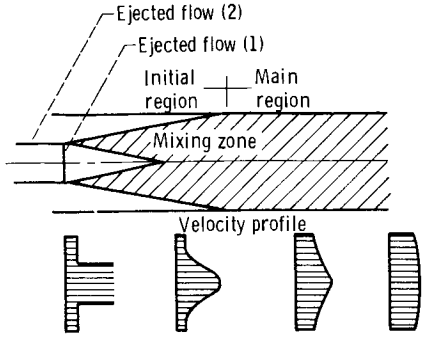

(a) Flow pattern in mixing chamber of an ejector.

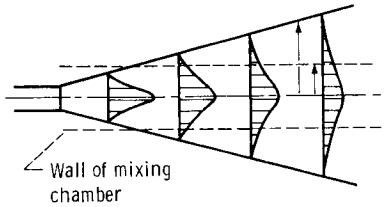

(b) Analogy between the fluid flow in a free jet and in the mixing chamber of an ejector.

Figure 108. - Analogy between free jet and jet ejector (from Abramovich (1963)).

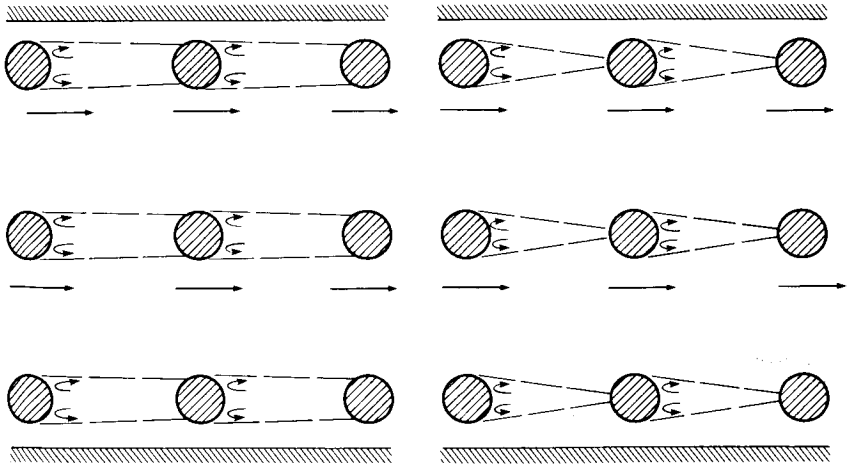

(a) Unexcited. (b) Excited.

Figure 109. - Schematic representation of flow past a tube bundle.

APPENDIX A

APPENDIX A

HOT-WIRE CALIBRATION PROCEDURE

(1) Initial constant temperature anemometer settings Square wave:off, H.F. Filter: 1, Volts: 1, Function:Standby, Probe type: wire, Decade resistance: 00.00, Gain: 1.

(2) Install shorted dummy probe, set function to 'Resistance measure' (CTA uses square wave in this position). Adjust 'zero ohms' so that meter deflects to red line.

(3) Determine Mach number versus Pressure Relationship (using program HOTWR on HP 9835A).

(4) To measure probe resistance set function to 'standby', remove dummy probe and install measuring probe with no air flow and cover with foam cup, set function swith to 'resistance measure' , set decade so that meter deflects to red line and record decade values. Reduce decade value by uncompensated lead resistance (0.9 for hot wire), readjust 'zero ohms' so that meter deflects to red line, set function to s'standby', multiply decade value by overheat ratio (1.8 for hot wire). Set new decade values and measure no-flow voltage.

(5) Square wave check: Remove foam cup, set CTA to 'operate', set square wave to 3.0 V, set calibrator flow to Mach 0.4, adjust gain, HF,L,Q for best square wave, shut off air, turn CTA to 'standby' and shut off square wave.

(6) Calibration table: Record probe voltages at various mach numbers from 0 to 0.4 at regular intervals, curve fit to (E**2 = a +b*(u)**0.5), where E=probe voltage, u = M*(Gamma*R*T)**0.5, M = Mach number.

Determine 'a' and 'b' and input into data acquisition program.

AXISYMMETRIC JET EXCITATION PROGRAM
Check Sheet and Run Summary

Test Date: _____ Configuration: _____

Test Eng.: _____ Mech. or Tech.: _____

Test Start Time: _____ Test End Time: _____

Total Run Time: _____ No. of Test Conditions: _____

START UP OPERATION

1. Put "Caution" sign on cell door and place warning light in hallway.

2. Close test cell door.

3. Open 8 in. VDJ handvalve.

4. Open 125 lb service air line.

5. Turn on cell exhaust air line.

6. Verify high limit setting of over-pressure switch.

7. Energize control room operational panel.

8. Press reset button on pressure alarm panel.

9. Read the barometer and record ambient static pressure.

10. Verify operation of four acoustic drivers.

11. Call Central Control (PAX 3200) for services (40 psig air at 6 lb sec).

12. Run jet at a tank gauge pressure of 1.0 psig for 10 minutes before setting the first condition. Adjust 8 in. butterfly valve for coarse control and 1-1/2 in. annin bypass for fine control. Determine nozzle exit velocity from appropriate pressure ratio and area ratio.

NOTE: Tank pressure must not exceed 35 psig.

SHUT DOWN OPERATION

___1. Close 8 in. butterfly valve and 1-1/2 in. annin bypass.

___2. Call Central Control to turn off 40 psig air service.

___3. De-energize control room operational panel.

___4. Close 125 lb service air line.

___5. Close 8 in. VDJ handvalve.

___6. Remove "Caution" sign and warning light.

APPENDIX B

SAMPLE CALCULATION FOR MOMENTUM THICKNESS

Experimental data in Tables C-6(a-f) and C-12(a-r) of Appendix C were used to calculate the momentum thicknesses presented in Table II.

For each case the data was curve-fitted using a hyperbolic tangent profile and the best fitting curve was integrated to give the momentum thickness. The form of the hyperbolic tangent profile used is similar to the one proposed by Michalke (1984)

$$\frac{U}{U_o} = 0.5 \left\{ 1 + \tanh \left[b \left(\frac{R}{\delta\gamma} - \frac{\delta\gamma}{R} \right) \right] \right\} \qquad \text{(B-1)}$$

where

$$b = 0.25\ R/\theta \qquad \text{(B 2)}$$

and it was found that

$$\frac{\theta}{R} = 0.06 \left(\frac{X}{D}\right) + 0.04 \qquad \text{(B-3)}$$

for their data.

In Equation (B-1) Michalke (1984) used $\delta = 1$. Figure (B-1) shows the best fit for the data in Table C-12(h) of Appendix C. At $X/D = 2$ the

curve in Equation (B-1) fitted best when δ was chosen to be 1.3 and b was 1.5625. A sample of the numerical integration to calculate the momentum thickness

$$\theta = \int_0^y \frac{U}{U_o}\left(1 - \frac{U}{U_o}\right)dy$$

is presented in Table (B-1).

TABLE B(1)

Δy	$\frac{U}{U_o}$	$\left(1 - \frac{U}{U_o}\right)$	$\frac{U}{U_o} * \left(1 - \frac{U}{U_o}\right) * \Delta y$
0.1	1.0	0.0	0.0
.2	1.0	.0	.0
.3	1.0	.0	.0
.4	1.0	.0	.0
.5	.999	.001	.0
.6	.995	.005	.001
.7	.984	.016	.003
.8	.959	.041	.007
.9	.913	.087	.014
1.0	.840	.160	.024
1.1	.741	.259	.034
1.2	.623	.377	.041
1.3	.500	.500	.044
1.4	.386	.614	.041
1.5	.290	.710	.036
1.6	.213	.787	.029
1.7	.155	.845	.023
1.8	.112	.888	.017
1.9	.081	.919	.013
2.0	.059	.941	.010
			θ = 0.336 in.

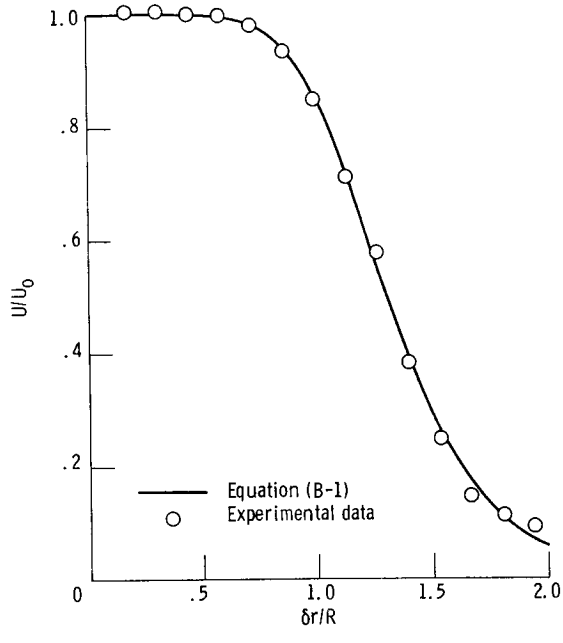

Figure B-1. - Curve fit of experimental data.

APPENDIX C

APPENDIX C - TABULATED DATA

KEY TO TABULATED DATA IN APPENDIX C

Table C-1(a-f) Axial traverse with hot wire along centerline, different locations and Mach numbers.

Table C-2 Radial traverse at X/D = 9 with and without excitation at a constant sound level.

Table C-3(a,b) Resonance characteristics of rig, with and without flow.

Table C-4(a-d) Excitation at Mach number = 0.1, hot-wire measurements, f = 650 to 1600 Hz.

Table C-5(a-d) Excitation at Mach number = 0.3, hot-wire measurements, f = 500 to 2450 Hz.

Table C-6(a-f) Radial velocity profiles, X/D = 1 and 2, Mach number 0.07, 0.2, and 0.435.

Table C-7(a-c) Felt test.

Table C-8 Resonance characteristics of modified rig.

Table C-9(a,b) Excitation at Mach number = 0.435, varying sound levels, Pitot probe measurements, X/D = 9, f = 700 to 1650 Hz.

Table C-10(a-c) Radial Traverse at X/D = 9, Pitot probe measurements at Mach numbers = 0.435 and 0.2 (quiet and noisy valve positions).

Table C-11(a-f) Radial traverse at X/D = 9, Mach number = 0.435 and 0.2.

Table C-12(a-r) Radial velocity profiles, Pitot probe measurements, X/D = 0, 1, and 2, Mach number = 0.435 and 0.2 (quiet and noisy valve positions), with and without excitation.

Table C-13(a-d) Axial velocity decay along centerline, single-hot-wire measurements, Mach number = 0.2 (quiet and noisy).

Table C-14(a-z) Sound level effects, Mach number = 0.435.

Table C-15(a-p) Sound level effects, Mach number = 0.2 (quiet valve).

Table C-16(a-l) Sound level effects, Mach number = 0.2 (noisy valve).

TABLE C-1

(a) Tank ΔP = 0.1 psi; jet Mach number = 0.100; main valve position = 3.7; bypass valve position = 14.8; noise peak = 128.6 dB at 850 Hz; nozzle diameter = 3.5 in.

Axial location, X/D	Velocity, ft/sec	Fluctuating velocity, ft/sec	Jet turbulence intensity
0.463	126.832	1.357	0.010
1.900	126.832	6.803	5.363×10^{-2}
3.320	126.089	9.049	7.177×10^{-2}
4.749	121.694	12.295	.101
6.178	110.809	16.631	.150
7.606	96.950	18.990	.195
9.035	85.993	18.825	.218
10.460	76.243	18.197	.238

(b) Tank ΔP = 0.2 psi; jet Mach number = 0.141; main valve position = 3.7; bypass valve position = 16.6; nozzle diameter = 3.5 in.

Axial location, X/D	Velocity, ft/sec	Fluctuating velocity, ft/sec	Jet turbulence intensity
0.463	177.143	2.630	1.484×10^{-2}
1.900	177.050	12.171	6.874×10^{-2}
3.320	176.285	14.397	8.166×10^{-2}
4.749	166.678	19.154	.114
6.178	148.151	25.273	.170
7.606	129.359	26.480	.204
9.035	112.365	25.200	.224
10.460	99.753	23.611	.236

(c) Tank ΔP = 0.3 psi; jet Mach number = 0.172; main valve position = 3.7; bypass valve position = 17.8; nozzle diameter = 3.5 in.

Axial location, X/D	Velocity, ft/sec	Fluctuating velocity, ft/sec	Jet turbulence intensity
0.463	212.151	2.910	1.371×10^{-2}
1.900	210.063	13.025	6.200×10^{-2}
3.320	208.894	16.529	7.912×10^{-2}
4.749	202.886	23.136	.114
6.178	177.236	29.179	.164
7.606	146.549	29.104	.198
9.035	138.160	29.986	.217
10.460	121.332	28.107	.231

TABLE C-1

(d) Tank ΔP = 0.4 psi; jet Mach number = 0.199; main valve position = 10; bypass valve position = 13.2; nozzle diameter = 3.5 in.

Axial location, X/D	Velocity, ft/sec	Fluctuating velocity, ft/sec	Jet turbulence intensity
0.463	244.609	1.967	8.045×10^{-3}
1.900	243.457	11.281	4.634×10^{-2}
3.320	242.883	13.087	5.388×10^{-2}
4.749	234.095	19.890	8.496×10^{-2}
6.178	214.518	29.255	.136
7.606	188.958	33.238	.175
9.035	167.035	32.808	.196
10.460	150.867	32.383	.214

(e) Tank ΔP = 0.5 psi; jet Mach number = 0.222; main valve position = 10; bypass valve position = 14.7; nozzle diameter = 3.5 in.

Axial location, X/D	Velocity, ft/sec	Fluctuating velocity, ft/sec	Jet turbulence intensity
0.463	268.734	2.106	7.839×10^{-3}
1.900	266.894	12.603	4.722×10^{-2}
3.320	267.414	16.925	0.063
4.749	256.330	25.303	9.871×10^{-2}
6.178	232.141	33.771	.145
7.606	204.901	36.922	.180
9.035	180.624	36.173	.200
10.460	162.391	35.124	.216

(f) Tank ΔP = 0.8 psi; jet Mach number = 0.280; main valve position = 10; bypass valve position = 14.7; nozzle diameter = 3.5 in.

Axial location, X/D	Velocity, ft/sec	Fluctuation velocity, ft/sec	Jet turbulence intensity
0.463	331.324	3.016	9.105×10^{-3}
1.900	329.095	16.362	0.049
3.320	327.615	21.813	6.658×10^{-2}
4.749	311.363	32.431	.104
6.178	279.639	41.376	.147
7.606	245.475	45.341	.184
9.035	218.021	44.784	.205
10.460	195.082	42.067	.215

TABLE C-2

[Date: August 15, 1985; Tank ΔP = 2.15 psi; Mach number = 0.45; frequency of excitation = 1590 Hz; pressure level = 135 3 dB re 20 μPa; axial location = 9 diameters downstream; Strouhal number = 0.920.]

Position, r, in.	Excited velocity, ft/sec	Unexcited velocity, ft/sec
0	373	400
.2	374.5	395
.4	376	395
.6	366	395.5
.8	364	381
1	358	371.5
1.2	347	361
1.4	330	342.2
1.6	317	326
1.8	303	309
2	288	290
2.2	277	274
2.4	264	257
2.6	244	246
2.8	231	219
3	226	215
3.2	197	198
3.4	189	193
3.6	172	169
3.8	167	162
4	158	151
4.2	149	138

TABLE C-3(a)

[Resonance characteristics of original rig; no flow test; Altec Lansing amplifiers at 10 V; date: June 28, 1985.]

Frequency, Hz	Pressure level, dB re 20 μPa
650	120
700	124.4
750	126.5
800	121
850	127.4
900	134.8
950	130.4
1000	123
1050	137.5
1100	136
1150	132.6
1200	129.3
1250	127
1300	124.8
1350	130
1400	121
1450	114
1500	131
1550	129.9
1600	132.3
1650	116.3
1700	117.3
1750	131
1800	125.8
1850	114
1900	117.7
1950	125.9
2025	127.35
2075	124.3
2125	115
2175	130.4
2225	114

TABLE C-3(b)

[Resonance characteristics of of original rig; Mach number = 0.3; test; Altec lansing amplifiers at 15 V; date: June 28, 1985.]

Frequency, Hz	Pressure level, dB re 20 μPa
600	133
650	128
700	129
750	130
800	128
850	137
900	137.9
950	134.5
1000	133
1050	139.5
1100	136.6
1150	133.4
1200	128.9
1275	131.4
1300	133.5
1350	132.4
1400	131
1450	113.8
1500	138.5
1550	133.5
1600	141.5
1650	129.5
1700	131.5
1750	121.2
1800	127.2
1850	125
1900	130.2
1950	122.8
2025	130.79
2075	127.5
2175	129
2200	120

TABLE C-4(a)

[Mach number = 0.1; tank ΔP = 0.104 psi; axial distance (X/D) = 1.90.]

Frequency, Hz	Velocity, ft/sec	Fluctuating velocity, ft/sec	Turbulence intensity, percent
700	137.831	6.247	4.533×10^{-2}
750	137.770	6.179	4.485×10^{-2}
800	137.731	6.209	4.508×10^{-2}
850	137.672	5.726	4.159×10^{-2}
900	137.800	6.028	4.374×10^{-2}
950	137.674	6.254	4.542×10^{-2}
1000	137.697	5.929	4.306×10^{-2}
1050	137.856	6.294	4.565×10^{-2}
1100	138.492	4.682	3.381×10^{-2}
1150	137.625	6.151	4.469×10^{-2}
1200	137.466	6.007	4.370×10^{-2}
1250	137.470	6.211	4.518×10^{-2}
1300	137.625	6.204	4.508×10^{-2}
1350	137.778	6.162	4.472×10^{-2}
1400	137.754	6.134	4.452×10^{-2}
1450	137.512	6.129	4.457×10^{-2}
1500	138.044	5.688	4.121×10^{-2}
1550	137.752	6.111	4.436×10^{-2}
1600	137.831	5.737	0.416

TABLE C-4(b)

[Mach number = 0.1; tank ΔP = 0.107 psi; axial distance (X/D) = 4.749.]

Frequency, Hz	Velocity, ft/sec	Fluctuating velocity, ft/sec	Turbulence intensity, percent
650	132.920	14.146	0.106
700	132.920	13.755	.103
750	129.302	13.883	.107
800	130.549	14.678	.112
850	129.571	13.515	.104
900	132.344	13.488	.101
950	130.877	15.165	.115
1000	131.153	13.579	.103
1050	131.784	14.505	.110
1100	132.761	12.869	.096
1150	130.527	14.985	.114
1200	132.687	14.241	.107
1250	130.881	14.716	.112
1300	130.774	15.031	.114
1350	132.561	18.855	.104
1400	130.493	14.366	.110
1450	130.852	13.207	.100
1500	131.967	13.350	.101
1550	132.334	15.107	.114
1600	132.920	13.005	.097

TABLE C-4(c)

[Mach number = 0.1; tank ΔP = 0.105 psi; axial distance (X/D) = 6.178.]

Frequency, Hz	Velocity, ft/sec	Fluctuating velocity, ft/sec	Turbulence intensity, percent
650	119.092	18.058	0.151
700	119.092	17.921	.150
750	117.063	17.409	.148
800	117.818	17.865	.151
850	117.480	17.697	.150
900	117.905	17.788	.150
950	117.947	18.291	.155
1000	118.374	17.897	.151
1050	119.592	18.562	.155
1100	122.176	17.352	.142
1150	117.697	17.530	.148
1200	116.502	17.893	.153
1250	117.754	18.579	.157
1300	117.893	18.577	.157
1350	118.002	17.421	.147
1400	118.136	18.078	.153
1450	117.130	17.334	.147
1500	119.509	17.453	.146
1550	118.494	17.715	.149
1600	119.092	17.604	.147

TABLE C-4(d)

[Mach number = 0.1; tank ΔP = 0.110 psi; axial distance (X/D) = 9.035.]

Frequency, Hz	Velocity, ft/sec	Fluctuating velocity, ft/sec	Turbulence intensity, percent
650	95.608	19.080	0.199
700	95.608	19.710	.206
750	93.053	18.976	.203
800	92.932	19.507	.209
850	93.876	19.531	.208
900	93.904	19.267	.205
950	94.326	19.186	.203
1000	92.578	18.957	.204
1050	91.272	18.897	.207
1100	94.217	18.715	.198
1150	91.824	18.968	.206
1200	91.852	19.283	.209
1250	92.051	19.190	.208
1300	90.617	18.771	.207
1350	91.536	18.997	.207
1400	91.391	18.734	.204
1450	96.693	19.767	.204
1500	96.670	19.962	.206
1550	96.214	19.172	.199
1600	95.608	19.571	.204

TABLE C-5(a)

[Mach number = 0.3; probe at X/D = 9.035; tank ΔP = 0.90; date: July 11, 1985.]

Frequency, Hz	Velocity, ft/sec	Fluctuating velocity, ft/sec	Turbulence intensity, percent
500	277.510	43.472	0.156
550	277.510	43.547	.156
600	264.087	44.398	.168
650	256.150	42.715	.166
700	257.710	40.719	.158
750	260.813	44.290	.169
800	266.884	44.214	.165
850	267.523	43.234	.161
900	259.980	43.142	.165
950	256.867	43.072	.167
1000	263.646	45.010	.170
1050	246.150	42.040	.170
1100	257.812	41.630	.161
1150	261.396	42.915	.164
1200	267.663	42.806	.159
1250	260.858	42.105	.161
1300	263.864	41.727	.158
1350	263.279	42.848	.162
1400	267.263	43.675	.163
1450	265.689	42.157	.158
1500	259.462	47.156	.181
1550	263.333	47.032	.178
1600	258.299	45.395	.175
1650	263.036	47.158	.179
1700	268.859	47.197	.175
1750	264.761	49.524	.187
1800	263.779	48.627	.184
1850	260.982	46.821	.179
1900	264.969	48.835	.184
1950	264.255	48.288	.182
2000	270.193	48.589	.179
2050	260.088	47.736	.183
2100	262.470	48.540	.184
2150	265.771	47.478	.178
2200	266.811	47.632	.178
2250	268.918	48.264	.179
2300	261.667	47.280	.180
2350	265.325	47.846	.180
2400	265.949	49.762	.187
2450	277.798	48.471	.174

TABLE C-5(b)

[Mach number = 0.3; probe at X/D = 6.178; tank ΔP = 0.90; date: July 11, 1985.]

Frequency, Hz	Velocity, ft/sec	Fluctuating velocity, ft/sec	Turbulence intensity, percent
550	334.354	40.967	0.122
600	333.229	39.249	.117
650	331.859	39.383	.118
700	334.570	38.745	.115
750	331.744	38.952	.117
800	332.533	38.472	.115
850	339.008	40.856	.120
900	327.221	40.261	.123
950	329.752	39.631	.120
1000	325.855	39.680	.121
1050	320.313	41.393	.129
1100	325.111	41.326	.127
1150	326.751	38.887	.119
1200	332.361	36.965	.111
1250	334.151	37.960	.113
1300	331.432	39.248	.118
1350	326.501	39.364	.120
1400	331.190	38.177	.115
1450	332.165	37.126	.111
1500	323.373	39.041	.120
1550	324.594	39.385	.121
1600	329.517	39.373	.119
1650	329.802	37.853	.114
1700	333.053	37.152	.111
1750	336.700	37.869	.112
1800	327.268	39.611	.121
1850	331.415	37.854	.114
1900	330.833	38.017	.114
1950	334.331	38.272	.114
2000	331.221	37.591	.113
2050	328.379	37.269	.113
2100	335.613	37.442	.111
2150	329.865	37.180	.112
2200	333.932	38.058	.113
2250	327.140	36.035	.110
2300	326.785	37.855	.115
2350	332.024	35.862	.108
2400	327.566	37.228	.113
2450	334.354	35.228	.105

TABLE C-5(c)

[Mach number = 0.3; probe at X/D = 4.749; tank ΔP = 0.90; date: July 11, 1985.]

Frequency, Hz	Velocity, ft/sec	Fluctuating velocity, ft/sec	Turbulence intensity, percent
500	360.411	27.529	7.638×10^{-2}
550	360.411	29.774	8.261×10^{-2}
600	358.707	29.108	8.114×10^{-2}
650	357.338	27.629	7.732×10^{-2}
700	357.167	28.603	8.008×10^{-2}
750	355.541	28.143	7.915×10^{-2}
800	356.682	28.249	7.920×10^{-2}
850	358.326	27.750	0.077
900	353.751	29.030	8.206×10^{-2}
950	355.145	28.037	7.894×10^{-2}
1000	359.032	28.569	7.957×10^{-2}
1050	349.214	30.978	8.870×10^{-2}
1100	351.400	29.192	8.307×10^{-2}
1150	357.979	29.785	8.320×10^{-2}
1200	355.538	27.248	7.664×10^{-2}
1250	361.102	27.888	7.723×10^{-2}
1300	359.176	28.664	0.079
1350	358.688	29.538	8.235×10^{-2}
1400	360.491	28.559	7.922×10^{-2}
1450	357.449	28.315	7.921×10^{-2}
1500	354.043	28.662	8.0957×10^{-2}
1550	356.180	27.904	7.834×10^{-2}
1600	356.782	28.866	8.088×10^{-2}
1650	358.137	28.674	8.006×10^{-2}
1700	356.433	28.077	7.877×10^{-2}
1750	355.978	28.225	7.929×10^{-2}
1800	355.868	27.158	7.631×10^{-2}
1850	359.877	26.639	7.402×10^{-2}
1900	361.195	26.349	7.295×10^{-2}
1950	361.012	27.249	7.548×10^{-2}
2000	361.510	26.833	7.422×10^{-2}
2050	360.120	27.210	7.555×10^{-2}
2100	359.842	27.724	0.077
2150	358.766	26.753	7.456×10^{-2}
2200	356.970	26.813	7.511×10^{-2}
2250	360.218	27.447	7.619×10^{-2}
2300	358.616	26.763	7.463×10^{-2}
2350	361.712	26.781	7.404×10^{-2}
2400	361.050	26.935	0.074
2450	360.411	26.068	7.232×10^{-2}

TABLE C-5(d)

[Mach number = 0.3; probe at X/D = 1.90; tank ΔP = 0.90; date: July 11, 1985.]

Frequency, Hz	Velocity, ft/sec	Fluctuating velocity, ft/sec	Turbulence intensity, percent
500	373.394	15.770	4.223×10^{-2}
550	373.394	19.853	5.316×10^{-2}
600	372.146	16.403	0.440
650	372.343	15.744	4.228×10^{-2}
700	373.015	16.199	4.342×10^{-2}
750	372.305	16.491	7.915×10^{-2}
800	372.827	16.094	4.316×10^{-2}
850	372.349	15.993	4.295×10^{-2}
900	372.019	16.607	4.464×10^{-2}
950	372.595	16.236	4.357×10^{-2}
1000	372.330	16.612	4.461×10^{-2}
1050	370.419	19.012	5.132×10^{-2}
1100	372.030	18.138	4.875×10^{-2}
1150	371.039	16.976	4.575×10^{-2}
1200	371.845	16.216	4.360×10^{-2}
1250	372.227	16.375	4.399×10^{-2}
1300	373.226	16.839	4.511×10^{-2}
1350	372.252	16.718	4.491×10^{-2}
1400	371.590	16.410	4.416×10^{-2}
1450	372.449	15.689	4.212×10^{-2}
1500	372.550	16.515	4.433×10^{-2}
1550	371.803	16.090	4.327×10^{-2}
1600	372.529	15.565	4.178×10^{-2}
1650	372.300	15.918	4.275×10^{-2}
1700	372.069	15.687	4.216×10^{-2}
1750	372.521	15.723	0.422
1800	372.049	15.669	4.211×10^{-2}
1850	372.579	15.587	4.183×10^{-2}
1900	371.913	15.371	4.133×10^{-2}
1950	371.895	15.672	4.214×10^{-2}
2000	372.117	15.425	4.145×10^{-2}
2050	372.012	15.609	4.195×10^{-2}
2100	371.621	15.757	4.240×10^{-2}
2150	372.947	15.266	4.093×10^{-2}
2200	371.579	15.862	4.269×10^{-2}
2250	372.048	15.648	.042
2300	371.913	15.370	4.132×10^{-2}
2350	372.224	14.897	4.002×10^{-2}
2400	371.671	15.584	4.193×10^{-2}
2450	373.394	14.682	0.393

TABLE C-6(a)

[Date: August 8, 1985; Mach number = 0.07; tank ΔP = 0.05 psi; X/D = 1; unexcited case; temperature = 533 °R; pressure = 14.35 psi.]

Position, r, in.	Velocity, ft/sec	Tank ΔP, psi
0.223	24.848	0.050
.462	26.679	.051
.706	26.631	.052
.944	25.001	.050
1.183	26.917	.051
1.428	26.343	.048
1.669	24.693	.051
1.903	24.745	.054
2.139	26.727	.053
2.379	24.276	.052
2.624	26.870	.052
2.869	23.257	.051
3.100	26.148	.045
3.245	29.753	.055
3.588	43.062	.053
3.822	49.126	.051
4.059	73.666	.054
4.308	79.131	.052
4.545	78.744	.051
4.777	79.792	.047
5.018	79.388	.054
5.260	79.660	.053
5.505	79.002	.053
5.739	79.259	.048
5.989	79.275	.052
6.217	79.596	.048
6.459	79.099	.048
6.697	79.580	.053
6.940	78.013	.048
7.183	68.748	.053
7.426	47.214	.053
7.665	32.183	.053
7.906	25.305	.048
8.148	23.583	.051
8.379	26.965	.044
8.625	25.755	.048
8.863	23.799	.052
9.108	26.584	.052
9.346	25.103	.045
9.580	24.118	.052
9.825	25.305	.051
10.057	27.757	.051
10.308	25.506	.047
10.549	24.899	.054
10.780	25.001	.053
11.022	24.118	.050
11.259	25.804	.048
11.498	24.224	.053

TABLE C-6(b)

[Date: August 8, 1985; Mach number = 0.07; Tank ΔP = 0.05 psi; X/D = 2; unexcited case; temperature = 533 °R; pressure = 14.35 psi.]

Position, r, in.	Velocity, ft/sec	Tank ΔP, psi
0.226	24.899	0.057
.465	22.869	.056
.706	23.257	.055
.958	22.645	.054
1.185	24.590	.051
1.418	25.796	.059
1.659	23.147	.058
1.908	24.796	.056
2.145	21.607	.059
2.385	23.257	.060
2.618	22.981	.055
2.864	25.952	.062
3.104	32.183	.059
3.337	40.719	.055
3.582	50.753	.060
3.817	65.212	.060
4.058	76.097	.056
4.297	83.482	.060
4.538	86.004	.060
4.785	85.231	.060
5.026	85.589	.053
5.268	85.782	.060
5.497	86.461	.061
5.749	85.648	.059
5.989	85.425	.060
6.223	85.142	.058
6.468	85.410	.055
6.709	83.375	.061
6.937	75.002	.060
7.183	63.949	.057
7.428	49.093	.060
7.668	39.991	.061
7.899	31.904	.057
8.140	24.329	.061
8.386	21.190	.059
8.618	23.092	.062
8.871	22.869	.059
9.099	23.036	.062
9.338	22.702	.061
9.586	23.311	.062
9.828	24.329	.060
10.075	23.237	.060
10.300	22.017	.056
10.539	25.848	.060
10.785	22.476	.056
11.030	23.366	.061
11.269	24.796	.061
11.508	21.901	.057

TABLE C-6(c)

[Date: August 8, 1985; Mach number = 0.2; tank ΔP = 0.4 psi; X/D = 1; unexcited case; temperature = 533 °R; pressure = 14.35 psi.]

Position, r, in.	Velocity, ft/sec	Tank ΔP, psi
0.223	10.352	0.413
.459	17.129	.439
.697	10.352	.418
.938	11.953	.419
1.179	10.595	.417
1.417	15.812	.413
1.665	8.893	.418
1.900	7.660	.419
2.138	3.194	.415
2.385	8.749	.418
2.623	22.419	.417
2.862	59.939	.417
3.103	124.030	.419
3.342	189.770	.420
3.579	220.421	.418
3.822	226.027	.419
4.057	226.685	.419
4.300	226.850	.419
4.537	226.894	.419
4.777	227.037	.419
5.024	227.219	.411
5.259	227.214	.419
5.504	227.065	.420
5.737	226.839	.420
5.978	226.817	.418
6.226	226.624	.418
6.460	216.968	.420
6.699	176.013	.419
6.944	100.839	.414
7.194	37.011	.419
7.419	16.132	.410
7.664	9.975	.418
7.899	11.066	.410
8.137	11.066	.420
8.378	16.367	.417
8.625	8.893	.420
8.858	17.858	.412
9.102	13.833	.420
9.338	12.475	.420
9.588	12.778	.418
9.824	14.813	.415
10.060	13.172	.415
10.302	12.678	.416
10.544	10.142	.416
10.705	15.069	.419
11.024	10.102	.419
11.257	12.778	.420
11.502	14.899	.410

TABLE C-6(d)

[Date: August 8, 1985; Mach number = 0.2; tank ΔP = 0.4 psi; X/D = 2; unexcited case; temperature = 533 °R; pressure = 14.35 psi.]

Position, r, in.	Velocity, ft/sec	Tank ΔP, psi
0.223	19.628	0.421
.458	19.628	.424
.698	19.234	.423
.937	22.419	.423
1.189	20.393	.422
1.418	19.497	.423
1.665	19.757	.421
1.903	18.352	.420
2.142	21.608	.414
2.379	21.548	.421
2.620	30.723	.421
2.859	37.660	.423
3.099	69.412	.414
3.342	86.456	.410
3.586	131.992	.423
3.818	162.437	.416
4.062	197.001	.421
4.303	216.118	.418
4.545	226.284	.423
4.777	227.258	.418
5.024	227.846	.422
5.257	227.988	.422
5.502	227.999	.417
5.739	227.840	.418
5.982	227.867	.422
6.217	226.944	.413
6.462	225.984	.422
6.700	213.915	.422
6.943	196.675	.421
7.184	164.729	.412
7.422	124.856	.42
7.658	90.725	.420
7.902	63.228	.417
8.143	39.860	.422
8.385	26.439	.422
8.622	22.362	.416
8.866	20.765	.422
9.100	22.362	.422
9.344	23.257	.417
9.584	20.330	.421
9.823	19.366	.427
10.058	19.432	.412
10.302	22.758	.42
10.542	20.393	.421
10.783	19.822	.419
11.022	21.430	.413
11.257	19.950	.419
11.500	20.826	.417

TABLE C-6(e)

[Date: August 8, 1985; Mach number = 0.435; tank ΔP = 1.99 psi; X/D = 1; unexcited case; temperature = 533 °R; pressure = 14.35 psi.]

Position, r, in.	Velocity, ft/sec	Tank ΔP, psi
0.226	23.257	1.987
.462	23.475	1.995
.705	25.606	1.988
.945	24.118	1.989
1.183	24.118	1.993
1.426	21.842	1.997
1.669	23.529	1.994
1.904	22.075	1.991
2.139	21.842	1.990
2.379	21.548	1.995
2.624	15.237	1.999
2.865	17.424	2.001
3.097	18.282	1.998
3.342	68.767	2.000
3.586	156.326	1.998
3.822	299.663	1.996
4.059	426.297	2.001
4.304	481.879	1.999
4.539	490.318	1.999
4.786	491.141	1.996
5.028	491.159	2.002
5.257	491.273	2.003
5.508	491.427	2.003
5.746	491.396	1.999
5.982	491.223	1.998
6.223	491.375	2.002
6.464	490.911	1.993
6.704	490.610	2.003
6.948	481.443	1.994
7.191	426.384	1.999
7.420	281.217	1.991
7.662	137.860	1.997
7.899	38.231	1.996
8.143	15.893	1.999
8.389	19.757	1.994
8.618	18.627	1.998
8.858	22.190	2.000
9.102	23.637	2.001
9.340	22.758	2.001
9.589	22.532	1.999
9.817	24.118	2.001
10.062	22.981	2.001
10.299	24.590	2.005
10.538	23.799	1.999
10.784	23.906	2.000
11.026	23.852	1.996
11.265	24.012	2.000
11.503	23.691	1.996

TABLE C-6(f)

[Date: August 8, 1985; Mach number = 0.435; tank ΔP = 1.99 psi; X/D = 2; unexcited case; temperature = 533 °R; pressure = 14.35 psi.]

Position, r, in.	Velocity, ft/sec	Tank ΔP, psi
0.223	19.563	1.988
.462	19.757	1.993
.706	17.351	1.988
.945	19.628	1.987
1.183	18.142	1.988
1.426	18.282	1.988
1.657	20.765	1.986
1.906	13.647	1.983
2.142	15.404	1.985
2.383	15.153	1.988
2.626	39.864	1.988
2.859	63.329	1.978
3.102	120.419	1.985
3.348	173.335	1.988
3.580	248.906	1.984
3.829	333.605	1.976
4.064	407.431	1.986
4.309	456.242	1.987
4.551	479.345	1.984
4.784	488.322	1.986
5.024	489.565	1.979
5.270	489.589	1.982
5.504	489.477	1.988
5.746	489.679	1.989
5.979	489.272	1.982
6.224	488.858	1.989
6.465	483.906	1.987
6.706	467.916	1.988
6.946	420.843	1.987
7.179	358.978	1.985
7.420	274.876	1.986
7.660	189.273	1.986
7.900	125.454	1.977
8.145	69.960	1.986
8.377	47.295	1.987
8.618	23.637	1.988
8.859	16.523	1.981
9.100	21.190	1.986
9.338	22.190	1.986
9.586	22.248	1.984
9.826	21.430	1.984
10.062	21.901	1.977
10.298	24.171	1.983
10.537	21.370	1.983
10.783	23.959	1.976
11.028	23.092	1.979
11.266	26.001	1.983
11.503	22.589	1.982

TABLE C-7

(a) Pressure = 14.37 psi;
temperature = 79 °F;
date: August 26, 1985;
felt thickness = 1/8 in.

Tank ΔP, psi	Velocity, ft/sec
0.29	0
.45	0
.95	16.057
1.43	20.311
1.92	23.269
2.43	27.343
2.92	29.168
3.42	30.885
3.88	32.112
4.39	33.294
4.87	34.060

(b) Pressure = 14.37 psi;
temperature = 79 °F;
date: August 26, 1985;
felt thickness = 1/8 in.

Tank ΔP, psi	Velocity, ft/sec
0.6	8.696
1	12.298
1.5	16.652
2	19.445
2.5	22.453
3	24.596
3.5	26.566
4	29.274
4.5	30.948
5	32.921

(c) Pressure = 14.47 psi;
temperature = 71 °F;
date: August 28, 1985;
felt thickness = 3/8 in.

Tank ΔP, psi	Velocity, ft/sec
0.71	8.696
1	10.041
1.5	12.298
2	14.201
2.5	15.062
3	16.652
3.5	18.102
4	19.445
4.5	21.884
5	22.453

TABLE C-8

[Resonance characteristics of modified rig no flow test; Altec Lansing amplifiers at 10 V; date: September 6, 1985.]

Frequency, Hz	Pressure level, dB re 20 μPa
600	137.9
625	130.1
650	130.7
675	132.9
700	132.2
725	131.8
750	133.6
775	133.1
800	130
825	138.8
850	141.1
875	135.1
900	138.3
925	144.3
950	140.7
975	139.9
1000	136.9
1025	139.4
1050	141.4
1075	140.8
1100	139.9
1125	138
1150	137.2
1175	141.1
1200	137.6
1225	139.8
1250	135.6
1275	136.7
1300	135.6
1325	136.6
1350	132.2
1375	129.9
1400	132.2
1425	134.5
1450	117.3
1475	126.2
1500	139.4
1525	141.9
1550	138.6
1550	138.6
1575	134.5

TABLE C-9(a)

[Date: September 10, 1985; exit Mach number = 0.435; pressure = 14.3 psi; temperature = 85 °F; tank ΔP = 1.99 psi; pressure drop across felt = 0.15 psi; main valve position = 11.0; bypass position = 17.1; Altec Lansing amplifiers at 10 V; Pitot probe at 90, centerline.]

Strouhal number	Pressure level, dB re 20 μPa	Velocity, ft/sec	Velocity $U_{excited}$/ Velocity $U_{unexcited}$	Frequency, Hz
0.417	129	373	0.987	700
.446	132	369	.976	750
.476	133	360	.952	800
.506	137	348	.921	850
.536	133	365	.966	900
.565	134	360	.952	950
.595	135	357	.944	1000
.625	138	342	.905	1050
.655	137	340	.899	1100
.685	136	343	.907	1150
.714	133	355	.939	1200
.744	135	344	.91	1250
.774	137	335	.886	1300
.804	128	364	.963	1350
.833	129	362	.958	1400
.863	123	372	.984	1450
.893	135	346	.915	1500
.923	137	339	.897	1550
.952	131	364	.963	1600
.982	131	358	.947	1650

TABLE C-9(b)

[Date: September 10, 1985; exit Mach number = 0.435; pressure = 14.3 psi; temperature = 85 °F; tank ΔP = 1.99 psi; pressure drop across felt = 0.15 psi; main valve position = 11.0; bypass position = 17.1; Altec Lansing amplifiers at 10 V; Pitot probe at 9D, centerline.]

Strouhal number	Pressure level, dB re 20 μPa	Velocity, ft/sec	Velocity $U_{excited}$/ Velocity $U_{unexcited}$	Frequency, Hz
0.417	132	365	0.973	700
.446	128	372	.992	750
.476	136	352	.939	800
.506	139	342	.912	850
.536	134	357	.952	900
.565	136	352	.939	950
.595	137	343	.915	1000
.625	141	334	.891	1050
.655	140	332	.885	1100
.685	140	332	.885	1150
.714	135	346	.923	1200
.744	137	340	.907	1250
.774	139	335	.893	1300
.804	130	362	.965	1350
.833	132	359	.957	1400
.863	124	370	.987	1450
.893	137	340	.907	1500
.923	139	334	.891	1550
.952	134	351	.936	1600
.982	134	349	.931	1650

TABLE C-10(a)

[Date: September 26, 1985; Mach number = 0.435; tank ΔP = 2; frequency = 850 Hz; pressure level, = 140 dB re 20 μPa; Pitot probe at 9D; Strouhal number St_d = 0.5.]

Position, r, in	Unexcited		Excited	
	Velocity, ft/sec	U/U_c	Velocity, ft/sec	U/U_c
0	385.76	1	349.0	0.9047
.2	391.42	1.01	353.91	.9174
.4	393.28	1.018	346.15	.897
.6	380.01	.9851	341.84	.886
.8	366.88	.9511	329.29	.8536
1.0	364.19	.9441	322.43	.8358
1.2	348.28	.9028	304.14	.7884
1.4	327.02	.8477	294.11	.7624
1.6	310.63	.8052	280.14	.7262
1.8	298.33	.7733	278.35	.7215
2.0	278.35	.7215	264.45	.6855
2.2	260.61	.6756	245.65	.636
2.4	243.59	.6314	225.22	.5838
2.6	229.67	.5953	208.83	.5413
2.8	216.01	.5599	197.55	.5121
3.0	205.14	.5318	190.99	.4751
3.2	184.18	.477	182.79	.4738
3.4	165.16	.428	168.23	.436
3.6	155.57	.4033	145.35	.3768
3.8	147.11	.3814	147.11	.3818

TABLE C-10(b)

[Date: September 26, 1985; Mach number = 0.2 (quiet); tank ΔP = 0.4; frequency = 550 Hz; pressure level = 140 dB re 20 μPa; Pitot probe at 9D; Strouhal number St_d = 0.5.]

Position, r, in	Unexcited		Excited	
	Velocity, ft/sec	U/U_c	Velocity, ft/sec	U/U_c
0	184.18	1	168.23	0.9134
.2	174.20	.9458	162.031	.8797
.4	175.67	.9538	165.16	.8967
.6	178.55	.9694	165.16	.8967
.8	165.16	.8967	158.84	.8622
1.0	166.70	.9051	160.44	.871
1.2	163.60	.8823	147.11	.7987
1.4	148.84	.808	153.92	.8357
1.6	148.84	.808	145.35	.7892
1.8	143.54	.7796	124.40	.6754
2.0	138.11	.7499	130.45	.7082
2.2	118.03	.6408	124.40	.6754
2.4	128.47	.6975	139.95	.7598
2.6	128.47	.6975	115.83	.6287
2.8	99.0	.5375	108.96	.59161
3.0	96.4	.523	88.03	.4779
3.2	104.13	.5654	106.57	.5786
3.4	96.42	.5235	93.71	.5088
3.6	78.75	.4276	90.91	.4936
3.8	101.62	.5517	71.89	.3903

TABLE C-10(c)

[Date: September 26, 1985; Mach number = 0.2 (noisy); tank ΔP = 0.4; frequency = 550 Hz; pressure level = 140 dB re 20 μPa; Pitot probe at 9D; Strouhal number St_d = 0.5.]

Position, r, in	Unexcited		Excited	
	Velocity, ft/sec	U/U_c	Velocity, ft/sec	U/U_c
0	157.75	1.0	145.76	0.9275
.2	157.11	.9959	145.60	.9265
.4	158.19	.99	144.37	.9186
.6	153.22	.9713	143.37	.9123
.8	142.77	.9049	140.00	.891
1.0	142.36	.9023	135.11	.8597
1.2	137.55	.8718	127.27	.8098
1.4	133.90	.8487	123.22	.7841
1.6	125.84	.7977	119.14	.7581
1.8	122.12	.7741	111.69	.711
2.0	114.13	.7235	115.41	.7343
2.2	104.49	.6623	102.86	.6545
2.4	99.51	.6308	97.28	.619
2.6	93.43	.5922	94.96	.6043
2.8	91.10	.577	82.89	.5274
3.0	82.58	.523	79.92	.5085
3.2	76.46	.4846	79.68	.5070
3.4	69.69	.4417	69.86	.4445
3.6	68.57	.4346	60.98	.388
3.8	57.68	.3655	60.14	.3827

TABLE C-11(a)

[Date: September 26, 1985; Pitot probe at X/D = 9; temperature = 537 °R; pressure = 14.26 psi; exit Mach number = 0.2; tank ΔP = 0.4 psi; noisy valve setting subsonic cold jet with excitation.]

Position, r, in.	Tank ΔP, psi	Velocity, ft/sec
0	0.395	145.758
.2	.405	145.603
.4	.401	144.373
.6	.410	143.371
.8	.405	140.003
1	.397	135.109
1.2	.402	127.270
1.4	.400	123.225
1.6	.406	119.146
1.8	.405	111.694
2	.398	115.416
2.2	.404	102.861
2.4	.405	97.281
2.6	.407	94.969
2.8	.406	82.893
3	.400	79.920
3.2	.405	79.684
3.4	.399	69.858
3.6	.402	60.983
3.8	.406	60.143

TABLE C-11(b)

[Date: September 26, 1985; Pitot probe at X/D = 9; temperature = 537 °R; pressure = 14.26 psi; exit Mach number = 0.2; tank ΔP = 0.4 psi; noisy valve setting subsonic cold jet without excitation.]

Position, r, in.	Tank ΔP, psi	Velocity, ft/sec
0	0.408	157.750
.2	.408	157.107
.4	.407	158.191
.6	.413	153.218
.8	.405	142.768
1	.408	142.359
1.2	.405	137.545
1.4	.409	133.898
1.6	.402	125.838
1.8	.403	122.121
2	.406	114.133
2.2	.394	104.494
2.4	.396	99.512
2.6	.406	93.431
2.8	.406	91.100
3	.405	82.584
3.2	.407	76.457
3.4	.404	69.692
3.6	.399	68.571
3.8	.404	57.678

TABLE C-11(c)

[Date: September 26, 1985; Pitot probe at X/D = 9; temperature = 537 °R; pressure = 14.26 psi; exit Mach number = 0.2; tank ΔP = 0.4 psi; quiet valve setting subsonic cold jet with excitation.]

Position, r, in.	Tank ΔP, psi	Velocity, ft/sec
0	0.405	168.231
.2	.412	162.030
.4	.405	165.161
.6	.405	165.161
.8	.402	158.837
1	.404	160.442
1.2	.412	147.106
1.4	.409	153.921
1.6	.405	145.351
1.8	.400	124.401
2	.405	130.454
2.2	.409	124.401
2.4	.401	139.953
2.6	.407	115.834
2.8	.406	108.963
3	.401	88.031
3.2	.412	106.573
3.4	.409	93.706
3.6	.411	90.913
3.8	.402	71.894

TABLE C-11(d)

[Date: September 26, 1985; Pitot probe at X/D = 9; temperature = 537 °R; pressure = 14.26 psi; exit Mach number = 0.2; tank ΔP = 0.4 psi; quiet valve setting subsonic cold jet without excitation.]

Position, r, in.	Tank ΔP, psi	Velocity, ft/sec
0	0.408	184.188
.2	.408	174.207
.4	.405	175.668
.6	.401	178.555
.8	.405	165.161
1	.395	166.703
1.2	.409	163.603
1.4	.411	148.839
1.6	.408	148.839
1.8	.403	143.575
2	.407	138.106
2.2	.410	118.035
2.4	.407	128.468
2.6	.403	128.568
2.8	.408	99.055
3	.408	96.418
3.2	.399	104.128
3.4	.408	96.418
3.6	.406	78.749
3.8	.402	101.624

TABLE C-11(e)

[Date: September 26, 1985; Pitot probe at X/D = 9; temperature = 537 °R; pressure = 14.26 psi; exit Mach number = 0.435; tank ΔP = 0.2 psi; subsonic cold jet with excitation.]

Position, r, in.	Tank ΔP, psi	Velocity, ft/sec
0	1.392	274.712
.2	1.995	353.906
.4	1.999	346.149
.6	1.992	341.837
.8	2.007	329.286
1	2.001	322.426
1.2	2.000	304.137
1.4	2.001	294.109
1.6	2.002	280.144
1.8	1.992	279.346
2	1.997	264.447
2.2	1.996	245.653
2.4	1.993	225.217
2.6	2.023	208.830
2.8	2.006	197.552
3	2.001	190.990
3.2	1.997	182.796
3.4	2.013	168.231
2.6	2.002	145.351
3.8	2.001	147.106

TABLE C-11(f)

[Date: September 26, 1985; Pitot probe at X/D = 9; temperature = 537 °R; pressure = 14.26 psi; exit Mach number = 0.435; tank ΔP = 0.2 psi; subsonic cold jet without excitation.]

Position, r, in.	Tank ΔP, psi	Velocity, ft/sec
0.2	2	385.765
.4	2	391.420
.6	2	393.285
.8	2	380.016
1	2.02	366.882
1.2	2	264.192
1.4	2	348.283
1.6	2	327.016
1.8	2.04	310.630
2	2.02	270.331
2.2	2.04	278.346
2.4	2	260.609
2.6	2	243.586
2.8	2	229.677
3	2	216.011
3.2	2	205.142
3.4	2.02	184.188
3.6	2.02	165.161
3.8	1.98	155.577
4	2	147.106

TABLE C-12(a)

[Date: September 27, 1985; Pitot probe at X/D = 0; temperature = 540 °R; pressure = 14.3 psi; exit Mach number = 0.2; tank ΔP = 0.39 psi; quiet valve setting subsonic cold jet with no excitation.]

Position, r, in.	Tank ΔP, psi	Velocity, ft/sec
0.220	0.394	11.835
0.462	.398	10.438
0.706	.4	12.985
0.938	.399	15.364
1.179	.393	14.315
1.424	.393	12.371
1.656	.398	15.022
1.901	.396	14.315
2.138	.398	14.495
2.382	.398	9.252
2.617	.399	14.133
2.859	.394	12.579
3.098	.398	13.084
3.339	.399	202.057
3.583	.399	226.562
3.818	.399	227.408
4.059	.399	227.833
4.299	.400	228.240
4.545	.401	228.212
4.776	.396	228.218
5.018	.398	228.351
5.259	.392	228.535
5.498	.399	228.546
5.743	.392	228.374
5.987	.394	228.129
6.223	.394	228.246
6.461	.391	228.023
6.705	.391	226.613
6.940	.399	29.123
7.181	.395	12.052
7.422	.398	9.797
7.663	.389	12.783
7.905	.392	15.615
8.138	.399	14.761
8.382	.397	18.851
8.626	.399	13.084
8.861	.390	14.761
9.100	.398	19.192
9.340	.399	15.780
9.585	.396	15.780
9.820	.392	18.363
10.061	.396	16.425
10.303	.398	16.582
10.537	.397	16.106
10.788	.397	17.862
11.020	.393	17.569
11.268	.398	19.856
11.496	.392	23.339

TABLE C-12(c)

[Date: September 27, 1985; Pitot probe at X/D = 1; temperature = 540 °R; pressure = 14.3 psi; exit Mach number = 0.2; tank ΔP = 0.39 psi; quiet valve setting subsonic cold jet with no excitation.]

Position, r, in.	Tank ΔP, psi	Velocity, ft/sec
0.226	0.397	12.579
0.462	.398	14.224
0.704	.401	10.186
0.944	.399	10.438
1.427	.398	12.579
1.662	.395	13.378
1.900	.401	14.584
2.148	.403	11.502
2.382	.396	11.274
2.619	.403	13.948
2.865	.401	56.171
3.104	.400	136.640
3.342	.403	208.975
3.580	.401	226.512
3.826	.394	227.822
4.056	.403	228.296
4.307	.402	228.335
4.539	.397	228.696
4.780	.403	228.880
5.020	.397	228.668
5.262	.394	228.713
5.497	.405	228.696
5.737	.403	228.841
5.988	.397	228.641
6.220	.405	228.401
6.464	.402	220.500
6.699	.403	165.925
6.937	.397	82.639
7.185	.398	25.414
7.416	.401	12.371
7.657	.399	10.804
7.896	.403	7.020
8.140	.397	10.186
8.376	.404	15.615
8.617	.403	11.388
8.862	.399	13.948
9.106	.401	16.186
9.338	.402	13.571
9.576	.401	14.224
9.822	.402	12.475
10.065	.404	16.425
10.302	.396	15.532
10.543	.404	13.855
10.785	.394	14.041
11.025	.394	12.371
11.264	.403	12.052
11.505	.398	11.944

TABLE C-12(d)

[Date: September 27, 1985; Pitot probe at X/D = 1; temperature = 540 °R; pressure = 14.3 psi; exit Mach number = 0.2; tank ΔP = 0.39 psi; quiet valve setting subsonic cold jet with excitation.]

Position, r, in.	Tank ΔP, psi	Velocity, ft/sec
0.219	0.391	15.279
0.459	.395	15.279
0.703	.395	11.041
0.938	.396	14.041
1.176	.391	11.388
1.418	.397	14.133
1.656	.394	8.212
1.903	.398	14.041
2.138	.398	7.554
2.385	.395	0
2.627	.392	10.313
2.859	.394	45.774
3.104	.394	148.172
3.340	.399	193.034
3.583	.390	222.803
3.818	.400	227.157
4.057	.397	227.269
4.298	.392	227.643
4.542	.391	227.710
4.777	.398	227.749
5.027	.400	227.637
5.263	.399	227.554
5.502	.390	227.375
5.737	.399	227.537
5.985	.392	227.285
6.217	.389	225.070
6.465	.393	208.033
6.700	.399	168.237
6.943	.399	84.650
7.181	.400	10.186
7.419	.394	0
7.656	.394	10.683
7.898	.399	14.761
8.144	.399	14.584
8.380	.397	10.058
8.629	.399	13.666
8.856	.399	12.475
9.102	.393	16.660
9.339	.399	14.936
9.590	.400	12.579
9.819	.389	16.425
10.057	.396	12.371
10.301	.390	14.761
10.539	.389	15.364
10.778	.398	14.673
11.028	.397	15.532
11.257	.396	14.495
11.501	.398	13.948

TABLE C-12(e)

[Date: September 27, 1985; Pitot probe at X/D = 2; temperature = 540 °R; pressure = 14.3 psi; exit Mach number = 0.2; tank ΔP = 0.39 psi; quiet valve setting subsonic cold jet without excitation.]

Position, r, in.	Tank ΔP, psi	Velocity, ft/sec
0.220	0.390	11.835
.465	.385	16.968
.697	.392	14.673
.938	.386	9.797
1.179	.383	14.495
1.418	.386	14.584
1.662	.391	8.967
1.897	.392	16.186
2.138	.391	16.892
2.376	.391	38.177
2.617	.383	61.013
2.862	.390	86.763
3.104	.391	130.250
3.345	.390	167.794
3.583	.382	199.986
3.822	.390	214.604
4.064	.389	223.987
4.298	.385	225.041
4.537	.384	225.290
4.786	.382	225.409
5.021	.382	225.476
5.266	.390	225.516
5.504	.382	225.392
5.745	.382	225.521
5.981	.385	223.663
6.226	.389	217.904
6.461	.382	201.519
6.699	.392	170.118
6.944	.390	127.823
7.188	.386	90.111
7.416	.391	59.855
7.664	.391	36.864
7.902	.386	20.688
8.138	.390	11.388
8.379	.391	13.571
8.623	.385	12.266
8.860	.383	14.673
9.100	.385	13.281
9.338	.386	15.022
9.584	.390	12.783
9.823	.390	14.315
10.059	.389	14.133
10.306	.392	15.364
10.539	.383	11.835
10.779	.386	15.698
11.023	.390	12.266
11.264	.391	16.815
11.506	.386	17.271

TABLE C-12(f)

[Date: September 27, 1985; Pitot probe at X/D = 2; temperature = 540 °R; pressure = 14.3 psi; exit Mach number = 0.2; tank ΔP = 0.39 psi; quiet valve setting subsonic cold jet with excitation.]

Position, r, in.	Tank ΔP, psi	Velocity, ft/sec
0.223	0.394	15.022
.465	.385	12.985
.706	.387	15.364
.947	.394	13.666
1.188	.393	15.944
1.421	.387	12.266
1.658	.388	11.274
1.900	.388	27.284
2.148	.385	36.118
2.376	.389	42.331
2.624	.388	40.131
2.856	.393	75.092
3.101	.394	127.853
3.345	.385	172.231
3.586	.385	199.295
3.825	.389	211.553
4.060	.387	221.048
4.313	.391	224.889
4.551	.391	226.118
4.792	.385	226.017
5.018	.391	226.158
5.260	.391	226.102
5.502	.394	225.888
5.746	.393	225.465
5.976	.395	223.606
6.223	.393	215.457
6.462	.394	202.121
6.703	.393	171.499
5.947	.386	125.358
7.180	.395	83.014
7.430	.393	47.333
7.659	.389	46.392
7.900	.386	40.676
8.145	.395	22.776
8.383	.394	20.750
8.618	.389	15.780
8.857	.389	13.761
9.110	.394	13.378
9.336	.390	15.279
9.593	.387	12.371
9.831	.396	15.194
10.069	.396	16.025
10.304	.393	17.862
10.551	.392	12.160
10.786	.395	16.425
11.031	.394	15.022
11.257	.396	16.025
11.498	.392	15.615

TABLE C-12(g)

[Date: September 27, 1985; Pitot probe at X/D = 0; temperature = 540 °R; pressure = 14.3 psi; exit Mach number = 0.2; tank ΔP = 0.39 psi; noisy valve setting subsonic cold jet with no excitation.]

Position, r, in.	Tank ΔP, psi	Velocity, ft/sec
0.217	0.399	18.007
.459	.400	11.725
.703	.392	18.363
.944	.400	18.504
1.186	.397	17.569
1.421	.399	9.928
1.662	.391	11.944
1.900	.400	15.022
2.148	.398	13.084
2.379	.398	12.266
2.618	.399	12.579
2.856	.391	11.041
3.100	.397	8.967
3.339	.398	211.016
3.577	.392	226.085
3.825	.401	227.816
4.057	.403	228.357
4.298	.402	228.446
4.545	.403	228.807
4.783	.402	228.652
5.018	.397	228.262
5.263	.402	228.596
5.497	.400	228.630
5.743	.400	228.474
5.976	.396	228.140
6.223	.400	228.463
6.462	.400	227.850
6.697	.393	223.891
6.939	.398	71.579
7.179	.394	8.212
7.423	.400	11.388
7.659	.398	13.855
7.903	.398	14.405
8.141	.395	10.313
8.376	.397	14.041
8.618	.399	12.371
8.859	.400	13.571
9.101	.393	17.716
9.339	.397	12.579
9.577	.399	14.936
9.818	.393	18.007
10.059	.397	12.475
10.304	.394	14.315
10.541	.394	16.660
10.785	.398	11.041
11.021	.393	16.815
11.262	.398	16.503
11.503	.393	16.737

TABLE C-12(h)

[Date: September 27, 1985; Pitot probe at X/D = 0; temperature = 540 °R; pressure = 14.3 psi; exit Mach number = 0.2; tank ΔP = 0.39 psi; noisy valve setting subsonic cold jet with excitation.]

Position, r, in.	Tank ΔP, psi	Velocity, ft/sec
0.231	0.395	16.345
.468	.398	16.503
.715	.400	19.259
.941	.400	14.224
1.189	.395	15.108
1.418	.400	17.271
1.665	.401	16.892
1.902	.394	18.504
2.141	.393	12.682
2.386	.393	14.315
2.627	.391	14.495
2.869	.400	13.281
3.097	.399	15.022
3.352	.399	210.344
3.578	.400	227.308
3.831	.401	227.917
4.067	.401	228.095
4.301	.403	228.240
4.536	.402	228.585
4.784	.394	228.618
5.020	.403	228.307
5.256	.403	228.618
5.505	.394	228.262
5.747	.398	228.457
5.988	.395	228.084
6.227	.401	228.156
6.457	.402	228.318
6.700	.396	221.559
6.938	.399	72.210
7.179	.393	10.313
7.434	.393	14.849
7.659	.398	14.849
7.904	.393	17.196
8.145	.394	11.944
8.386	.400	15.944
8.618	.399	18.574
8.878	.397	15.615
9.098	.393	16.025
9.339	.397	16.737
9.577	.396	14.041
9.822	.394	17.196
10.057	.396	15.279
10.304	.393	17.934
10.548	.393	17.934
10.780	.392	13.378
11.017	.399	18.078
11.266	.397	15.698
11.517	.398	17.421

TABLE C-12(i)

[Date: September 27, 1985; Pitot probe at X/D = 1; temperature = 540 °R; pressure = 14.3 psi; exit Mach number = 0.2; tank ΔP = 0.39 psi; noisy valve setting subsonic cold jet with no excitation.]

Position, r, in.	Tank ΔP, psi	Velocity, ft/sec
0.221	0.389	14.315
.465	.396	13.855
.703	.398	15.108
.938	.392	14.315
1.186	.396	17.346
1.425	.397	16.186
1.659	.398	13.281
1.897	.399	13.183
2.141	.396	10.561
2.384	.391	10.058
2.624	.397	19.986
2.857	.388	43.776
3.103	.398	117.267
3.345	.389	175.527
3.580	.396	211.257
3.831	.395	224.906
4.072	.397	226.888
4.310	.392	227.056
4.548	.397	227.531
4.792	.396	227.492
5.026	.392	227.531
5.263	.392	227.732
5.511	.398	227.531
5.746	.392	227.559
5.997	.390	227.699
6.229	.399	227.140
6.457	.394	220.927
6.706	.399	188.094
6.947	.393	123.983
7.184	.397	60.372
7.419	.390	23.116
7.661	.400	10.438
7.896	.393	15.788
8.144	.401	10.804
8.379	.400	12.985
8.620	.390	16.892
8.868	.398	10.186
9.100	.393	12.579
9.341	.398	15.862
9.588	.390	13.855
9.820	.398	12.682
10.071	.391	13.571
10.296	.398	14.761
10.537	.392	17.196
10.797	.399	15.194
11.026	.393	15.364
11.277	.400	11.614
11.518	.397	17.196

TABLE C-12(j)

[Date: September 27, 1985; Pitot probe at X/D = 1; temperature = 540 °R; pressure = 14.3 psi; exit Mach number = 0.2; tank ΔP = 0.39 psi; noisy valve setting subsonic cold jet with excitation.]

Position, r, in.	Tank ΔP, psi	Velocity, ft/sec
0.223	0.399	15.448
.468	.390	15.364
.712	.393	15.448
.938	.399	18.007
1.179	.398	14.849
1.420	.400	16.106
1.659	.400	14.761
1.906	.397	14.761
2.151	.400	11.725
2.385	.391	6.640
2.633	.401	0
2.865	.396	44.452
3.110	.398	117.553
3.344	.390	174.663
3.586	.398	209.883
3.825	.397	223.982
4.056	.399	227.000
4.310	.401	227.364
4.542	.394	227.520
4.786	.401	227.827
5.037	.394	227.548
5.257	.398	227.727
5.501	.400	227.649
5.743	.399	227.772
5.977	.397	227.587
6.223	.400	226.253
6.461	.391	217.681
6.705	.398	187.105
6.959	.401	127.510
7.193	.399	50.254
7.416	.398	12.682
7.664	.399	15.862
7.897	.400	16.025
8.155	.393	13.761
8.381	.398	17.789
8.637	.399	15.862
8.856	.397	15.022
9.112	.397	14.495
9.341	.393	17.716
9.581	.400	18.292
9.827	.398	17.271
10.074	.398	18.363
10.300	.397	17.934
10.547	.393	16.968
10.782	.397	19.327

TABLE C-12(k)

[Date: September 27, 1985; Pitot probe at X/D = 2; temperature = 540 °R; pressure = 14.3 psi; exit Mach number = 0.2; tank ΔP = 0.39 psi; noisy valve setting subsonic cold jet with no excitation.]

Position, r, in.	Tank ΔP, psi	Velocity, ft/sec
0.223	0.393	13.183
.458	.386	18.434
.697	.389	15.364
.941	.393	16.345
1.176	.396	16.186
1.418	.397	12.985
1.662	.390	18.221
1.902	.398	20.116
2.145	.395	24.318
2.376	.397	32.768
2.621	.395	55.778
2.859	.399	86.029
3.097	.397	130.438
3.343	.392	161.025
3.577	.396	191.944
3.819	.388	211.908
4.060	.393	222.705
4.301	.389	226.675
4.540	.390	226.966
4.780	.399	227.554
5.024	.392	227.643
5.266	.393	227.241
5.505	.400	227.677
5.737	.399	226.764
5.982	.393	224.419
6.228	.394	214.461
6.459	.399	195.299
6.703	.394	164.971
6.941	.399	131.284
7.179	.400	29.712
7.417	.394	72.030
7.665	.393	49.001
7.899	.399	37.284
8.144	.400	20.244
8.376	.397	20.937
8.621	.399	14.673
8.862	.390	19.593
9.101	.399	14.405
9.339	.395	15.108
9.577	.393	13.761
9.824	.394	18.782
10.063	.399	16.660
10.301	.394	14.584
10.539	.394	13.666
10.780	.401	14.495
11.018	.400	15.194
11.259	.394	17.716
11.497	.394	16.737

TABLE C-12(1)

[Date: September 27, 1985; Pitot probe at X/D = 2; temperature = 540 °R; pressure = 14.3 psi; exit Mach number = 0.2; tank ΔP = 0.39 psi; noisy valve setting subsonic cold jet with excitation.]

Position, r, in.	Tank ΔP, psi	Velocity, ft/sec
0.220	0.397	17.569
.458	.399	13.666
.700	.394	13.084
.945	.398	18.851
1.176	.393	17.196
1.418	.398	18.221
1.665	.394	21.183
1.898	.397	24.584
2.139	.394	34.389
2.386	.402	40.803
2.621	.398	62.481
2.862	.400	87.918
3.104	.400	125.091
3.339	.400	170.321
3.581	.397	195.011
3.825	.393	214.325
4.060	.400	221.801
4.298	.399	226.691
4.536	.396	227.593
4.784	.392	228.140
5.022	.394	227.799
5.262	.399	227.727
5.496	.399	227.866
5.741	.399	226.798
5.985	.397	224.317
6.217	.394	215.528
6.456	.399	202.272
6.700	.399	173.817
6.945	.391	134.723
7.179	.399	88.475
7.424	.399	63.591
7.659	.400	57.403
7.903	.397	37.526
8.145	.400	13.761
8.388	.399	18.150
8.618	.397	19.791
8.866	.391	13.761
9.101	.400	10.804
9.339	.398	16.345
9.577	.4	12.579
9.822	.391	15.448
10.057	.394	14.761
10.301	.397	16.503
10.545	.400	7.724
10.783	.390	16.968
11.027	.400	13.948
11.259	.399	14.224
11.501	.390	14.133

TABLE C-12(m)

[Date: September 27, 1985; Pitot probe at X/D = 0; temperature = 540 °R; pressure = 14.3 psi; exit Mach number = 0.435; tank ΔP = 2 psi; subsonic cold jet with no excitation.]

Position, r, in.	Tank ΔP, psi	Velocity, ft/sec
0.220	1.988	14.041
0.464	1.988	17.862
0.700	1.993	12.985
0.944	2.008	11.835
1.185	2.008	11.158
1.421	2.003	0
1.662	2.007	15.108
1.903	2.004	7.890
2.143	2.009	0
2.386	2.006	0
2.624	2.012	0
2.858	2.013	0
3.098	2.006	0
3.340	2.010	292.325
3.584	2.009	495.285
3.918	2.008	497.680
4.060	2.011	498.850
4.302	2.011	499.593
4.543	2.018	500.188
4.784	2.013	500.332
5.025	2.014	500.417
5.264	2.012	500.294
5.506	2.018	500.407
5.747	2.015	500.143
5.986	2.015	499.952
6.227	2.013	499.546
6.466	2.007	498.569
6.701	2.012	495.443
6.945	2.007	41.496
7.177	2.004	0
7.418	2.004	0
7.661	1.998	0
7.898	2.003	14.761
8.144	1.998	9.252
8.389	1.996	3.601
8.616	1.993	17.271
8.860	2.001	15.108
9.105	1.996	11.725
9.343	2.007	15.448
9.580	2.001	10.923
9.819	2.007	17.716
10.057	2.007	16.737
10.302	2.007	13.948
10.540	2.000	12.160
10.784	2.005	15.108
11.019	2.006	11.041
11.257	2.006	17.495
11.499	2.006	14.041

TABLE C-12(n)

[Date: September 27, 1985; Pitot probe at X/D = 0; temperature = 540 °R; pressure = 14.3 psi; exit Mach number = 0.435; tank ΔP = 2 psi; subsonic cold jet with excitation.]

Position, r, in.	Tank ΔP, psi	Velocity, ft/sec
0.223	2.000	14.224
0.468	1.999	15.698
0.706	1.999	15.944
0.947	2.000	15.364
1.176	1.999	13.948
1.421	1.994	8.967
1.662	1.999	7.890
1.900	1.997	6.640
2.151	1.998	0
2.382	1.992	0
2.621	2.000	0
2.865	1.999	0
3.101	1.999	0
3.336	1.998	276.259
3.583	1.996	495.022
3.831	2.004	497.727
4.060	1.999	498.462
4.307	2.003	498.959
4.551	2.012	499.510
4.783	2.007	499.839
5.024	2.014	499.822
5.260	2.006	499.846
5.498	2.016	499.796
5.740	2.014	499.742
5.979	2.013	499.560
6.221	2.008	498.853
6.457	2.006	497.005
6.696	1.995	494.831
6.941	1.992	59.224
7.188	1.984	0
7.426	1.988	0
7.667	1.995	0
7.906	1.992	16.025
8.138	2.002	14.041
8.385	1.999	11.944
8.616	1.993	14.584
8.862	1.999	14.936
9.109	1.993	17.495
9.341	1.997	12.052
9.576	1.998	14.761
9.825	1.997	18.363
10.062	1.997	12.985
10.303	2.000	13.475
10.543	1.997	17.643
10.776	1.989	19.527
11.026	2.000	16.503
11.265	1.992	15.364
11.496	1.993	16.025

TABLE C-12(o)

[Date: September 27, 1985; Pitot probe at X/D = 1; temperature = 540 °R; pressure = 14.3 psi; exit Mach number = 0.435; tank ΔP = 2 psi; subsonic cold jet with no excitation.]

Position, r, in.	Tank ΔP, psi	Velocity, ft/sec
0.226	1.992	13.475
.463	1.991	14.761
.697	1.987	11.158
.944	1.983	14.673
1.186	1.979	9.391
1.436	1.974	10.313
1.665	1.977	7.020
1.907	1.981	9.111
2.138	1.977	7.203
2.386	1.988	9.252
2.618	1.989	8.673
2.862	1.980	116.351
3.098	1.985	283.447
3.337	1.984	445.665
3.586	1.983	489.045
3.822	1.983	495.874
4.066	1.982	496.232
4.302	1.985	496.639
4.536	1.982	496.789
4.777	1.983	496.665
5.022	1.990	496.653
5.260	1.988	496.177
5.496	1.985	495.786
5.743	1.979	495.171
5.979	1.979	494.896
6.217	1.974	494.097
6.462	1.973	487.321
6.700	1.974	419.402
6.944	1.963	250.695
7.179	1.970	110.583
7.423	1.984	29.565
7.657	1.995	13.571
7.906	2.003	16.186
8.147	2.004	14.673
8.389	2.003	16.815
8.628	2.006	11.835
8.862	1.995	17.196
9.104	2.002	17.495
9.339	2.005	14.495
9.580	2.006	16.968
9.821	1.998	16.582
10.072	1.998	18.782
10.298	2.003	14.673
10.538	2.008	17.346
10.782	2.010	27.271
11.033	2.004	15.780
11.262	2.010	16.266
11.507	2.006	18.504

TABLE C-12(p)

[Date: September 27, 1985; Pitot probe at X/D = 1; temperature = 540 °R; pressure = 14.3 psi; exit Mach number = 0.435; tank ΔP = 2 psi; subsonic cold jet with excitation.]

Position, r, in.	Tank ΔP, psi	Velocity, ft/sec
0.223	1.997	15.448
.466	1.996	9.797
.706	1.997	12.266
.936	1.991	14.224
1.182	1.998	14.041
1.418	1.996	14.405
1.665	1.987	15.615
1.900	1.983	11.725
2.151	1.992	12.579
2.382	1.992	0
2.621	1.992	0
2.761	1.993	83.092
3.099	1.991	246.064
3.342	1.988	415.727
3.581	1.993	483.898
3.819	2.007	496.567
4.057	2.004	497.824
4.307	1.997	498.005
4.544	1.999	498.159
4.777	1.997	498.287
5.021	1.993	498.325
5.258	2.002	498.303
5.508	2.001	498.341
5.740	1.997	498.296
5.982	2.003	498.355
6.217	1.998	498.102
6.458	1.999	490.460
6.699	1.997	422.444
6.943	2.000	252.692
7.181	2.002	114.020
7.423	1.997	30.557
7.658	1.994	13.183
7.902	2.005	10.923
8.138	2.000	11.502
8.379	2.003	12.371
8.617	2.003	15.862
8.859	2.003	14.495
9.100	2.002	11.388
9.347	2.006	12.266
9.576	2.002	16.266
9.823	1.996	15.698
10.065	1.999	17.862
10.306	1.995	11.614
10.537	2.000	16.106
10.778	2.002	16.106
11.022	2.004	15.615
11.261	2.003	15.108
11.505	1.996	13.378

TABLE C-12(q)

[Date: September 27, 1985; Pitot probe at X/D = 2; temperature = 540 °R; pressure = 14.3 psi; exit Mach number = 0.435; tank ΔP = 2 psi; subsonic cold jet with no excitation.]

Position, r, in.	Tank ΔP, psi	Velocity, ft/sec
0.223	2.012	14.315
.459	2.002	9.663
.700	2.004	6.442
.942	2.007	13.948
1.176	2.007	12.579
1.418	2.013	12.682
1.662	2.006	14.315
1.901	2.014	9.252
2.148	2.019	15.108
2.376	1.998	50.125
2.621	1.989	93.616
2.859	2.007	154.169
3.101	2.006	242.729
3.336	2.005	340.041
3.580	2.001	416.923
3.816	2.008	471.054
4.063	2.004	494.389
4.302	2.005	497.774
4.542	2.005	498.365
4.777	2.007	498.566
5.022	1.996	498.663
5.260	2.008	498.777
5.502	2.000	498.661
5.744	2.006	498.545
5.979	2.007	497.212
6.220	2.002	488.018
6.456	2.009	452.994
6.708	2.011	371.417
6.941	2.011	275.492
7.176	2.011	188.264
7.420	2.010	114.922
7.668	2.002	53.935
7.897	2.01	20.436
8.139	2.000	9.528
8.377	2.009	11.725
8.618	2.007	9.528
8.856	2.005	13.281
9.104	2.001	14.495
9.342	2.007	12.371
9.579	1.997	16.106
9.825	1.999	16.425
10.063	1.998	10.923
10.307	2.003	15.944
10.548	1.994	14.936
10.776	2.000	11.274
11.020	2.000	13.475
11.265	1.995	15.022
11.507	2.000	15.780

TABLE C-12(r)

[Date: September 27, 1985; Pitot probe at X/D = 2; temperature = 540 °R; pressure = 14.3 psi; exit Mach number = 0.435; tank ΔP = 2 psi; subsonic cold jet with excitation.]

Position, r, in.	Tank ΔP, psi	Velocity, ft/sec
0.223	2.012	8.522
.462	2.018	14.495
.702	2.020	12.160
.950	2.035	9.391
1.176	2.043	14.405
1.424	2.026	11.274
1.656	2.028	3.945
1.897	2.013	0
2.142	1.997	23.996
2.385	2.002	50.869
2.627	2.000	106.224
2.856	2.002	162.793
3.104	2.000	253.931
3.342	1.988	338.981
3.583	1.989	413.815
3.822	1.987	458.973
4.056	1.985	488.050
4.301	1.994	496.001
4.539	1.985	495.970
4.780	1.985	495.402
5.024	1.979	495.185
5.264	1.974	494.748
5.496	1.968	494.121
5.746	1.967	493.635
5.981	1.960	491.480
6.217	1.962	478.211
6.458	1.956	432.480
6.670	1.904	572.__7
6.940	1.953	281.398
7.178	1.946	187.084
7.433	2.011	112.010
7.661	2.001	60.222
7.902	1.999	0
8.147	1.997	0
8.388	1.999	0
8.626	1.997	8.967
8.859	2.002	11.725
9.109	1.998	6.026
9.339	1.999	1.610
9.582	1.992	18.087
9.830	1.995	17.196
10.074	2.004	13.761
10.312	2.000	13.666
10.547	2.003	17.643
10.782	2.004	18.363
11.026	1.999	15.279
11.261	2.005	13.281
11.506	1.995	15.862

TABLE C-13

(a) Quiet background; pressure level ≈ 115 dB re 20 μPa

Axial distance, X/D	Mean velocity, ft/sec	Fluctuating velocity, ft/sec	Turbulence intensity, percent	Tank ΔP, psi
9	226.492	40.579	17.916	0.40927
7.6	261.0169	39.0429	14.958	.4083
6.2	289.253	33.068	11.43	.40704
4.75	310.36	22.744	7.328	.40664
3.3	315.339	12.694	4.025	.4069
1.9	316.868	7.7518	2.446	.4074

(b) Excitated; frequency = 550 Hz; pressure level = 140.8 dB re 20 μPa

Axial distance, X/D	Mean velocity, ft/sec	Fluctuating velocity, ft/sec	Turbulence intensity, percent	Tank ΔP, psi
9	204.45	41.3045	20.20	0.4072
7.6	227.86	41.8221	18.354	.4071
6.2	254.64	38.9595	15.299	.40754
4.75	285.349	32.158	11.269	.40795
3.3	303.722	21.929	7.22	.40705
1.9	302.046	14.21	4.704	.4078

(c) Unexcited; noisy background; pressure level ≈ 125 dB re 20 μPa

Axial distance, X/D	Mean velocity, ft/sec	Fluctuating velocity, ft/sec	Turbulence intensity, percent	Tank ΔP, psi
9	205.61	37.95	18.46	0.4033
7.6	238.83	40.541	16.975	.4048
6.2	268.389	37.82	14.091	.4037
4.75	292.68	27.083	9.25	.4036
3.3	302.56	18.201	6.01	.40411
1.9	302.27	12.526	4.144	.404256

(d) Excited; frequency = 550 Hz; pressure level = 140.7 dB re 20 μPa

Axial distance, X/D	Mean velocity, ft/sec	Fluctuating velocity, ft/sec	Turbulence intensity, percent	Tank ΔP, psi
9	194.328	40.35	20.76	0.40086
7.6	217.4039	41.126	18.92	.40437
6.2	243.058	37.58	15.46	.4027
4.75	273.75	32.74	11.96	.4022
3.3	292.56	26.61	9.095	.4021
1.9	291.02	17.68	6.078	.4022

TABLE C-14. - PRESSURE LEVEL DEPENDENCE

[Pitot probe at X/D = 9; Mach number = 0.435; date: September 17, 1985; pressure = 14.41 psi; temperature = 80 °F; main valve position = 11; bypass valve position = 17; tank ΔP = 1.99 psi; frequency range = 450 to 2400; Strouhal numbers = 0.268 to 1.428.]

(a) Frequency = 450 Hz; $U_{unexcited}$ = 374 ft/sec

Pressure level, dB re 20 μPa	$U_{excited}$, ft/sec	$\frac{U_{excited}}{U_{unexcited}}$	Tank ΔP, psi
125.73	373.65	0.999	1.988
126.93	369.81	.988	1.997
127.52	369.24	.987	1.999
127.92	371.72	.993	1.998
129.20	371.73	.993	1.991

(b) Frequency = 500 Hz, $U_{unexcited}$ = 385 ft/sec

Pressure level, dB re 20 μPa	$U_{excited}$, ft/sec	$\frac{U_{excited}}{U_{unexcited}}$	Tank ΔP, psi
119	385	1	2.0043
124.81	384.66	0.999	1.993
123.77	383	.995	1.997
124.53	384.99	1	1.993
127.86	382.60	.994	1.998
125.96	388.03	1.007	1.991
127.47	384.49	.998	1.993

(c) Frequency = 550 Hz; $U_{unexcited}$ = 373 ft/sec

Pressure level, dB re 20 μPa	$U_{excited}$, ft/sec	$\frac{U_{excited}}{U_{unexcited}}$	Tank ΔP, psi
123.54	373.13	1	1.9982
125.94	375.74	1.007	1.9943
128.55	369.24	.989	1.992
130.91	372.88	.999	2.0015
133.15	370.36	.993	1.9968
135.52	370.12	.992	1.9968
136.63	370.24	.993	2.0002
137.91	363.67	.975	1.993

TABLE C-14. - Continued.

(d) Frequency = 600 Hz, $U_{unexcited}$ = 385 ft/sec

Pressure level, dB re 20 μPa	$U_{excited}$, ft/sec	$\frac{U_{excited}}{U_{unexcited}}$	Tank ΔP, psi
118	385	1	1.992
123.14	380.08	0.987	1.990
125.17	380.74	.989	1.993
125.88	382.87	.994	1.992
128.73	380.32	.988	1.994
129.23	382.19	.993	1.996
129.35	381.92	.992	1.996
130.44	382.08	.992	1.994
130.75	381.12	.990	1.993
131.61	378.92	.984	1.992
135.06	378.03	.982	2
136.76	373.62	.970	1.992
137.21	374.62	.973	1.999

(e) Frequency = 650 Hz, $U_{unexcited}$ = 371 ft/sec

Pressure level, dB re 20 μPa	$U_{excited}$, ft/sec	$\frac{U_{excited}}{U_{unexcited}}$	Tank ΔP, psi
120.01	371	1	2.001
124.68	372.87	1.005	2.001
127.56	374.02	1.008	2.002
129.91	371.72	1.002	2
131.08	364.87	.983	2
133.01	366.44	.987	2.002

(f) Frequency = 750 Hz, $U_{unexcited}$ = 374 ft/sec

Pressure level, dB re 20 μPa	$U_{excited}$, ft/sec	$\frac{U_{excited}}{U_{unexcited}}$	Tank ΔP, psi
123.53	371.80	0.994	1.994
124.14	371.55	.993	1.991
124.52	374.95	1.002	2
127.78	371.20	.993	1.994
128.14	369.86	.989	1.993
128.92	369.42	.987	1.994

TABLE C-14. - Continued.

(g) Frequency = 800 Hz, $U_{unexcited}$ = 372 ft/sec

Pressure level, dB re 20 μPa	$U_{excited}$, ft/sec	$\frac{U_{excited}}{U_{unexcited}}$	Tank ΔP, psi
122.58	372	1	1.995
123.46	370.01	0.995	2
124.23	371.34	.997	1.992
127.11	363.84	.978	2.005
129.53	365.92	.984	1.994
132.67	363.35	.976	1.998
133.27	356.04	.957	2
134.49	355.76	.956	1.999
135.41	351.75	.945	1.997
135.93	349.19	.939	1.998
136.97	349.26	.939	1.998

(h) Frequency = 850 Hz, $U_{unexcited}$ = 388 ft/sec

Pressure level, dB re 20 μPa	$U_{excited}$, ft/sec	$\frac{U_{excited}}{U_{unexcited}}$	Tank ΔP, psi
119.75	389.53	1.003	1.998
120.37	388.85	1.002	1.989
122.39	387.8	.999	1.996
126.12	385.65	.994	2.002
128.36	378.57	.976	1.996
130.10	380.54	.981	1.991
131.81	376.97	.971	1.988
132.88	370.75	.955	1.992
134.07	369.74	.953	1.994
135.15	361.17	.931	1.989
136.16	363.84	.937	1.995
137.33	355.84	.917	1.992
138.02	351.51	.905	1.994

(i) Frequency = 900 Hz, $U_{unexcited}$ = 390 ft/sec

Pressure level, dB re 20 μPa	$U_{excited}$, ft/sec	$\frac{U_{excited}}{U_{unexcited}}$	Tank ΔP, psi
122.80	390	1	1.996
126.13	386.10	0.989	1.994
127.48	382.92	.981	1.995
128.56	380.84	.976	1.988
132.64	376.80	.966	1.993
133.38	374.80	.961	1.997
134.53	368.30	.944	1.996
134.77	368.62	.945	1.988

TABLE C-14. - Continued.

(j) Frequency = 950 Hz, $U_{unexcited}$ = 373 ft/sec

Pressure level, dB re 20 μPa	$U_{excited}$, ft/sec	$\frac{U_{excited}}{U_{unexcited}}$	Tank ΔP, psi
122.86	373	1	1.993
126.48	370.28	0.993	1.994
127.79	370.80	.994	1.993
129.49	363.87	.975	1.999
130.74	364.33	.977	1.991
131.19	361.19	.968	1.995
132.80	355.03	.951	1.996
133.38	355.31	.952	1.993
134.70	352.50	.945	1.994
135.62	350.51	.940	1.998

(k) Frequency = 1000 Hz, $U_{unexcited}$ = 388 ft/sec

Pressure level, dB re 20 μPa	$U_{excited}$, ft/sec	$\frac{U_{excited}}{U_{unexcited}}$	Tank ΔP, psi
123.06	388	1	1.993
125.33	387.51	0.999	1.993
127.03	383.45	.988	1.991
129.47	381.60	.983	1.990
130.72	377.79	.974	1.993
132.03	376.13	.969	1.992
132.99	371.52	.957	1.992
133.80	365.99	.943	1.996
135.07	363.17	.936	1.992
136.17	357.94	.922	1.991
136.67	360.74	.929	1.993

(l) Frequency = 1050 Hz, $U_{unexcited}$ = 393 ft/sec

Pressure level, dB re 20 μPa	$U_{excited}$, ft/sec	$\frac{U_{excited}}{U_{unexcited}}$	Tank ΔP, psi
117.57	393	1	1.991
118.77	390.17	0.993	1.996
119.77	388.36	.988	1.997
120.19	387.81	.986	1.995
120.92	388.73	.989	1.995
125.77	380.19	.967	1.993
128.46	379.26	.965	1.989
131.42	374.05	.952	1.996
132.17	369.06	.939	1.997
133.86	368.49	.937	1.995
135.22	361.48	.919	1.994
135.68	361.60	.920	1.999
136.66	355.91	.905	1.998
138.24	347.93	.885	1.993
139.17	342.08	.870	1.991
140.05	339.0	.862	1.991

TABLE C-14. - Continued.

(m) Frequency = 1100 Hz, $U_{unexcited}$ = 370 ft/sec

Pressure level, dB re 20 μPa	$U_{excited}$, ft/sec	$\frac{U_{excited}}{U_{unexcited}}$	Tank ΔP, psi
121.37	370.95	1.002	1.991
122.97	368.80	.997	1.989
123.98	372.91	1.007	1.993
126.45	368.64	.996	1.991
127.74	366.01	.989	1.986
128.96	363.08	.981	1.993
130.86	359.87	.973	1.993
132.15	356.89	.964	1.994
133.02	353.54	.955	1.989
133.57	349.66	.945	1.996
135.17	348.95	.943	1.992
135.83	342.84	.926	1.996

(n) Frequency = 1200 Hz, $U_{unexcited}$ = 376 ft/sec

Pressure level, dB re 20 μPa	$U_{excited}$, ft/sec	$\frac{U_{excited}}{U_{unexcited}}$	Tank ΔP, psi
123.93	376	1	1.988
124.64	373.82	0.994	1.992
127.88	364.64	.970	1.996
129.52	359.38	.956	1.998
130.36	361.47	.961	1.994
131.41	356.58	.948	1.995
132.54	350.34	.932	1.990
133.07	353.58	.940	1.990
133.89	348.47	.927	1.987

(o-1) Frequency = 1300 Hz, $U_{unexcited}$ = 388 ft/sec

Pressure level, dB re 20 μPa	$U_{excited}$, ft/sec	$\frac{U_{excited}}{U_{unexcited}}$	Tank ΔP, psi
116.92	388	1	1.989
122.17	383.65	0.989	1.992
125.71	382.31	.985	1.992
128.18	382.57	.986	1.998
129.71	377.39	.973	2.002
131.38	373.50	.963	1.989
132.59	369.39	.952	1.986
133.80	367.55	.947	1.993
134.76	362.97	.935	1.997
135.72	356.18	.918	1.986
136.72	351.65	.906	1.987
137.38	349.40	.900	1.993

TABLE C-14. - Continued.

(u) Frequency = 1900 Hz, $U_{unexcited}$ = 382 ft/sec

Pressure level, dB re 20 μPa	$U_{excited}$, ft/sec	$\frac{U_{excited}}{U_{unexcited}}$	Tank ΔP, psi
122.56	382.00	1.000	1.996
124.72	376.95	0.987	1.992
127.85	376.60	.986	1.996
129.86	370.76	.970	2.000
131.04	368.18	.964	2.000
132.47	365.46	.957	1.993
133.08	362.62	.949	1.998
134.07	361.96	.947	2.004
134.88	358.10	.937	1.995

(v) Frequency = 2000 Hz, $U_{unexcited}$ = 382 ft/sec

Pressure level, dB re 20 μPa	$U_{excited}$, ft/sec	$\frac{U_{excited}}{U_{unexcited}}$	Tank ΔP, psi
119.79	382	1.000	2.001
126.47	378.72	0.991	1.994
129.21	375.55	.983	2.001
128.07	376.13	.985	1.999
131.36	371.31	.972	1.991
132.90	369.03	.966	1.993
133.94	367.99	.963	2.003
134.59	366.63	.959	2.000
135.15	365.47	.957	2.002

(w) Frequency = 2100 Hz, $U_{unexcited}$ = 385.6 ft/sec

Pressure level, dB re 20 μPa	$U_{excited}$, ft/sec	$\frac{U_{excited}}{U_{unexcited}}$	Tank ΔP, psi
127.92	376.21	0.976	1.998
129.30	375.70	.974	1.993
130.15	377.16	.977	1.996
131.33	372.99	.967	1.994
131.82	372.32	.966	1.997
132.16	369.72	.959	1.994
132.41	368.28	.955	1.997
133.47	368.57	.955	1.997
134.92	365.51	.948	2.002

TABLE C-14. - Concluded.

(x) Frequency = 2200 Hz, $U_{unexcited}$ = 385 ft/sec

Pressure level, dB re 20 μPa	$U_{excited}$, ft/sec	$\frac{U_{excited}}{U_{unexcited}}$	Tank ΔP, psi
124.75	374.91	0.974	1.987
126.44	378.08	.982	1.997
127.67	377.92	.982	1.996
128.66	371.71	.965	1.9934
129.99	374.35	.972	1.995

(y) Frequency = 2300 Hz, $U_{unexcited}$ = 382 ft/sec

Pressure level, dB re 20 μPa	$U_{excited}$, ft/sec	$\frac{U_{excited}}{U_{unexcited}}$	Tank ΔP, psi
119.73	382.00	1.000	1.989
127.31	376.16	0.985	1.992
128.76	377.26	.987	2.000
131.15	374.34	.979	1.998
132.85	369.23	.966	1.997
133.66	373.87	.978	1.998
134.83	374.52	.980	1.993

(z) Frequency = 2400 Hz, $U_{unexcited}$ = 384 ft/sec

Pressure level, dB re 20 μPa	$U_{excited}$, ft/sec	$\frac{U_{excited}}{U_{unexcited}}$	Tank ΔP, psi
119.94	384.00	1.000	2.004
127.29	381.25	0.994	1.996
127.67	380.73	.992	1.996
129.10	381.92	.996	1.997
131.17	378.52	.987	1.995
133.15	376.73	.982	1.998
135.15	376.26	.980	1.995

TABLE C-15

[Pitot probe at X/D = 9; Mach number = 0.2; quiet valve position; date: September 20, 1985; pressure = 14.41 psi; temperature = 81 °F; main valve = 10.1; bypass closed = 3.8; tank ΔP = 0.4 psi; frequency range = 250 to 1300 Hz; Strouhal number range = 0.3 to 1.56.]

(a) Frequency = 250 Hz, $U_{unexcited}$ = 160 ft/sec

Pressure level, dB re 20 μPa	$U_{excited}$, ft/sec	$\frac{U_{excited}}{U_{unexcited}}$	Tank ΔP, psi
128.36	151.70	0.948	0.396
129.39	154.48	.965	.396

(b) Frequency = 450 Hz, $U_{unexcited}$ = 160 ft/sec

Pressure level, dB re 20 μPa	$U_{excited}$, ft/sec	$\frac{U_{excited}}{U_{unexcited}}$	Tank ΔP, psi
113.32	160.00	1.000	0.387
114.65	160.00	1.000	.388
128.00	143.83	.898	.395
129.98	141.44	.884	.395
131.38	140.59	.878	.389

(c) Frequency = 700 Hz, $U_{unexcited}$ = 161 ft/sec

Pressure level, dB re 20 μPa	$U_{excited}$, ft/sec	$\frac{U_{excited}}{U_{unexcited}}$	Tank ΔP, psi
116.03	161.00	1.00	0.391
126.79	149.30	.927	.392
128.52	150.88	.937	.398
130.79	145.02	.90	.392
132.68	145.94	.906	.399
134.18	145.30	.902	.393
134.78	144.82	.899	.394

TABLE C-15. - Continued.

(d) Frequency = 650 Hz, $U_{unexcited}$ = 161(FPS)

Pressure level, dB re 20 μPa	$U_{excited}$, ft/sec	$\frac{U_{excited}}{U_{unexcited}}$	Tank ΔP, psi
114.64	161.00	1.000	0.398
126.21	153.18	.951	.399
127.27	149.81	.390	.401
128.57	147.21	.914	.395
130.88	145.18	.902	.391
132.84	145.24	.902	.391
133.81	143.45	.891	.391
135.39	142.23	.882	.402
135.90	140.99	.876	.402
137.04	139.81	.868	.392

(e) Frequency = 750 Hz, $U_{unexcited}$ = 161 ft/sec

Pressure level, dB re 20 μPa	$U_{excited}$, ft/sec	$\frac{U_{excited}}{U_{unexcited}}$	Tank ΔP, psi
115.70	161.00	1.000	0.396
123.84	154.59	.960	.397
129.47	150.58	.935	.391
130.96	150.47	.935	.396
132.18	148.43	.922	.396
132.75	148.8	.924	.396

(f) Frequency = 900 Hz, $U_{unexcited}$ = 161 ft/sec

Pressure level, dB re 20 μPa	$U_{excited}$, ft/sec	$\frac{U_{excited}}{U_{unexcited}}$	Tank ΔP, psi
116.30	161.00	1.000	0.392
127.45	155.47	.965	.391
128.89	156.08	.969	.395
131.46	153.86	.955	.397
133.26	151.44	.940	.394
134.64	151.20	.939	.394

(g) Frequency = 950 Hz, $U_{unexcited}$ = 161 ft/sec

Pressure level, dB re 20 μPa	$U_{excited}$, ft/sec	$\frac{U_{excited}}{U_{unexcited}}$	Tank ΔP, psi
114.28	161	1	0.395
128.23	155.10	.963	.391
130.97	154.92	.962	.404
132.99	154.41	.959	.397
134.64	155.81	.967	.395

TABLE C-15. - Continued.

(h) Frequency = 1000 Hz, $U_{unexcited}$ = 160 ft/sec

Pressure level, dB re 20 μPa	$U_{excited}$, ft/sec	$\frac{U_{excited}}{U_{unexcited}}$	Tank ΔP, psi
115.18	160	1	0.395
127.83	156.5	.978	.392
128.69	155.45	.972	.394
130.96	157.46	.984	.395
132.86	157.56	.985	.399
134.33	154.72	.967	.399
134.94	154.76	.967	.393
135.65	154.40	.965	.398

(i) Frequency = 1050 Hz, $U_{unexcited}$ = 161 ft/sec

Pressure level, dB re 20 μPa	$U_{excited}$, ft/sec	$\frac{U_{excited}}{U_{unexcited}}$	Tank ΔP, psi
114.28	161.00	1.000	0.395
127.81	157.28	.977	.396
129.72	157.16	.976	.395
131.38	158.20	.982	.392
132.65	157.67	.979	.396
134.80	156.84	.974	.393
135.78	155.67	.967	.399

(j) Frequency = 550 Hz, $U_{unexcited}$ = 160 ft/sec

Pressure level, dB re 20 μPa	$U_{excited}$, ft/sec	$\frac{U_{excited}}{U_{unexcited}}$	Tank ΔP, psi
130.76	145.37	0.908	0.389
134.13	140.36	.877	.394
135.56	139.93	.875	.392
136.58	137.34	.858	.383
140.08	140.51	.878	.394
142.43	143.43	.896	.402
144.33	143.16	.895	.389

TABLE C-15. - Concluded.

(n) Frequency = 1150 Hz, $U_{unexcited}$ = 160 ft/sec

Pressure level, dB re 20 μPa	$U_{excited}$, ft/sec	$\frac{U_{excited}}{U_{unexcited}}$	Tank ΔP, psi
125.58	160.00	1.000	0.400
128.19	160.84	1.005	.399
130.11	162.29	1.014	.395
130.80	158.99	.994	.397
131.69	160.1	1.00	.394
132.42	158.69	.992	.394
133.32	156.99	.98	.397
134.98	160.92	1.005	.394

(o) Frequency = 1200 Hz, $U_{unexcited}$ = 159 ft/sec

Pressure level, dB re 20 μPa	$U_{excited}$, ft/sec	$\frac{U_{excited}}{U_{unexcited}}$	Tank ΔP, psi
115.44	159.00	1.000	0.394
127.76	163.59	1.028	.399
128.95	163.77	1.03	.392
129.97	164.63	1.035	.398
132.01	160.59	1.009	.393
132.81	162.36	1.021	.401
134.23	163.33	1.027	.402
134.73	161.77	1.017	.397

(p) Frequency = 1300 Hz, $U_{unexcited}$ = 160 ft/sec

Pressure level, dB re 20 μPa	$U_{excited}$, ft/sec	$\frac{U_{excited}}{U_{unexcited}}$	Tank ΔP, psi
112.78	160.00	1.000	0.401
127.58	163.99	1.025	.399
130.74	165.14	1.032	.398
131.72	165.61	1.035	.399
133.12	162.6	1.016	.393
134.34	167.33	1.046	.394
134.84	166.82	1.043	.400

TABLE C-16

[Pitot probe at X/D = 9; Mach number = 0.2; noisy valve position; date: September 24, 1985; pressure = 14.4 psi; temperature = 80 °F; main valve almost closed = 8.7; bypass valve almost fully open = 18.2; ΔP = 0.4 psi; frequency range = 450 to 1300 Hz; Strouhal number range = 0.54 to 1.56.]

(a) Frequency = 450 Hz, $U_{unexcited}$ = 167.7 ft/sec

Pressure level, dB re 20 μPa	$U_{excited}$, ft/sec	$\frac{U_{excited}}{U_{unexcited}}$	Tank ΔP, psi
127.74	167.7	1.000	0.4
130.96	163.12	.973	.394
131.67	156.75	.935	.4
132.13	158.37	.944	.395
133.13	159.97	.954	.395

(b) Frequency = 525 Hz, $U_{unexcited}$ = 173 ft/sec

Pressure level, dB re 20 μPa	$U_{excited}$, ft/sec	$\frac{U_{excited}}{U_{unexcited}}$	Tank ΔP, psi
131	167.74	0.969	0.395
133.34	180.86	1.045	.393
134.62	172.23	1.0	.399

(c) Frequency = 550 Hz, $U_{unexcited}$ = 159 ft/sec

Pressure level, dB re 20 μPa	$U_{excited}$, ft/sec	$\frac{U_{excited}}{U_{unexcited}}$	Tank ΔP, psi
127.22	161.55	1.016	0.386
129.04	164.67	1.035	.402
131.25	167.74	1.055	.389
131.71	164.67	1.035	.388
132.72	167.74	1.055	.397
133.96	161.55	1.016	.391
135.23	170.74	1.073	.392
135.50	164.67	1.035	.391
135.74	163.12	1.026	.392
137.48	169.25	1.064	.396
137.67	158.37	.996	.394
137.82	163.12	1.026	.395
141.25	166.21	1.045	.397
143.75	151.79	.954	.391
145.45	164.67	1.035	.397

TABLE C-16. - Continued.

(d) Frequency = 575 Hz, $U_{unexcited}$ = 173 ft/sec

Pressure level, dB re 20 μPa	$U_{excited}$, ft/sec	$\frac{U_{excited}}{U_{unexcited}}$	Tank ΔP, psi
128.22	179.45	1.037	0.3927
130.02	166.21	.960	.397
130.28	173.69	1.004	.393
131.78	183.65	1.062	.394
133.64	169.25	.978	.393
135.44	167.74	.969	.396
135.62	170.74	.987	.403
135.64	173.70	1.004	.397
135.92	176.59	1.02	.3955
136.71	167.74	.969	.3935

(e) Frequency = 600 Hz, $U_{unexcited}$ = 166 ft/sec

Pressure level, dB re 20 μPa	$U_{excited}$, ft/sec	$\frac{U_{excited}}{U_{unexcited}}$	Tank ΔP, psi
127.49	166.21	1.001	.395
129.73	167.74	1.010	.403
130.02	175.15	1.055	.399
131.16	178.03	1.072	.406
131.75	166.21	1.001	.399
132.56	161.55	.973	.389
132.88	169.25	1.019	.396
135.41	172.22	1.037	.400
136.20	172.22	1.037	.400
137.29	169.25	1.019	.398

(f) Frequency = 700 Hz, $U_{unexcited}$ = 166 ft/sec

Pressure level, dB re 20 μPa	$U_{excited}$, ft/sec	$\frac{U_{excited}}{U_{unexcited}}$	Tank ΔP, psi
127.91	166.00	1.000	0.392
128.18	175.15	1.055	.389
130.38	175.15	1.055	.396
131.02	164.67	.992	.389
133.29	169.25	1.019	.395
134.24	180.86	1.089	.394
134.85	164.67	.991	.391

TABLE C-16. - Continued.

(g) Frequency = 850 Hz, $U_{unexcited}$ = 178 ft/sec

Pressure level, dB re 20 μPa	$U_{excited}$, ft/sec	$\frac{U_{excited}}{U_{unexcited}}$	Tank ΔP, psi
129.26	178	1	0.394
131.56	178	1.0	.398
131.88	175	.983	.396
138.14	178	1.0	.400

(h) Frequency = 575 Hz, $U_{unexcited}$ = 173 ft/sec

Pressure level, dB re 20 μPa	$U_{excited}$, ft/sec	$\frac{U_{excited}}{U_{unexcited}}$	Tank ΔP, psi
127.78	173.69	1.003	0.397
130.39	175.15	1.012	.396
130.85	178.03	1.029	.389
131.04	178.03	1.029	.396
133.00	180.86	1.045	.400
134.84	176.59	1.021	.397

(i) Frequency = 1050 Hz, $U_{unexcited}$ = 173 ft/sec

Pressure level, dB re 20 μPa	$U_{excited}$, ft/sec	$\frac{U_{excited}}{U_{unexcited}}$	Tank ΔP, psi
124.08	166.21	0.961	0.3884
130.16	178.03	1.029	.398
130.27	173.70	1.004	.392
130.62	169.25	.978	.399
132.74	173.69	1.004	.401
134.15	172.22	.995	.403
134.91	176.59	1.02	.403

(j) Frequency = 1150 Hz, $U_{unexcited}$ = 176 ft/sec

Pressure level, dB re 20 μPa	$U_{excited}$, ft/sec	$\frac{U_{excited}}{U_{unexcited}}$	Tank ΔP, psi
125.93	180.86	1.027	0.397
130.27	176.59	1.003	.397
131.57	173.69	.987	.408
131.81	172.23	.978	.400
132.03	182.26	1.035	.402
132.74	182.26	1.035	.401
133.99	183.65	1.043	.397
135.51	169.24	.962	.393
135.66	180.86	1.027	.393

TABLE C-16. - Concluded.

(k) Frequency = 1200 Hz, $U_{unexcited}$ = 178 ft/sec

Pressure level, dB re 20 μPa	$U_{excited}$, ft/sec	$\frac{U_{excited}}{U_{unexcited}}$	Tank ΔP, psi
127.78	175.15	0.983	0.395
128.93	178.03	1.000	.392
130.55	172.23	.967	.396
131.99	173.69	.976	.399
132.00	172.23	.967	.396
133.27	178.03	1.0	.398
134.29	166.21	.934	.392
135.25	175.15	.984	.397

(m) Frequency = 1300 Hz, $U_{unexcited}$ = 174 ft/sec

Pressure level, dB re 20 μPa	$U_{excited}$, ft/sec	$\frac{U_{excited}}{U_{unexcited}}$	Tank ΔP, psi
128.06	173.70	1.000	0.396
130.59	182.26	1.047	.398
131.95	167.74	.964	.394
132.99	176.59	1.015	.406
134.38	173.70	.998	.403
134.75	172.23	.989	.389

1. Report No.	2. Government Accession No.	3. Recipient's Catalog No.
NASA CR-175059		

4. Title and Subtitle	5. Report Date
Enhanced Mixing of an Axisymmetric Jet by Aerodynamic Excitation	March 1986
	6. Performing Organization Code
7. Author(s)	8. Performing Organization Report No.
Ganesh Raman	None
	10. Work Unit No.
9. Performing Organization Name and Address	11. Contract or Grant No.
Cleveland State University Department of Chemical Engineering Cleveland, Ohio 44115	NCC 3-49
	13. Type of Report and Period Covered
12. Sponsoring Agency Name and Address	Contractor Report
National Aeronautics and Space Administration Washington, D.C. 20546	14. Sponsoring Agency Code
	505-62-21

15. Supplementary Notes

Final report. Project Managers, Edward J. Rice and Jeffrey H. Miles, Internal Fluid Mechanics Division, NASA Lewis Research Center, Cleveland, Ohio 44135. This report was a thesis submitted in partial fulfillment of the requirements for the degree Master of Science in Chemical Engineering at Cleveland State University in March 1986.

16. Abstract

The main objective of acoustic excitation studies is to gain a high level of control over processes governing free shear flow characteristics. The basic premise is that inherent instability waves in free shear flows are excitable by external perturbations with frequencies close to the natural instability frequency of the flow. In the present work an 8.89 cm diameter axisymmetric jet was acoustically excited by four loudspeakers placed upstream of the nozzle exit. Measurements were made at Mach numbers of 0.435 and 0.2 (quiet and noisy valve conditions). A single hot-wire probe was used to obtain turbulence levels at the nozzle exit and along the centerline, and a microphone at the nozzle exit was used to study the resonance characteristics of the rig. A Pitot probe was stationed at X/D = 9 downstream along the nozzle axis to study the Strouhal number dependence and to look at threshold levels for excitation. The test results were obtained after a preliminary evaluation and facility improvement. Excitation at the correct Strouhal number enhanced mixing significantly. The effects were most prominent in the Strouhal number range between 0.4 and 1.0. The effects of acoustic excitation also depended considerably on the sound pressure level at the nozzle exit and were more pronounced at higher sound levels. Other factors which influenced the excitability were valve noise, exit turbulence levels, extraneous noise and a flanged nozzle. Analysis of the hot-wire signal, in conditions of optimum jet mixing, showed vortex pairing to occur between 2 and 3 diameters downstream.

17. Key Words (Suggested by Author(s))	18. Distribution Statement
Aerodynamic excitation; Discrete tone excitation; Instability waves; Axisymmetric jet; Turbulent jet; Coherent structures; Vortex pairing	Unclassified - unlimited STAR Category 02

19. Security Classif. (of this report)	20. Security Classif. (of this page)	21. No. of pages	22. Price*
Unclassified	Unclassified	187	A09

*For sale by the National Technical Information Service, Springfield, Virginia 22161